THIS BOOK IS OF POOR LEGIBILITY DUE TO LIGHT PRINTING THROUGH OUT IT'S ENTIRETY.

THIS IS AS RECEIVED FROM THE CUSTOMER.

THE DETERMINATION OF THE BUCKLING STRENGTH OF REINFORCED CONCRETE PLATES

by 613-8302

MARK YALE BERMAN

B. S. C. E., Kansas State University, 1971

A MASTER'S THESIS

submitted in partial fulfillment

of the requirements for the degree

MASTER OF SCIENCE

Department of Civil Engineering

KANSAS STATE UNIVERSITY
Manhattan, Kansas

1973

Approved by

Stuart E Swartz
Major Professor

TABLE OF CONTENTS

LIST OF TABLES

LIST OF FIGURES

LIST OF FIGURES (CONTINUED)

LIST OF FIGURES (CONTINUED)

LIST OF FIGURES (CONTINUED)

LIST OF FIGURES (CONTINUED)

INTRODUCTION

Reinforced concrete plates have been finding a varied number of uses in modern day structures, ranging from bearing walls in buildings to elements in box girder bridges. Due to their adaptability to precasting methods, and the advent of economical, prefabricated construction techniques, the use of reinforced concrete plates has been steadily growing. In these applications, these plates may be subjected to compressive stresses of considerable magnitude and the possibility of buckling should be considered. Previous research in this area, however, has been limited, and therefore no large volume of experimental work has been available for predicting the buckling load of a plate.

This paper is a direct result of the experimental testing of twenty-four simply supported, rectangular plates loaded in uniaxial compression to failure. Varying thicknesses were considered, as well as different total steel ratios.

The basic work of developing the experimental techniques used in this project was performed by Swartz, et al. (6) and Rogacki (4). The presentation and analysis of the experimental results obtained from the project falls within the domain of this paper.

The first objective herein is to present, in a coherent manner, such information as is necessary to produce an accurate

representation of the buckling characteristics of the test plates. This is accomplished through the use of appropriate graphs and tables. The second objective is to present the buckling loads determined for each plate and reference as to the procedure used in determining these loads. The third, and final objective, is to correlate the experimentally derived buckling loads with the available theoretical predictions. This is done by making analytical and graphical comparisons, and a final determination as to the most precise theoretical approach.

LITERATURE REVIEW

Previous investigations in determining the buckling strength of reinforced concrete plates have been quite limited. The only work done that closely approximated the present experiment was performed by Ernst (2) and Ernst, et al. (3), in which mortar plates 40 in. by 40 in. (1.02 m by 1.02 m) and 20 in. by 40 in. (0.51 m by 1.02 m) were tested. Plate thicknesses of 1/2 in. (1.27 cm), 3/4 in. (1.89 cm), 1 in. (2.54 cm), 1 1/4 in. (3.18 cm), and 1 1/2 in. (3.81 cm) were considered. These plates, however, were substantially smaller than the plates presently being considered (4 ft. by 8 ft.[1.22 m by 2.44 m]), and the edges not loaded were not free to rotate, but were stiffened with steel sections. The method of reinforcement was also different, with the plates being reinforced with mesh only in the central areas. The mode of failure observed by Ernst was that of biaxial curvature, the mode normally associated with plate buckling.

More recent work has been done with load bearing masonry walls by Yokel and Dikkers (8). These tests, however, were performed on specimens supported only along the loaded edges, so that the mode of failure was not that of plate buckling, but that of column buckling (uniaxial curvature).

Analysis of the buckling behavior of plates with a constant modulus of elasticity and behaving in a ductile

manner has been made by Timoshenko and Gere (7). Some experiments with the buckling of plates are described, and references are made to methods of experimentally determining the value of the buckling load.

Work on the theoretical aspects of reinforced concrete plate buckling has been recently performed by Swartz and Rosebraugh (5). Different theoretical approaches are considered, and some analytical examples are shown.

THEORETICAL BACKGROUND

For a thin, simply supported homogeneous plate subjected to uniaxial compression, the buckling load, P_{cr}, is given by Timoshenko and Gere (7) as:

$$P_{cr} = \frac{\pi^2 D}{a} \left(\frac{ma}{b} + \frac{b}{ma}\right)^2 \qquad (1)$$

where

$$D = \frac{Eh^3}{12\ (1-\nu^2)}$$

a = plate length

b = plate width

m = number of half waves of buckled surface in the direction parallel to the applied load

E = Young's Modulus

h = plate thickness

ν = Poisson's Ratio

For the present case, in which a = 2b, the plate would buckle into two half waves, m = 2, and P_{cr} would be:

$$P_{cr} = \frac{4\ \pi^2 D}{a} \qquad (2)$$

It must be restated that Eq. (1) is valid only for a material whose modulus of elasticity is constant, which is not the case for a reinforced concrete plate. In actuality, the value of E decreases with the increase of stress, and Eq. (1) would have to be modified to be applicable.

Swartz and Rosebraugh (5) have analyzed plate buckling behavior specifically for reinforced concrete. Two buckling theories are considered, the tangent modulus and double modulus approaches, and the material behavior is assumed to be either isotropic or orthotropic. The development assumes that the edges are simply supported with the load applied uniaxially with no eccentricity, and that the concrete stress-strain relationship is parabolic. The non-dimensionalized buckling strains, e_{cr}, for each of the cases considered are found from the following:

Isotropic-Tangent Modulus Approach

$$e_{cr}^2 - \left[2 + C' \left(\frac{m^2}{l^2} + \frac{l^2}{m^2} + 2\right) + D_{sl}\right] e_{cr} + C \left(D_{yl} + D_s\right)\left(\frac{m^2}{l^2} + \frac{l^2}{m^2}\right) + 2C' = 0 \qquad (3)$$

Isotropic-Double Modulus Approach

$$e_{cr}^2 - \left(2 + D_{sl}\right) e_{cr} + 4C' \left(\frac{m^2}{l^2} + \frac{l^2}{m^2} + 2\right)\frac{(1-e_{cr})}{\left(1+(1-e_{cr})^{\frac{1}{2}}\right)^2} + CD_s \left(\frac{m^2}{l^2} + \frac{l^2}{m^2}\right) = 0 \qquad (4)$$

Orthotropic-Tangent Modulus Approach

$$e_{cr}^2 - \left(2 + C' \frac{m^2}{l^2} + D_{sl}\right) e_{cr} + 2C' \left(1-e_{cr}\right)^{\frac{1}{2}} + C \left(D_{yl} + D_s\right)\left(\frac{m^2}{l^2} + \frac{l^2}{m^2}\right) = 0 \qquad (5)$$

Orthotropic-Double Modulus Approach

$$e_{cr}^2 - (2 + D_{sl})\, e_{cr} + 4C' \frac{(1-e_{cr})^{\frac{1}{2}}}{(1+(1-e_{cr})^{\frac{1}{2}})} \left[\frac{m^2}{l^2} \frac{(1-e_{cr})^{\frac{1}{2}}}{1+(1-e_{cr})^{\frac{1}{2}}} + 1\right]$$

$$+ C \left[D_s \left(\frac{m^2}{l^2} + \frac{l^2}{m^2}\right) + D_{yl} \frac{l^2}{m^2}\right] = 0 \qquad (6)$$

where

$$C = \frac{\pi^2}{hb^2\ (1-p)\ 0.85\ f'_c}$$

$$C' = \frac{\pi^2 h^2}{6\ (1-\nu_c)^2\ \varepsilon_o\ (1-p)\ b^2}$$

$$D_{yl} = \frac{1.7\ f'_c\ h^3}{12\ (1-\nu_c^2)\ \varepsilon_o}$$

$$D_s = E_s h \sum_{i=1}^{2} p_i\ \bar{Z}_i^2$$

$$D_{sl} = \frac{E_s\ \varepsilon_o\ p}{0.85\ f'_c\ (1-p)}$$

$$e_{cr} = \frac{\varepsilon_{cr}}{\varepsilon_o}$$

$$p = \frac{A_s}{bh}$$

$$p_i = \frac{A_{si}}{bh}$$

a = plate length

A_s = total steel area

A_{si} = steel area in $i^{\underline{th}}$ layer

b = plate width

E_s = steel modulus

f'_c = concrete cylinder strength

h = plate thickness

l = ratio of length to width of plate

m = buckling node number

$\bar{z}_i$ = distance of $i^{\underline{th}}$ steel layer from middle surface

ϵ_o = concrete strain at f'_c

ϵ_{cr} = concrete buckling stress

ν_c = Poisson's Ratio for concrete

Using the buckling strain, e_{cr}, as found in Eq. (3), (4), (5), or (6) above, the buckling stress in the concrete, f_{cr}, is given as (5):

$$f_{cr} = 0.85\, f'_c\, (2\, e_{cr} - e_{cr}^2) \qquad (7)$$

Furthermore, the plate buckling load, P_{cr}, is given by (5):

$$P_{cr} = f_{cr} (1-p) bh + E_s \varepsilon_o e_{cr} pbh \quad (8)$$

Methods of determining the experimental buckling load are numerous, but only three are considered generally applicable here. Timoshenko and Gere (7) give the Southwell method. This method utilizes a plot of the deflection/load at the point of maximum deflection. The inverse slope of the resulting straight line gives the buckling load.

Swartz, et al. (6) describes two further approaches. A plot of the deflection patterns is utilized in the first, and an empirical evaluation of the buckling load is made. In the second method, a plot of the load versus strain at contiguous strain gage locations is employed. When buckling occurs, the strain on the "tension" side of the plate should become less compressive. The buckling load, therefore, is the highest load at which the strain on the "tension" side is still increasingly compressive.

The "Rankine-Gordon" empirical approach to buckling failure is applied by Ernst (4) to reinforced concrete. For a rectangular reinforced concrete plate, simply supported and loaded on two opposite edges, the buckling stress in the

concrete, f_{cr}, is given by Ernst as:

$$f_{cr} = \frac{f'_c}{1 + C\left(\frac{f'_c}{p_{cr}}\right)}$$

where

f'_c = concrete cylinder strength

p_{cr} = elastic buckling stress

$$= \frac{\pi^2}{12\ (1-\nu^2)} \left(\frac{a}{b} + \frac{b}{a}\right)^2 \frac{E}{\left(\frac{b}{h}\right)^2}$$

C = experimental coefficient

= 3.0 (as proposed by Ernst)

EXPERIMENTAL SETUP

The test plates considered were rectangular in shape, measuring 4 ft. by 8 ft. (1.22 m by 2.44 m), with thicknesses of 1 in. (2.54 cm), 1 1/4 in. (3.18 cm), and 3/4 in. (1.89 cm). Reinforcing of the plates was in the form of two-way mesh made of No. 12 wire (0.105 in. [2.667 mm] in diameter) with a yield point of 76,800 psi (5.31×10^5 kN/m^2). The mesh was placed in one or two layers with steel ratios, $(A_s/bh) \times 100$, of 0.20, 0.50, 0.75, and 1.00 per cent. Two standard 6 in. (15.24 cm) diameter by 12 in. (30.48 cm) test cylinders were made for each plate, and tested on the day of the plate test (28th day from casting). Complete plate and cylinder properties are listed in Tables 1 and 2.

The plates were tested in a load frame with boundary conditions designed so that the edges of the plate were free to rotate, but with no displacement normal to the edges of the plate allowed. This meant, essentially, that the plates were simply supported on all edges. The load was applied along the short edges of the specimens. Dial gages and resistance strain gages were attached in various configurations, and the load applied axially in compression, as free from eccentricity as possible. Readings of deflections and strains were taken at various load levels until collapse occurred. For comprehensive explanations of the plate fabrication techniques, testing equipment, and testing procedures, see (4) and (6).

Table 1 - Plate Properties

Plate Number (1)	Average thickness, in inches (2)	Steel ratio, in per cent (3)	Number of steel layers (4)
1	0.996	0.20	1
2	1.000	0.20	1
3	1.010	0.50	2
4	1.005	0.50	2
5	1.00	0.75	2
6	1.04	0.75	2
7	0.99	1.00	2
8	0.97	1.00	2
9	1.25	0.20	1
10	1.25	0.20	1
11	1.255	0.50	2
12	1.243	0.50	2
13	1.25	0.75	2
14	1.27	0.75	2
15	1.28	1.00	2
16	1.24	1.00	2
17	0.757	0.20	1
18	0.763	0.20	1
19	0.757	0.50	1
20	0.747	0.50	1
21	0.76	0.75	1
22	0.758	0.75	1
23	0.763	1.00	1
24	0.782	1.00	1

Note: 1 in. = 2.54 cm.

Table 2 - Concrete Properties

Plate Number (1)	Average cylinder strength, f'_c, in pounds per square inch (2)	Average strain at f'_c, ε_o, in inches per inch x 10^{-3} (3)
1	3896	2.10
2	3802	1.92
3	3156	1.93
4	3430	1.69
5	3298	1.80
6	3546	2.30
7	3688	1.89
8	3201	1.80
9	2564	1.94
10	2653	1.76
11	2414	1.75
12	2600	2.40
13	2546	2.00
14	2873	1.87
15	2882	1.92
16	2590	2.02
17	3272	1.89
18	3386	1.72
19	3448	1.88
20	3546	1.98
21	3626	2.09
22	3590	1.98
23	3396	1.67
24	3917	1.87

Note: 1 psi = 6.89 kN/m^2.

EXPERIMENTAL RESULTS

The number of plates tested in the project was twenty-four, with properties as listed in Table 1. The plate thickness was an average value of the thickness measured at six different points on the plate. The steel ratio is listed in per cent, and the number of steel layers one or two.

The results of the tests on the standard test cylinders are listed in Table 2. Two cylinders were made and tested for each plate, and the values of the cylinder strength, f'_c, and the strain at f'_c, ε_o, are average values for these two cylinders. The design strengths for plates numbered 1 through 8 (1 in. [2.54 cm] thickness) and 17 through 24 (3/4 in. [1.89 cm] thickness) was 3,000 psi (2.067×10^4 kN/m^2), and 2,500 psi (1.723×10^4 kN/m^2) for plates numbered 9 through 16 (1 1/4 in. [3.18 cm] thickness).

Deflection profiles along the vertical centerlines for plates numbered 1 through 24 are shown in Appendix A, Figures A1 through A24. The deflections are adjusted values, that is, the values at the edges of the plates were adjusted to zero, so that all displacements were relative to the edges. A deflection profile is given for each load level at which deflection readings were taken. The actual loads at these load levels are listed in Table A1. The deflection profiles for the 3/4 in. (1.89 cm) plates (plates numbered 17 through 24)

show that buckling was by bulging into two or three panels. The 1 in. (2.54 cm) plates (plates numbered 1 through 8) buckled into both one and two panels. The 1 1/4 in. (3.18 cm) plates (plates numbered 9 through 16) all buckled into one panel. The reason for the varying buckling geometries is probably related to the difference in the relative bending stiffnesses of the plates. Most of the plates that buckled into more than one panel displayed contraflexure points that were relatively stable in location until the onset of buckling. The mode of buckling of all the panels was that of plate buckling (biaxial curvature), versus that of column buckling (uniaxial curvature). It should be noted that the deflection profile for plate number 5 (Figure A5) is incomplete. This was due to equipment difficulties which prevented deflection readings from being recorded for load levels 1 through 7. The adjusted profile for plate number 5 was set to zero at load level 8.

The centerline deflection profiles were used in making Southwell plots for each plate. The Southwell method involved determining the location of the largest deflection, and plotting deflection versus deflection/load, the inverse slope of the resulting straight line being the buckling load according to Timoshenko and Gere (7). Southwell plots for plates numbered 1 through 4 and 6 through 24 are presented in Appendix B, Figures B1 through B23. A Southwell plot for

plate number 5 is not presented due to the incompleteness of the deflection data. The value of the buckling load determined by this method is shown on each plot.

The last technique employed in determining the buckling loads was the utilization of the strain versus load plots at the strain gages closest to the point of the largest deflection. In the majority of cases, the strain on the "tension" face of the plate became less compressive at a distinct point, that point being the buckling load. Strain versus load plots are presented in Appendix C, Figures C1 through C20. Plots are lacking for plates numbered 1, 4, 5, and 6, due to their failure to show any distinct change on the part of the strain gages before collapse.

In determining the experimental buckling load, P_{cre}, the primary method used was that of the strain versus load plots. The reasons for this were numerous, as given in (6). The deflection profiles were inconclusive in showing any distinct change at the buckling load for most of the plates, due to the presence of unavoidable eccentricities in the loading. The effects of the eccentricities were very difficult to determine so that they could not readily be seen in the profiles. The Southwell plots yielded definite values for the experimental buckling loads, but in all cases except plate number 2, this load was higher in value than the experimental collapse load. The applicability of

Southwell's method in the present case is questionable (6) due to the fact that reinforced concrete is not a linearly elastic material. This method was developed for a linearly elastic material, as shown by Timoshenko and Gere (7), so that it is not surprising that the buckling loads obtained using it were not of acceptable accuracy. In all the cases for which the strain versus load plots yielded a distinct buckling load, this load was used. For the plates for which a strain versus load plot did not yield conclusive buckling loads, the other methods were utilized. For plates numbered 1 and 4, Southwell plots were available, and these were used in determining the buckling load. For plate number 5, for which the Southwell plot was not available, and plate number 6, the deflection profiles were used. For these plates, however, the deflection profiles did show definite points at which buckling appeared to occur, and these values were used. The values of the experimental buckling loads, P_{cre}, and the collapse loads, P_f, are shown in Table 3.

Table 3 - Comparison of the Buckling Results With the Tangent Modulus Formula

Plate number (1)	Experimental buckling load, P_{cre}, in Kips (2)	Collapse load, P_f, in Kips (3)	Tangent modulus buckling load, P_{crt}, in Kips (5) (4)
1	125.5[a]	110.2	116.0
2	100.4	113.9	119.0
3	90.6	99.9	105.0
4	125.7[a]	120.1	118.0
5	130.2[b]	140.2	113.0
6	133.4[b]	155.5	119.0
7	130.0	143.9	124.0
8	100.8	102.3	106.0
9	116.0	140.7	116.0
10	140.0	156.5	123.0
11	120.4	143.1	120.0
12	120.2	143.8	119.0
13	100.2	115.1	128.0
14	129.9	161.0	148.0
15	150.1	172.3	155.0
16	130.6	162.3	134.0
17	80.4	96.5	59.0
18	80.1	89.1	65.5
19	70.1	84.9	63.1
20	75.3	83.8	61.0
21	75.6	82.8	63.2
22	70.0	80.0	64.4
23	70.0	78.0	68.9
24	80.0	90.0	78.3

Note: 1 Kip = 4.448 kN
[a]Obtained from the Southwell Method
[b]Obtained from the Deflection Plot

Table 3 - Comparison of the Buckling Results With the Tangent Modulus Formula (Continued)

Plate number	$\frac{P_{cre}}{P_{crt}}$	$\frac{P_f}{P_{crt}}$	$\frac{P_f}{P_{cre}}$	Buckling stress in concrete, f_{cr}, in psi	$\frac{f_{cr}}{f'_c}$
(5)	(6)	(7)	(8)	(9)	(10)
1	1.08[a]	0.95	0.88[a]	2575[a]	0.661[a]
2	0.84	0.96	1.13	2065	0.543
3	0.86	0.95	1.10	1806	0.572
4	1.07[a]	1.02	0.96[a]	2530[a]	0.739[a]
5	1.15[b]	1.24	1.08[b]	2550[b]	0.773[b]
6	1.12[b]	1.31	1.16[b]	2470[b]	0.696[b]
7	1.05	1.16	1.11	2590	0.702
8	0.95	0.96	1.01	2050	0.641
9	1.00	1.21	1.21	1908	0.745
10	1.14	1.27	1.12	2275	0.866
11	1.00	1.19	1.19	1922	0.798
12	1.01	1.21	1.20	1924	0.740
13	0.78	0.90	1.15	1565	0.614
14	0.88	1.09	1.24	2027	0.706
15	0.97	1.11	1.15	2265	0.785
16	0.97	1.21	1.24	2030	0.785
17	1.36	1.64	1.20	2185	0.668
18	1.22	1.36	1.11	2160	0.638
19	1.11	1.34	1.21	1872	0.543
20	1.23	1.37	1.11	2040	0.575
21	1.20	1.31	1.10	2070	0.572
22	1.09	1.24	1.14	1854	0.516
23	1.02	1.13	1.11	1805	0.531
24	1.02	1.15	1.12	2010	0.513

Note: 1 psi = 6.89 kN/m^2

[a]Obtained from the Southwell Method

[b]Obtained from the Deflection Plot

CORRELATION OF EXPERIMENTAL RESULTS WITH THEORY

The major part of the correlation of the experimental results involved the experimental buckling loads. These loads were compared with different theoretical approaches and a determination was made as to the most accurate of these theories. The four approaches considered by Swartz and Rosebraugh (5) are examined here, as well as a determination of the validity of the "Rankine-Gordon" formula as proposed by Ernst (2). In order to decide upon the most applicable theory, it was necessary to non-dimensionalize the buckling parameters. To get an accurate comparison between the results of the plate experiments and those predicted by the theories, the concrete buckling stresses obtained experimentally, f_{cr}, were non-dimensionalized by dividing them by the average cylinder strength, f'_c, and the plate widths b, were non-dimensionalized by dividing them by the plate thicknesses, h. The experimentally obtained concrete buckling stresses and the f_{cr}/f'_c ratios for the plates are listed in Table 3. These ratios were averaged for each pair of plates and plotted in Figure 1. Also plotted were the representations of the four theoretical approaches given by Eqs. (3) through (7). It is apparent, upon inspection of Figure 1, that all but one of the average experimental values fall above the curve representing the isotropic-tangent modulus theory, whereas the representations

THIS BOOK CONTAINS NUMEROUS PAGES WITH DIAGRAMS THAT ARE CROOKED COMPARED TO THE REST OF THE INFORMATION ON THE PAGE.

THIS IS AS RECEIVED FROM CUSTOMER.

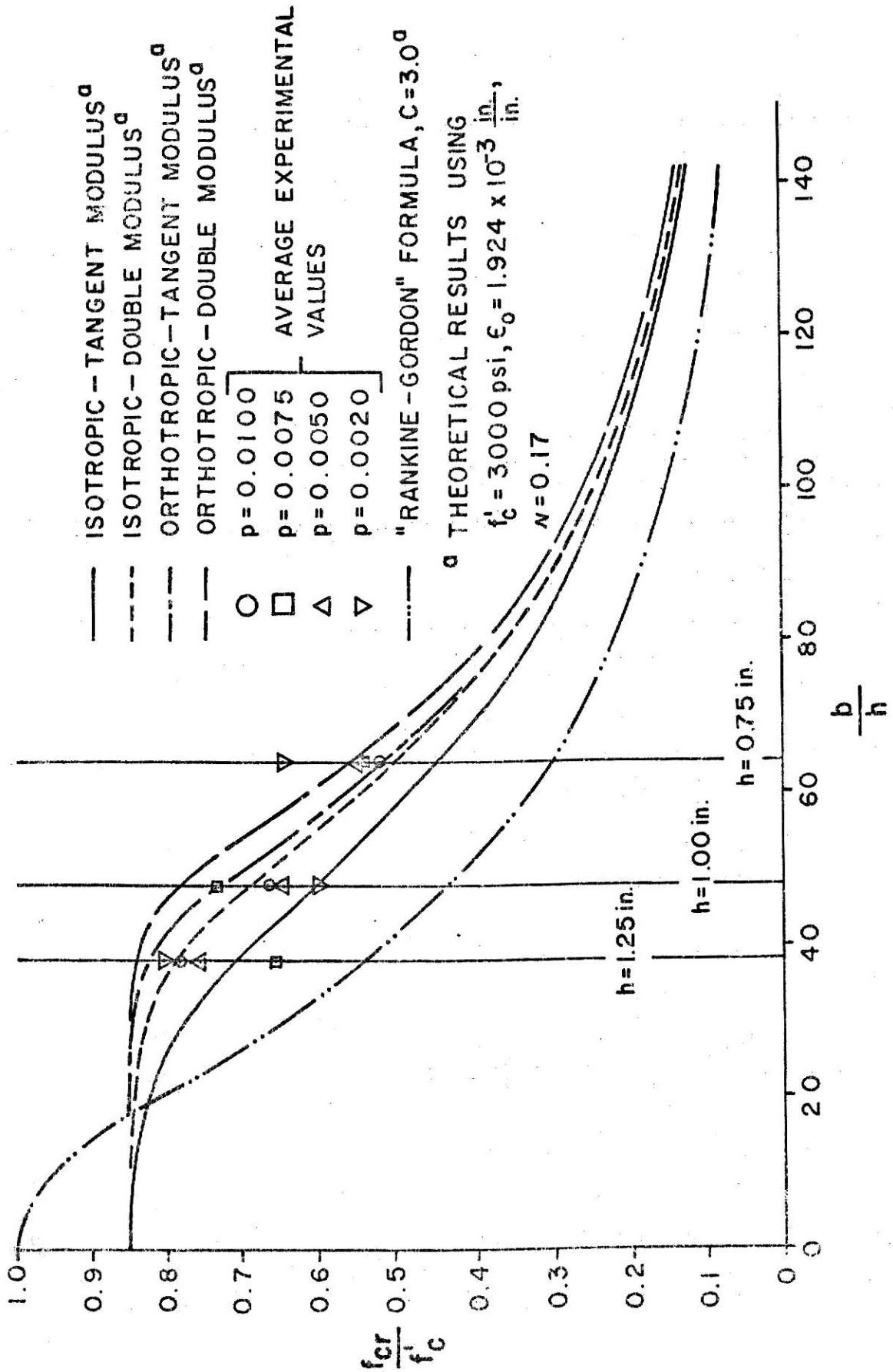

Figure 1 - Concrete Buckling Stress Versus Plate Thickness - Comparison of Experimental Results with Various Formulas (1 in. = 2.54 cm; 1 psi = 6.89 kN/m^2)

of the orthotropic-tangent modulus, isotropic-double modulus, and orthotropic-double modulus theories all appear to be unconservative and exceed the majority of the average experimental values. Therefore, the isotropic-tangent modulus theory has been selected as being the most accurate depiction of the plate buckling behavior.

The correlation with the "Rankine-Gordon" formula Eq. (9), as proposed by Ernst, was made in a similar manner as with the theoretical approaches. Concrete buckling stresses obtained from the "Rankine-Gordon" formula using the initial tangent modulus for E, were non-dimensionalized and plotted on Figure 1. The experimental constant, C = 3.0, proposed by Ernst was used, and it is obvious, that while the average experimental values are all well above the curve, the formula is overly conservative as compared to the isotropic-tangent modulus theory.

The isotropic-tangent modulus theory being chosen as the most precise of the approaches, further correlations were made with the experimental results. The theoretical values of the tangent-modulus buckling loads, P_{crt}, were determined for each plate, and are listed in Table 3. Ratios of P_{cre}, the experimental buckling loads, to P_{crt} were calculated for each plate, and plotted as shown in Figure 2. It is obvious from the plot that the tangent modulus theory is on the conservative side as compared to

the experimental buckling loads, the coefficient of variation being 13 per cent. The difference is not large considering the norms for experimental work. Another correlation was made between the experimental collapse loads, P_f, and P_{crt}. The ratios are listed in Table 3 and the results plotted in Figure 3. This plot points out the fact that the experimental collapse loads are generally above the tangent modulus buckling loads, an important consideration in terms of safety. The coefficient of variation was 14 per cent. Figure 3 helped to finalize the conclusion that the tangent modulus theory was precise, yet conservative, a major prerequisite for any further attempt to develop a practical design formula.

Two further correlations were made. The experimental collapse loads were compared with the experimental buckling loads in order to determine the post-buckling strength increase. The ratios of P_f/P_{cre} are listed in Table 3. These ratios show that, with the exceptions of plates numbered 1 and 4, the buckling loads were below the collapse loads. Plates numbered 1 and 4 did not conform because the buckling loads were obtained from the Southwell plots, which are thought to be unconservative. These results indicate that a post-buckling strength increase, while slight, is nevertheless present.

The final correlation made was that of the non-dimensionalized concrete buckling stresses with the total steel ratio.

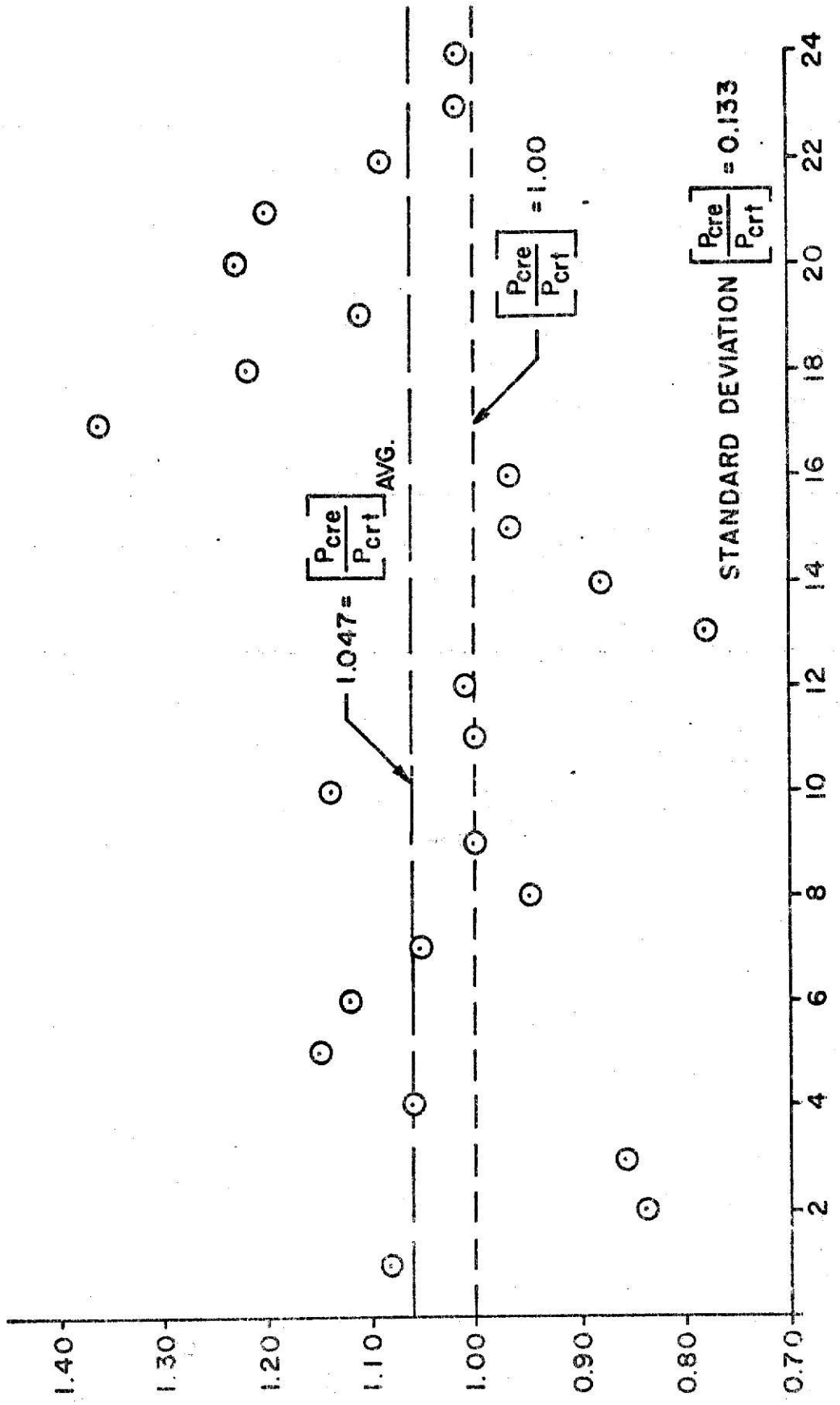

Figure 2 - P_{cre}/P_{crt}

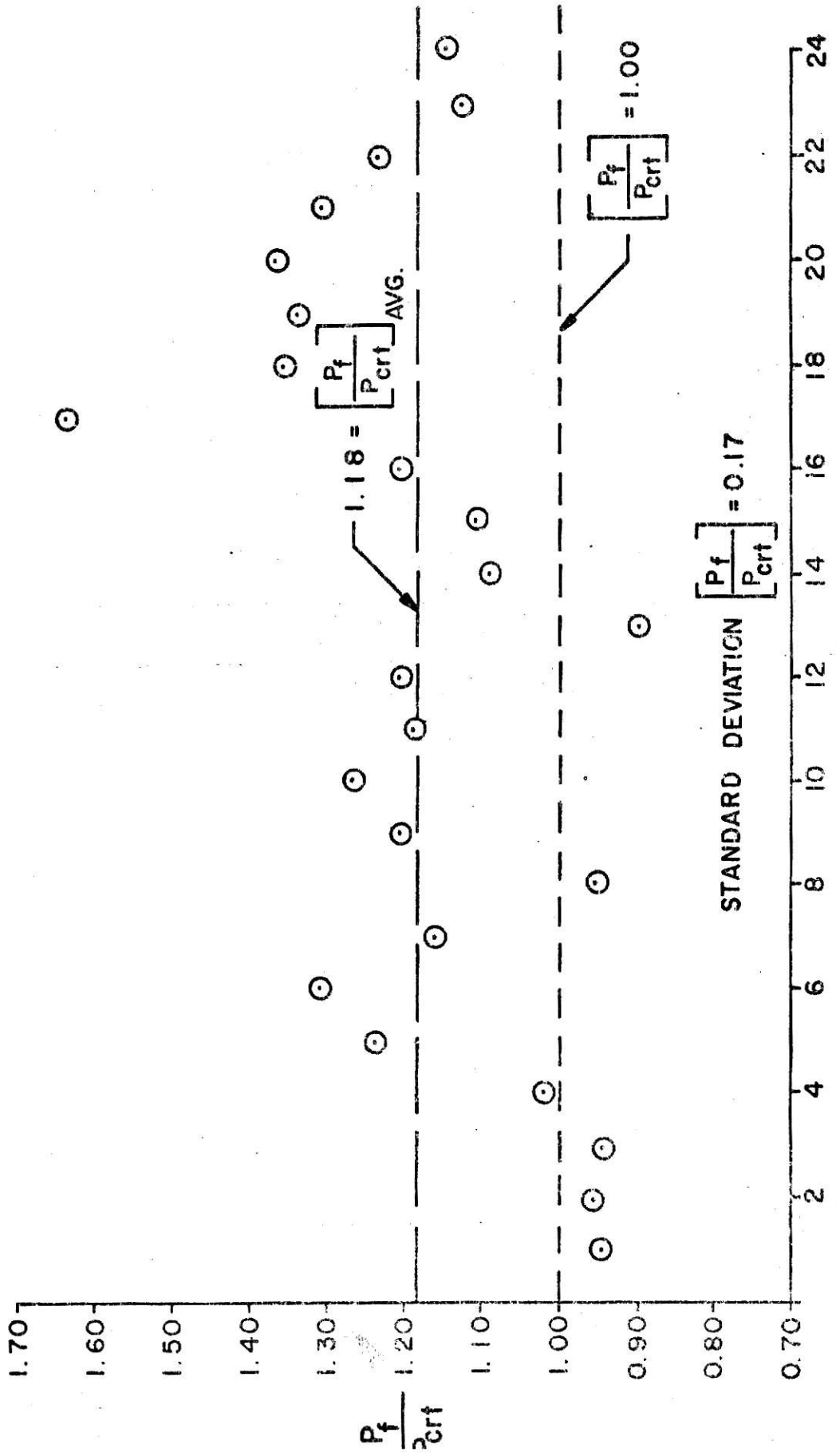

Figure 3 - P_f/P_{crt}

The comparison is shown in Figure 4. The average experimental values do not form any specific pattern, indicating that the total steel ratio did not influence the buckling stress to any large degree. The amount of steel present, however, would influence the behavior of a plate in other ways. A minimum total steel ratio would be required to satisfy temperature and shrinkage requirements. In addition, as shown by Figure 5, there is a definite relation between the total steel ratio and the ductility of the plates. Figure 5 presents a plot of load versus deflection for the 3/4 in. (1.89 cm) test plates at the point of largest deflection. It is observed that as the total steel ratio is increased, the maximum deflection achieved increases. This would indicate that as the total steel ratio increases, the ductility of a plate increases. The final relation of the total steel ratio to plate behavior is that if larger load carrying capacities are required, larger total steel ratios could be used.

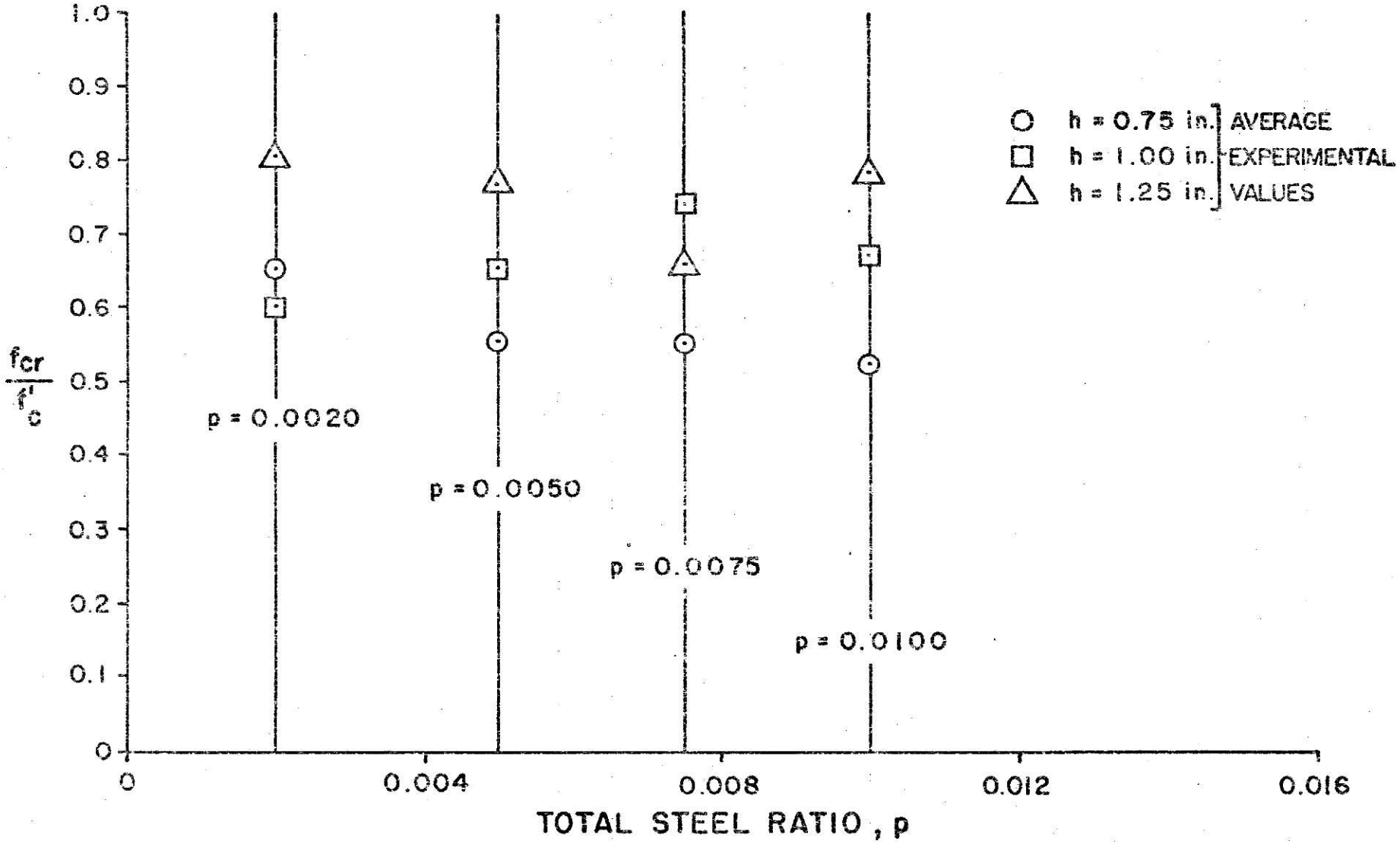

Figure 4 - Concrete Buckling Stress Versus Total Steel Ratio (1 in. = 2.54 cm)

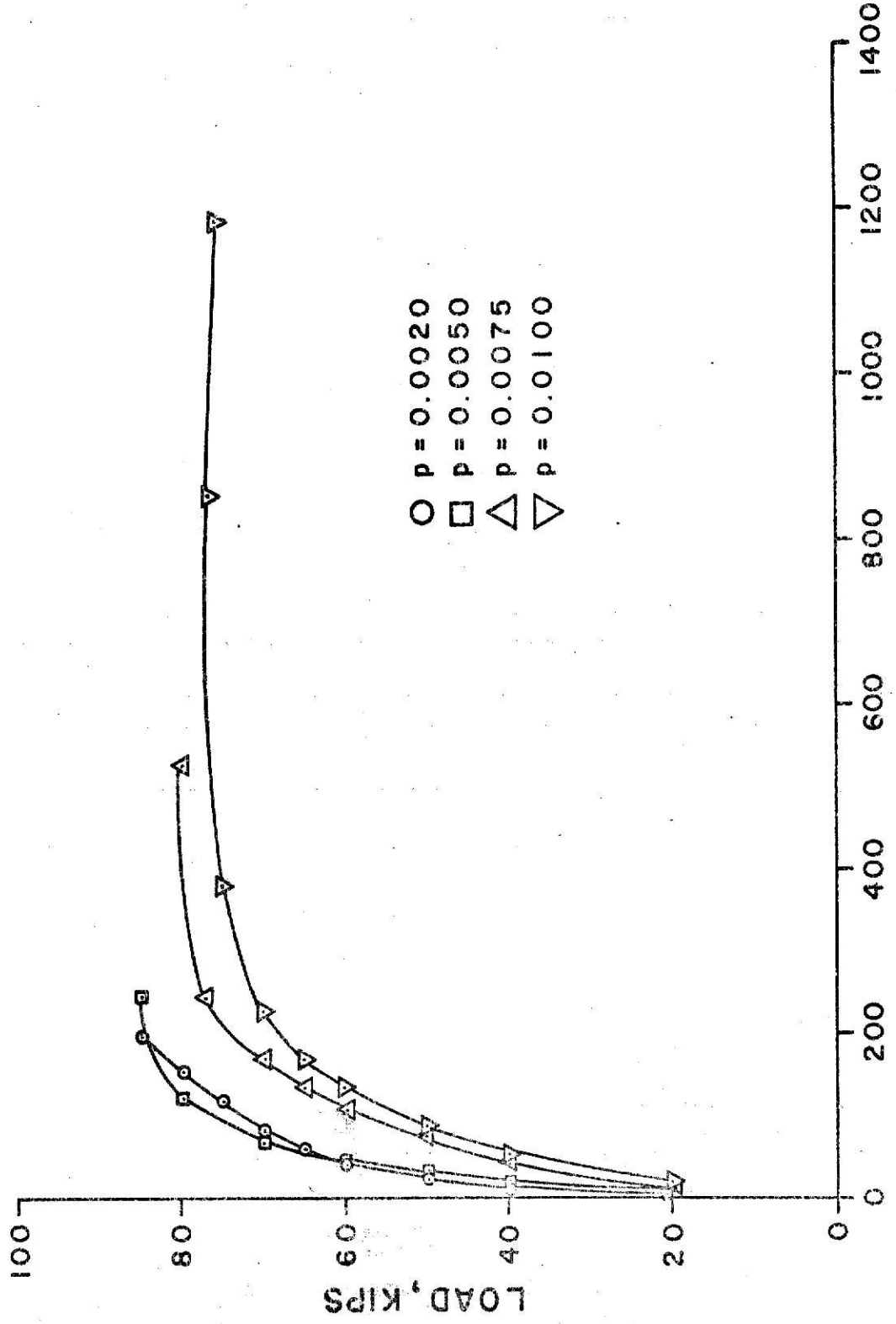

Figure 5 - Deflection Versus Load at Point of Maximum Deflection, 3/4 in. Plates
(1 in. = 2.54 cm; 1 Kip = 4.448 kN)

CONCLUSIONS

The principal method used in selecting the experimental buckling loads, that of the strain versus load plots, was found to be adequate. The centerline deflection profiles and the Southwell method failed to designate reasonable buckling loads. Due to the fact that it was necessary to use the Southwell plot method for two plates, and the deflection profile method for two plates, it should be noted that the results were accordingly affected to some degree.

The type of failure observed in the plates, biaxial curvature, was the correct mode, it being normally associated with plate buckling.

Of the four theoretical approaches considered, the isotropic-tangent modulus theory adequately predicted the buckling characteristics of the reinforced concrete plates. The variations of the tangent modulus theory from the experimental results, on the order of 13 per cent, was a reasonable deviation for experimental work of this kind. It is concluded that the isotropic-tangent modulus theory is an adequate basis from which to develop a practical design formula. The "Rankine-Gordon" formula as proposed by Ernst (2) was found to be unacceptable in adequately predicting the buckling behavior. Since it is basically an empirical equation, its failure does not propose any serious theoretical questions.

The effects of the total steel ratio were found not to be a major factor in determining concrete buckling stresses. It was shown, however, that increasing the total steel ratio would increase the ductility of the plates. In addition, total steel ratios affect temperature and shrinkage properties, as well as the total load carrying capacity.

The effects of loading eccentricity were difficult to determine, and were the reasons for the failure of the deflection profiles in determining the buckling. Since, in practical problems, eccentricities would be a major factor, further work in this area is also needed.

APPENDIX A

DEFLECTION PROFILES ALONG VERTICAL CENTERLINES

Table A1 - Load Levels

Plate number	Load level, in Kips						
	1	2	3	4	5	6	7
(1)	(2)	(3)	(4)	(5)	(6)	(7)	(8)
1	19.6	29.7	40.4	50.6	59.5	70.7	80.2
2	20.8	29.8	40.5	50.9	60.4	70.8	77.6
3	20.1	39.3	50.9	60.6	70.1	80.0	90.6
4	20.3	30.8	40.1	49.7	59.7	71.1	80.4
5	19.6	40.5	49.3	59.7	70.4	80.2	90.5
6	19.5	40.9	60.5	80.9	100.2	109.4	120.4
7	20.1	39.5	60.1	80.2	100.1	110.0	119.9
8	19.9	40.3	60.3	80.2	90.5	95.6	100.8
9	20.0	39.8	50.6	60.1	70.1	80.0	91.0
10	20.1	40.2	60.0	70.6	80.5	90.2	100.6
11	19.5	40.1	60.6	80.2	100.1	110.4	120.4
12	20.0	39.9	60.2	80.2	100.2	110.1	120.2
13	20.0	40.0	60.2	80.3	100.2	110.3	-----
14	19.9	40.0	60.4	81.0	100.3	110.1	120.2
15	20.0	39.9	60.0	80.3	100.6	110.5	120.5
16	20.3	39.7	60.5	80.3	100.3	110.6	120.5
17	20.4	29.9	40.1	50.2	55.1	60.2	65.4
18	21.1	40.4	50.0	60.1	55.4	70.1	75.2
19	20.8	39.8	50.0	60.2	70.1	80.2	84.9
20	19.6	40.3	50.1	60.2	64.9	70.2	75.3
21	20.1	40.1	50.0	60.1	65.2	70.0	75.6
22	20.2	40.1	49.9	60.0	65.2	70.0	76.7
23	20.1	40.0	50.0	60.0	65.0	70.0	75.0
24	20.0	40.0	50.0	60.0	65.0	70.0	75.0

Note: 1 Kip = 4.448 kN
Note: The symbol ----- denotes that deflection readings were terminated at that point.

Table A1 - Load Levels (Continued)

Plate number	Load level, in Kips					
	8	9	10	11	12	13
(9)	(10)	(11)	(12)	(13)	(14)	(15)
1	90.1	100.6	-----			
2	91.1	110.4	108.8	-----		
3	96.7	-----				
4	90.5	100.4	105.5	111.6	-----	
5	99.9	111.1	120.6	130.2	140.2	-----
6	126.1	133.4	140.0	-----		
7	130.5	-----				
8	-----					
9	100.0	110.6	-----			
10	110.2	120.0	124.6	-----		
11	130.2	-----				
12	-----					
13	-----					
14	129.9	-----				
15	130.4	140.1	150.1	-----		
16	130.6	140.6	-----			
17	70.5	75.4	80.4	84.6	90.4	95.8
18	80.1	84.5	-----			
19	-----					
20	80.3	-----				
21	80.2	-----				
22	80.0	-----				
23	76.9	76.5	-----			
24	80.0	85.0	90.0	-----		

Note: 1 Kip = 4.448 kN
Note: The symbol ----- denotes that deflection readings were terminated at that point.

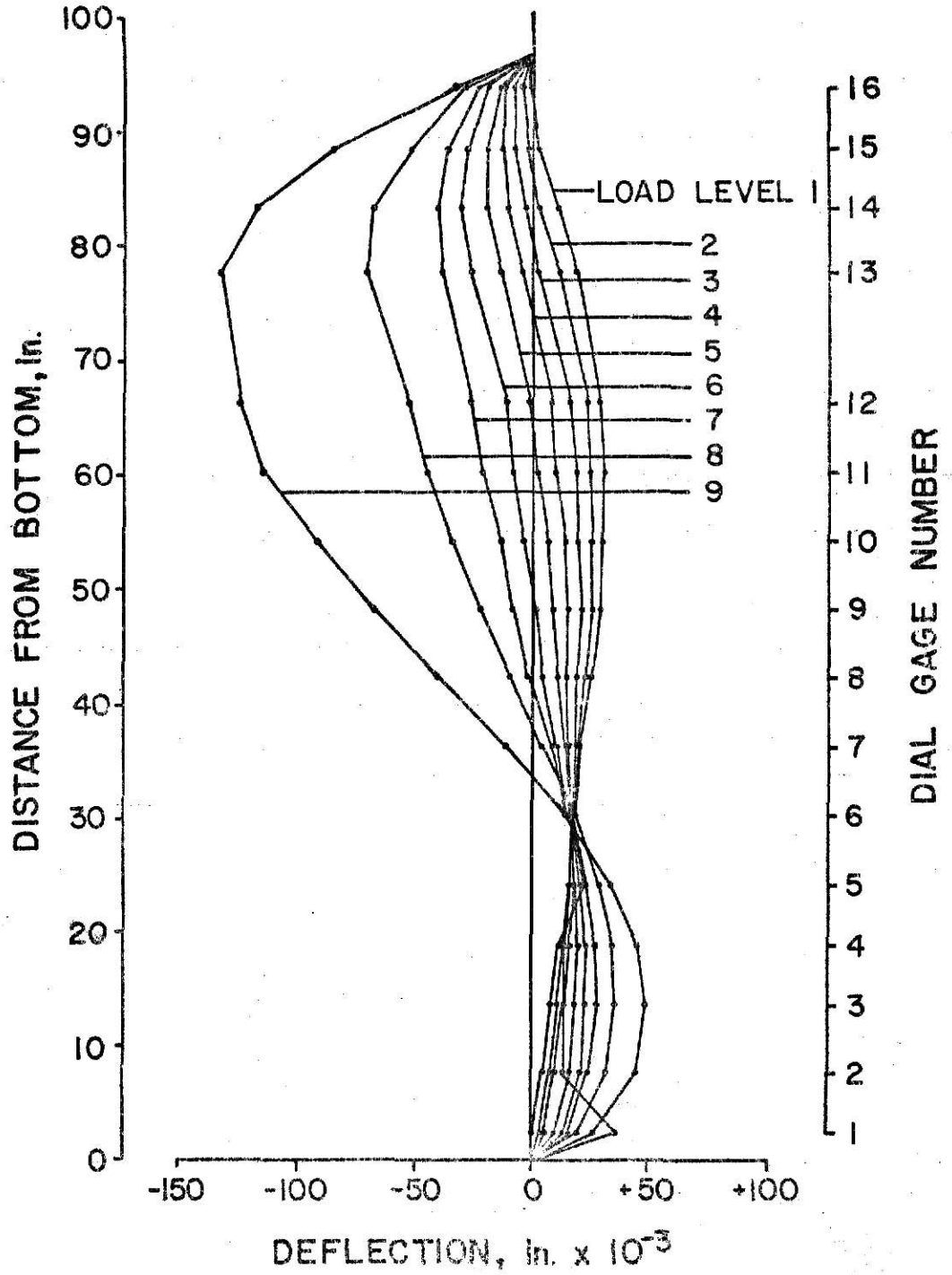

Figure A1 - Deflection Profile Along Vertical Centerline, Plate Number 1 (Adjusted Values) (1 in. = 2.54 cm.)

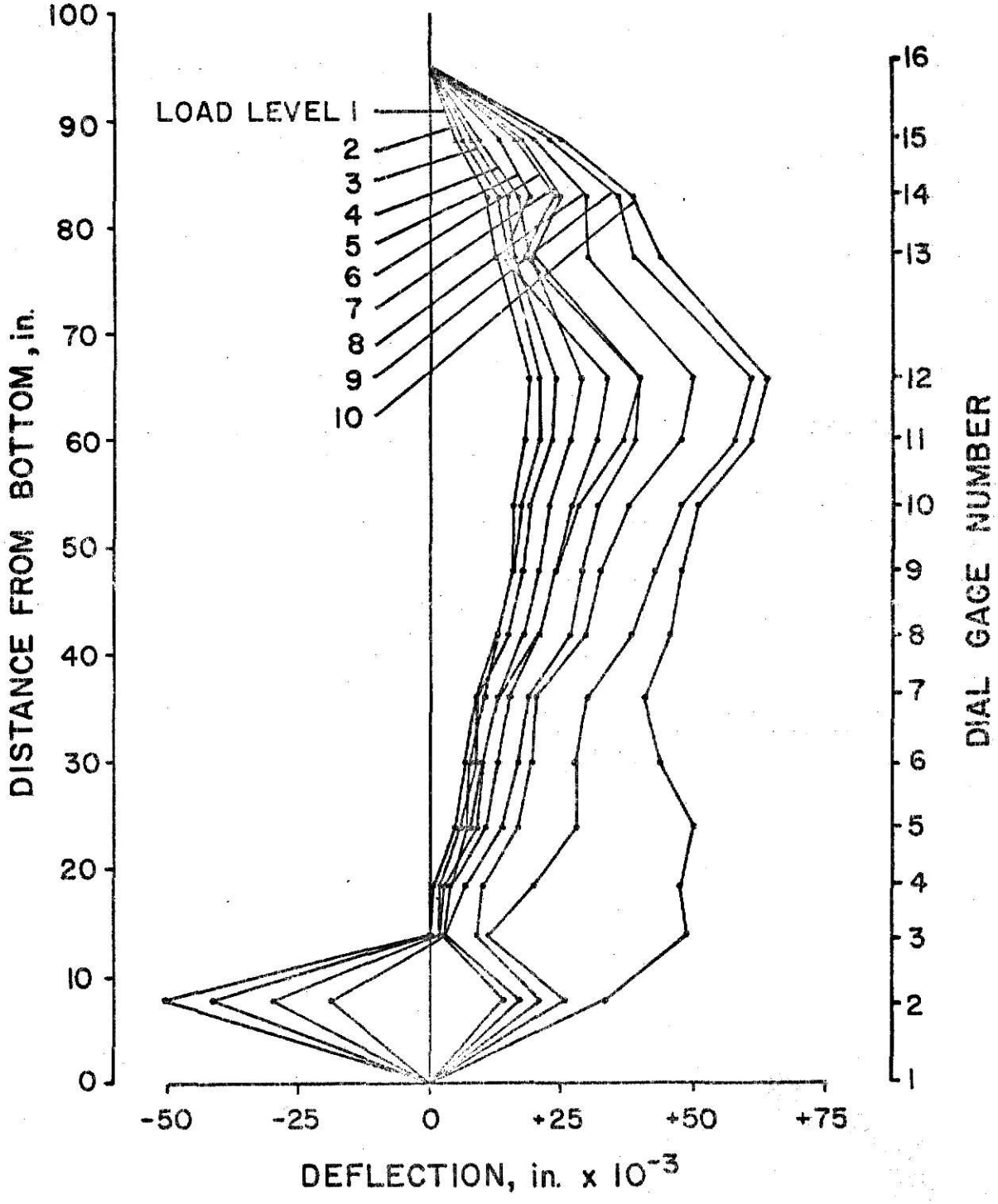

Figure A2 - Deflection Profile Along Vertical Centerline, Plate Number 2 (Adjusted Values) (1 in. = 2.54 cm.)

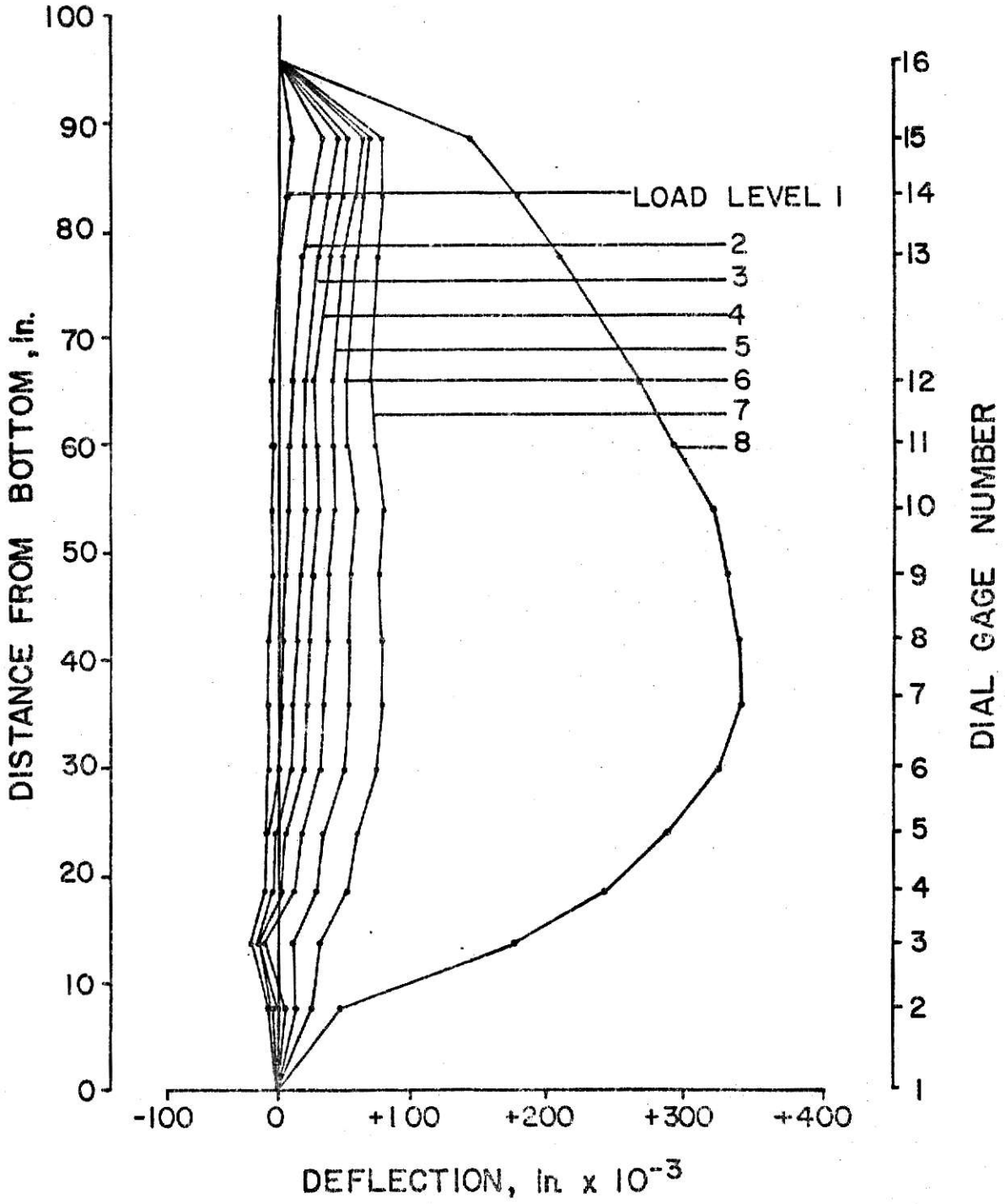

Figure A3 - Deflection Profile Along Vertical Centerline, Plate Number 3 (Adjusted Values)(1 in. = 2.54 cm.)

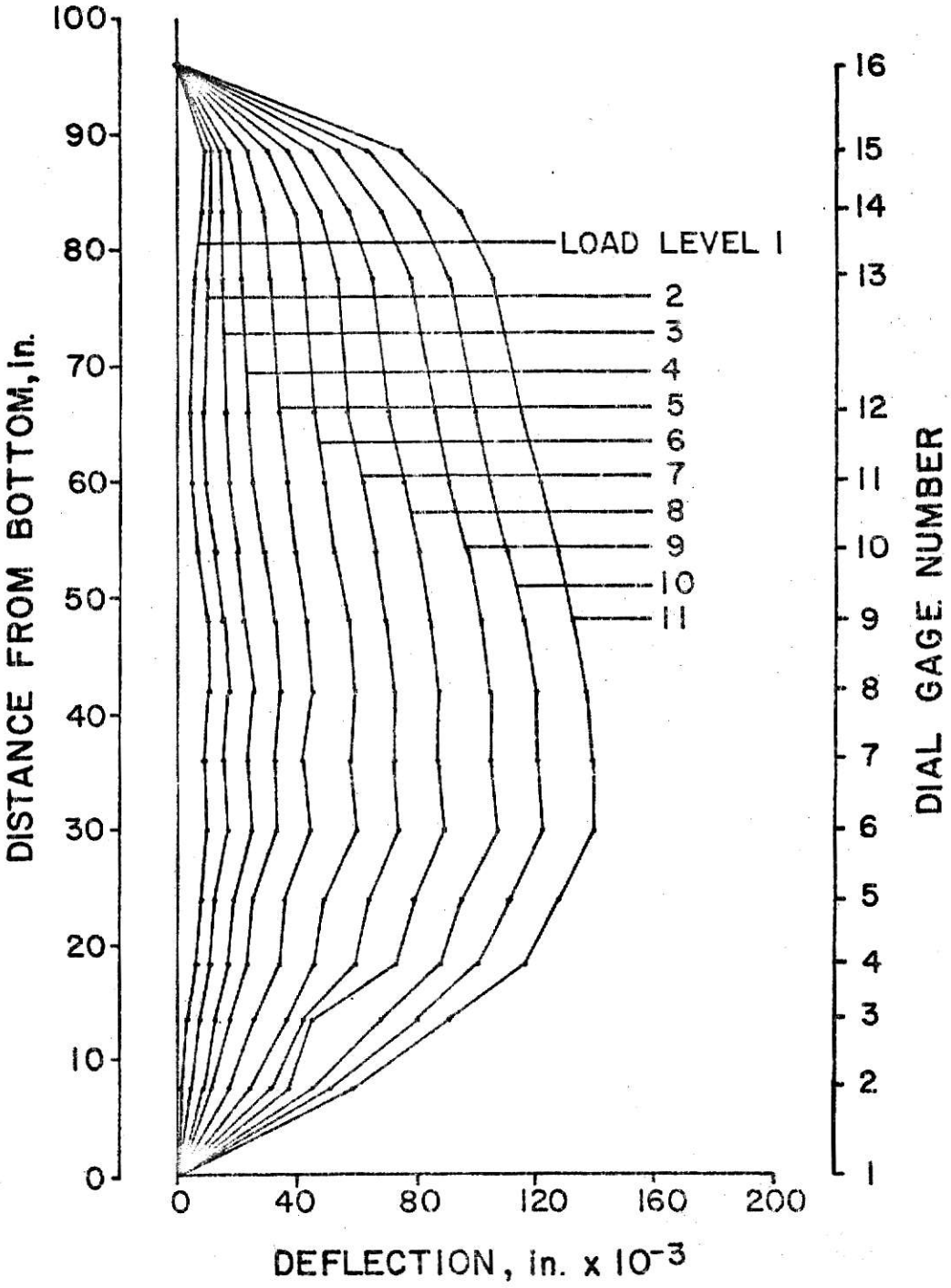

Figure A4 - Deflection Profile Along Vertical Centerline, Plate Number 4 (Adjusted Values)(1 in. = 2.54 cm.)

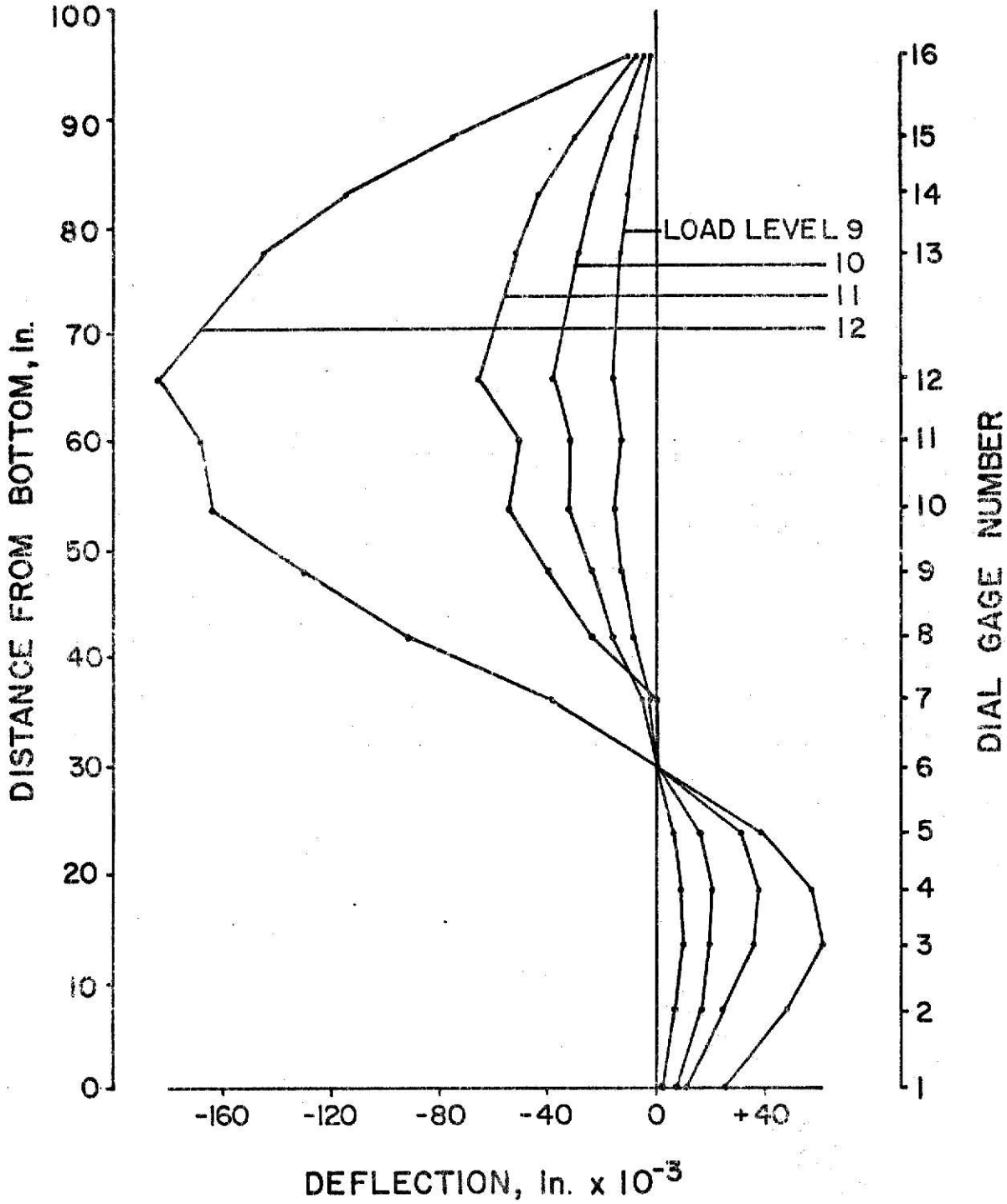

Figure A5 - Deflection Profile Along Vertical Centerline, Plate Number 5 (Unadjusted Values) (1 in. = 2.54 cm.)

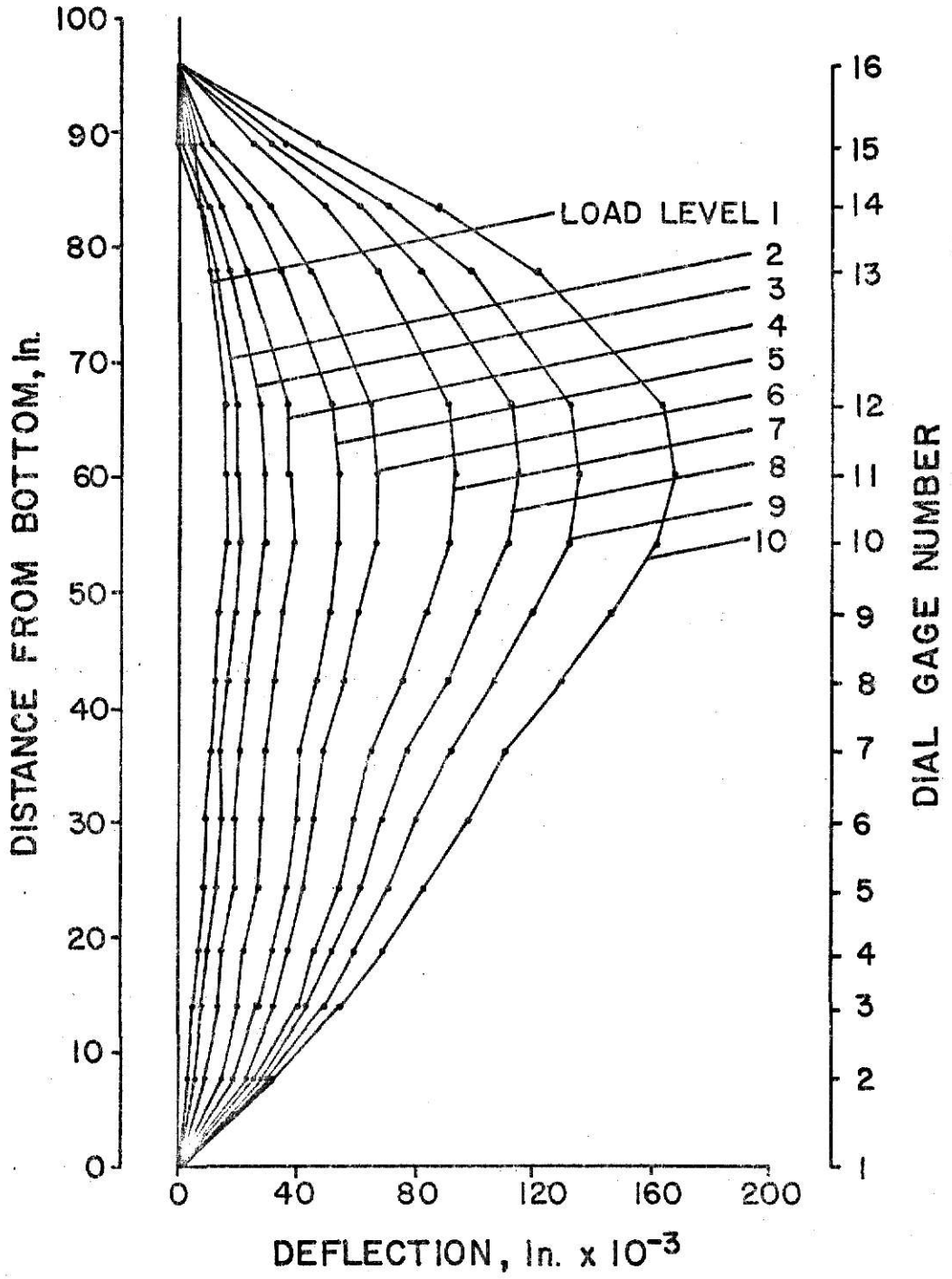

Figure A6 - Deflection Profile Along Vertical Centerline, Plate Number 6 (Adjusted Values) (1 in. = 2.54 cm.)

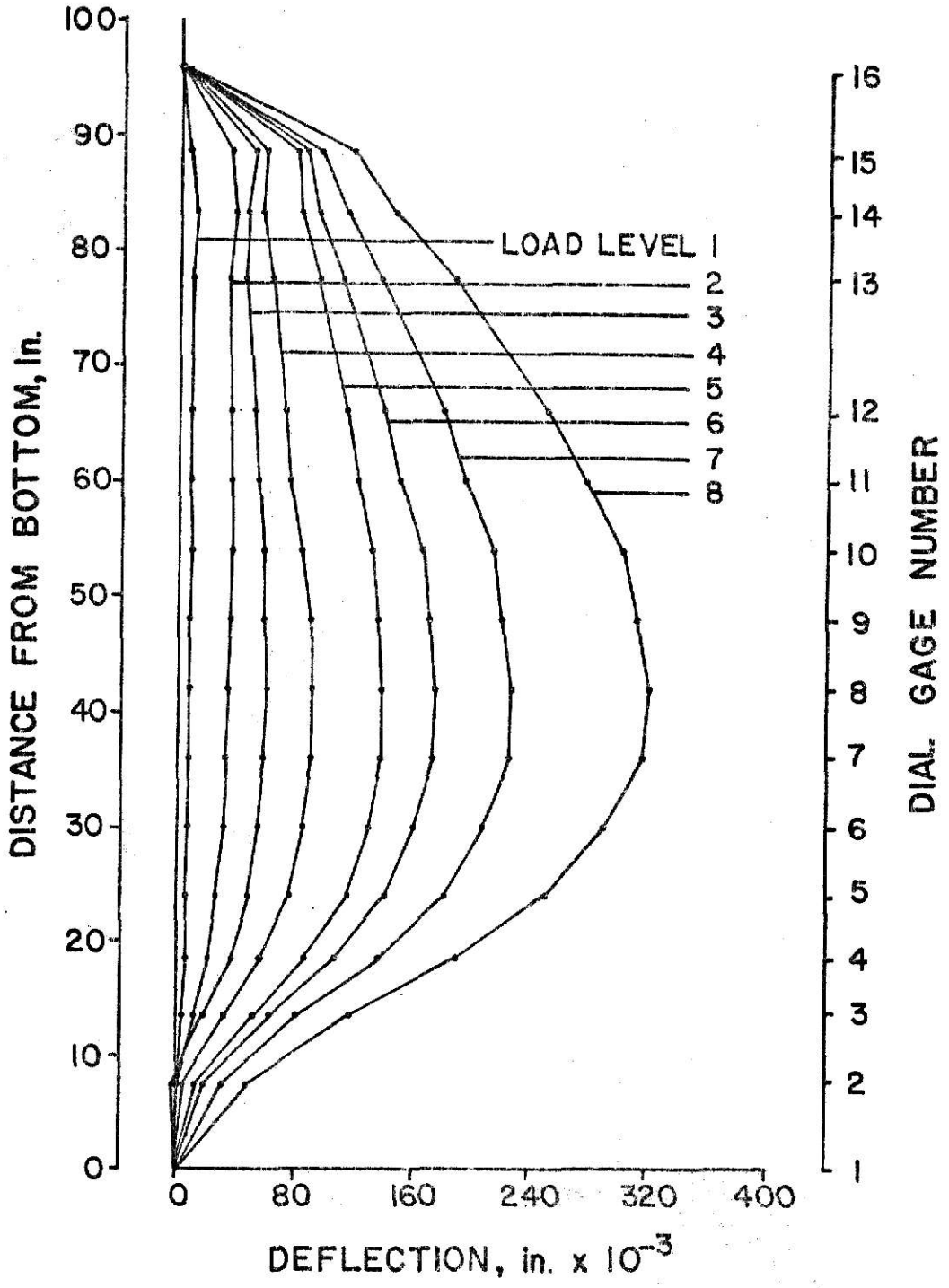

Figure A7 - Deflection Profile Along Vertical Centerline, Plate Number 7 (Adjusted Values)(1 in. = 2.54 cm.)

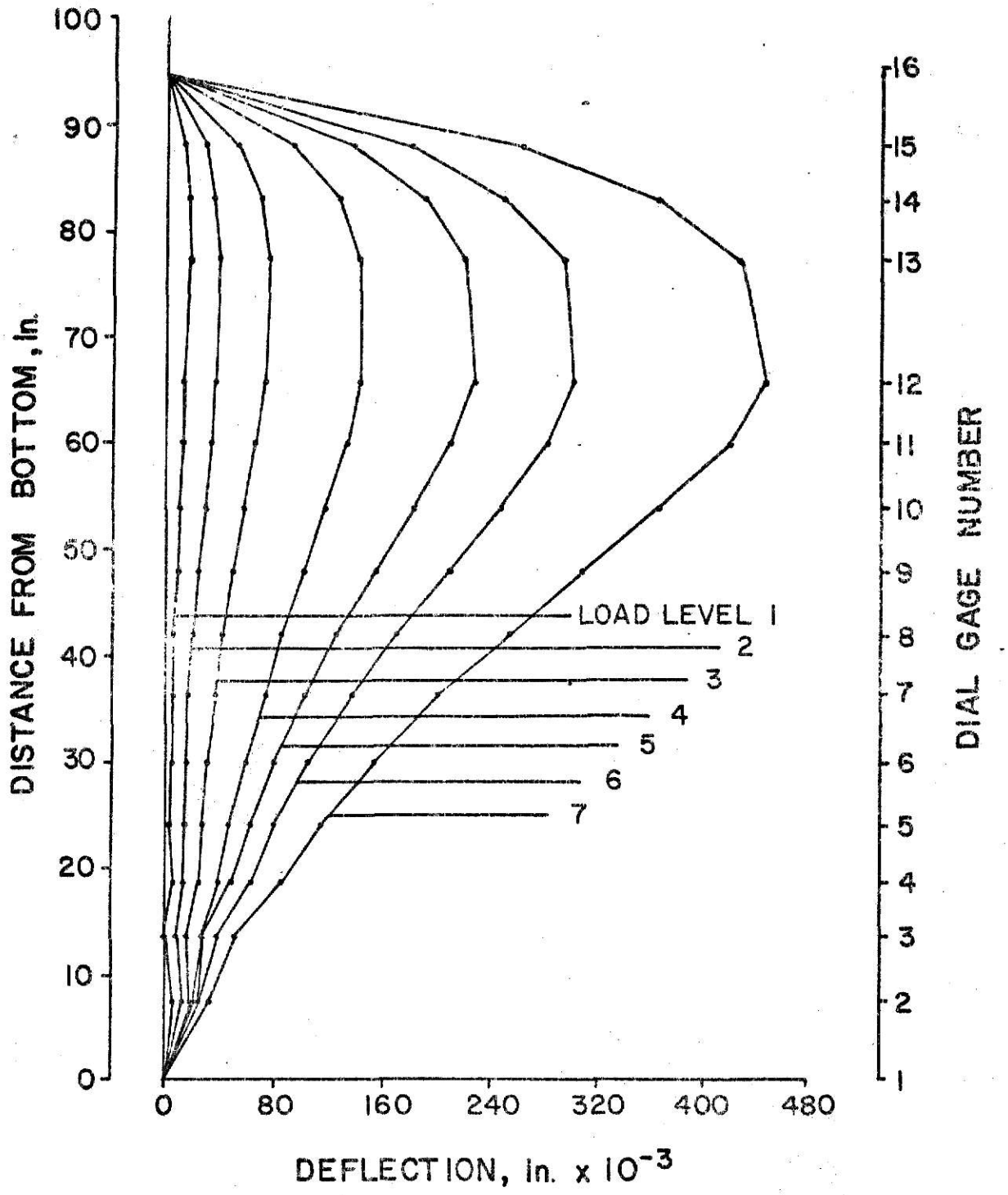

Figure A8 - Deflection Profile Along Vertical Centerline, Plate Number 8 (Adjusted Values)(1 in. = 2.54 cm.)

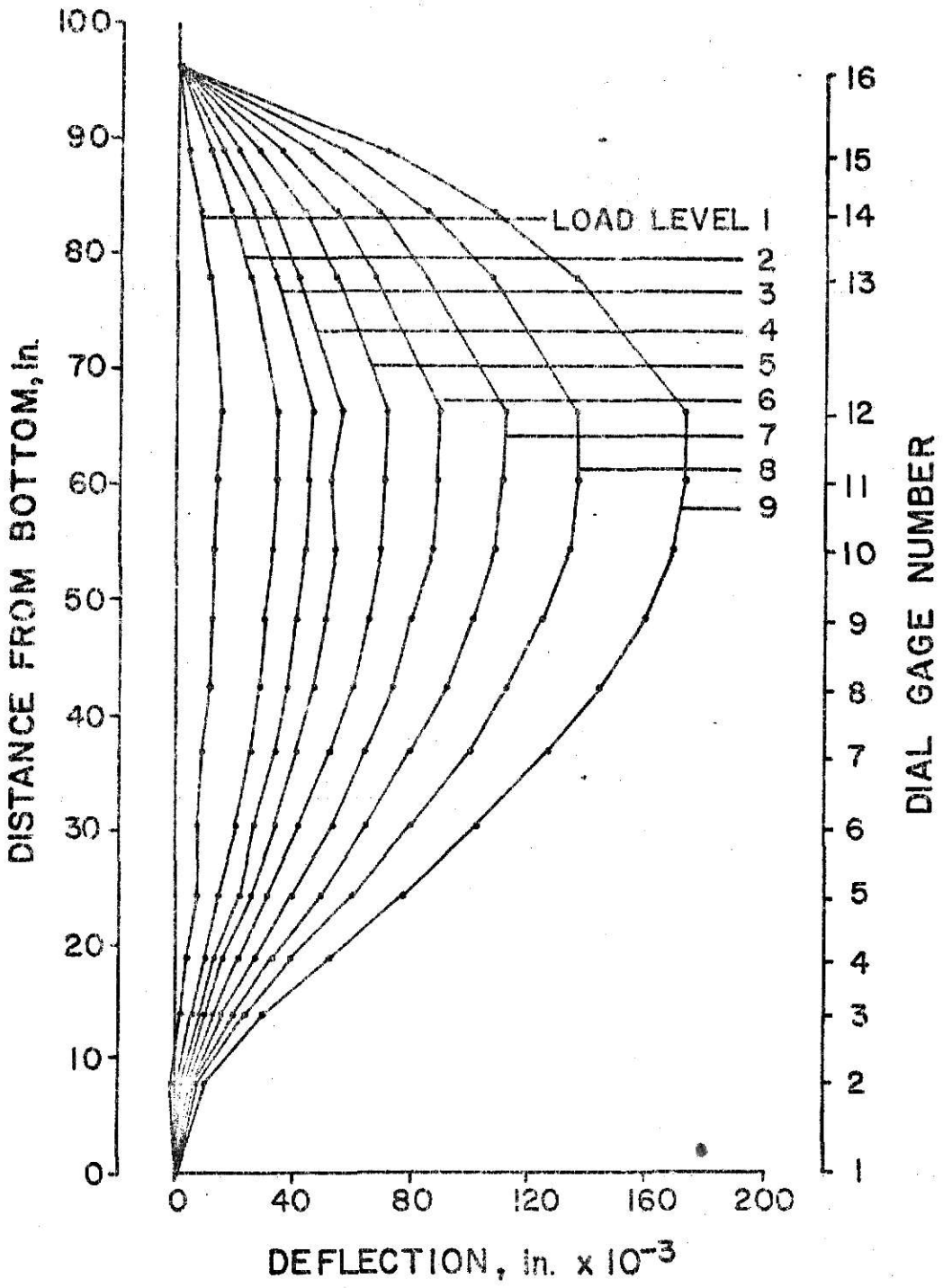

Figure A9 - Deflection Profile Along Vertical Centerline, Plate Number 9 (Adjusted Values)(1 in. = 2.54 cm.)

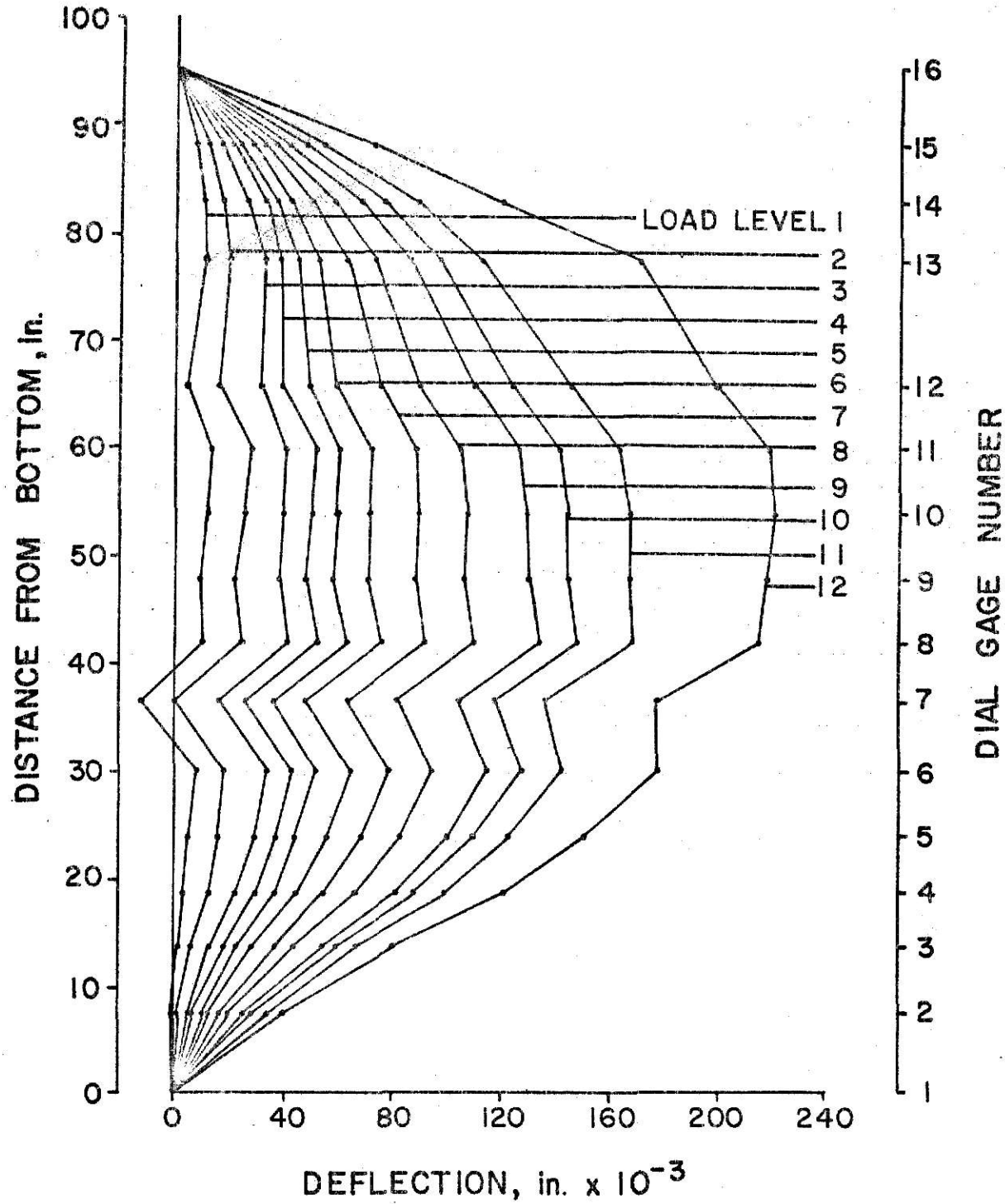

Figure A10 - Deflection Profile Along Vertical Centerline, Plate Number 10 (Adjusted Values) (1 in. = 2.54 cm.)

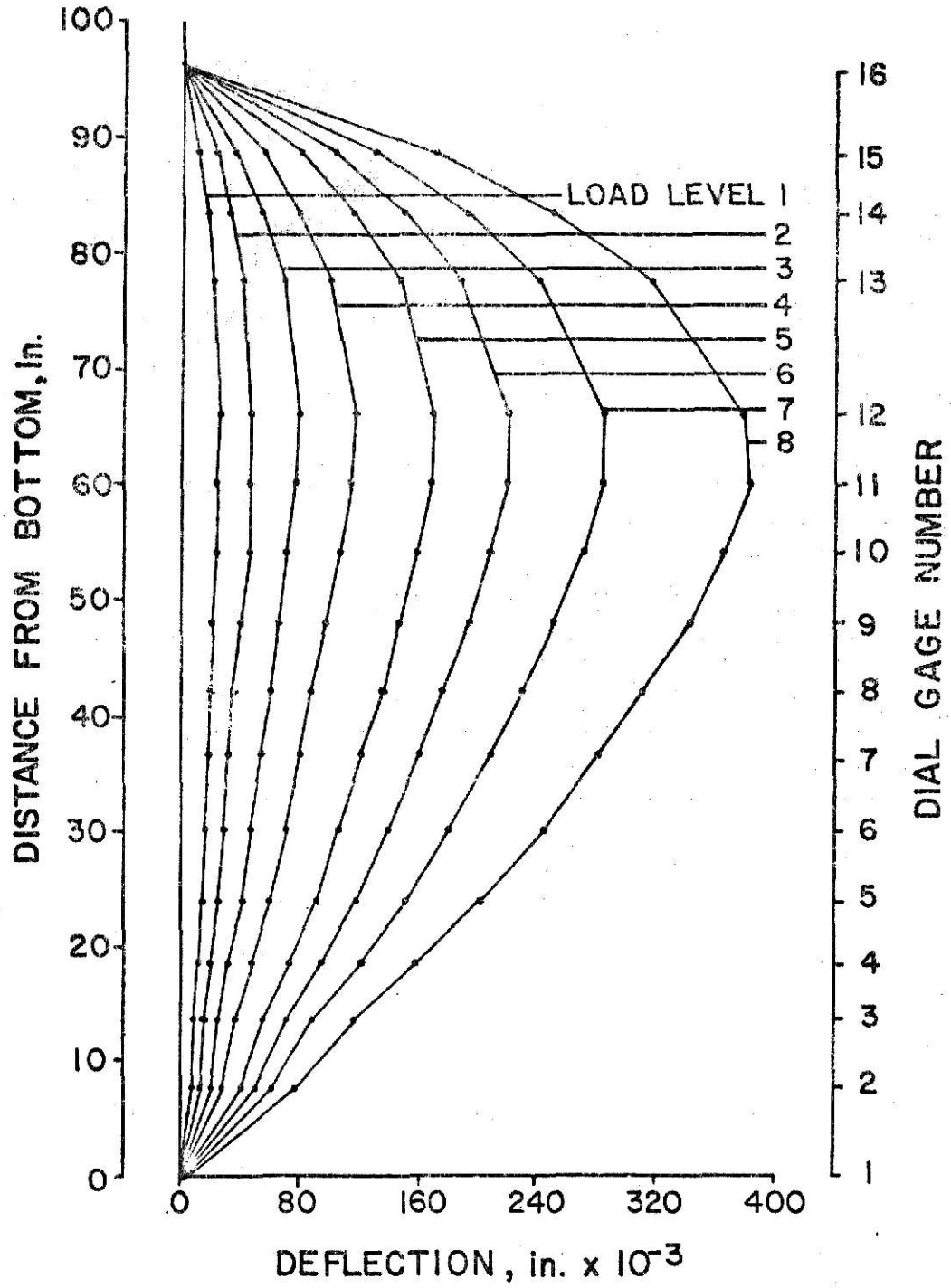

Figure A11 - Deflection Profile Along Vertical Centerline, Plate Number 11 (Adjusted Values)(1 in. = 2.54 cm.)

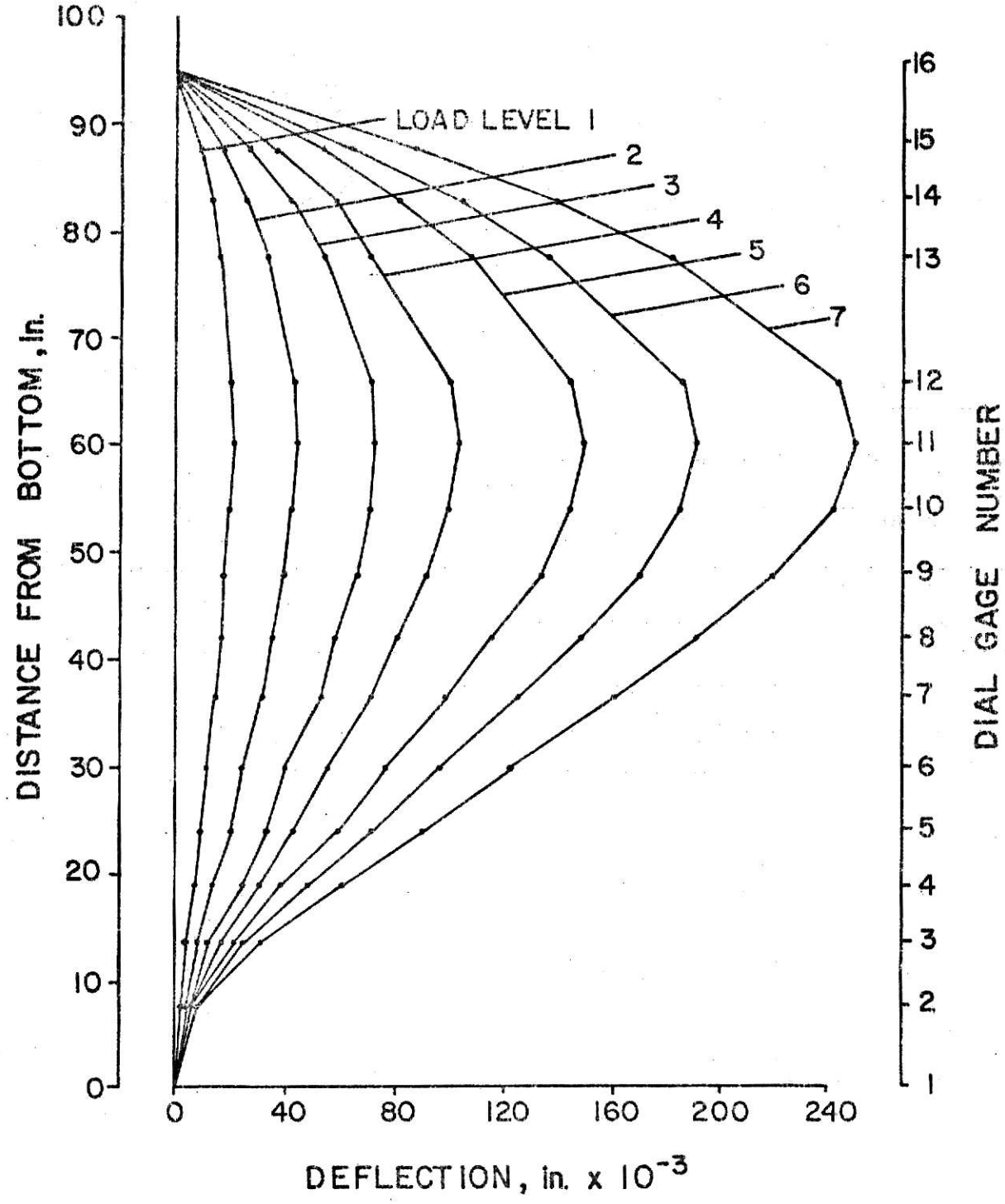

Figure A12 - Deflection Profile Along Vertical Centerline, Plate Number 12 (Adjusted Values)(1 in. = 2.54 cm.)

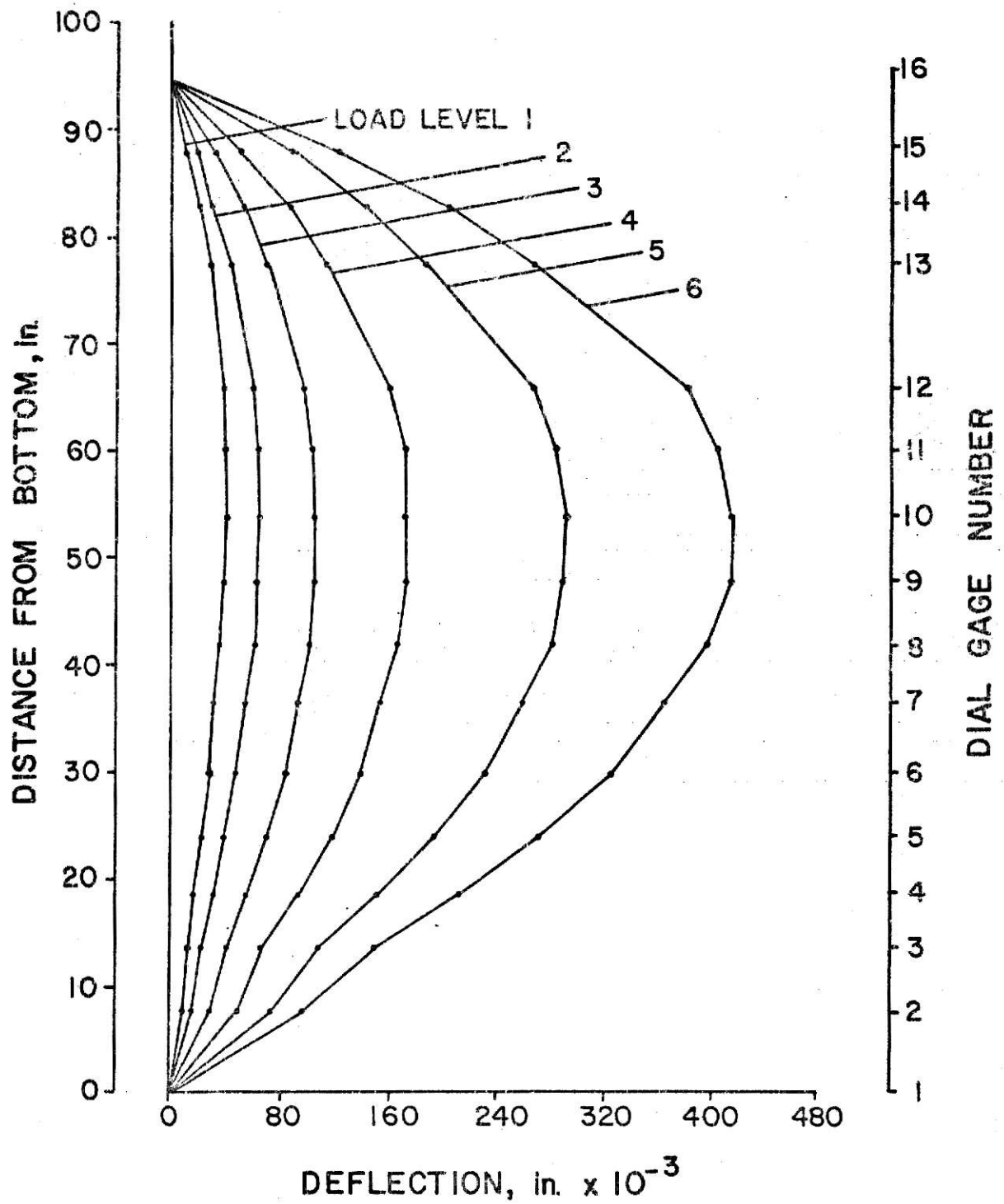

Figure A13 - Deflection Profile Along Vertical Centerline, Plate Number 13 (Adjusted Values)(1 in. = 2.54 cm.)

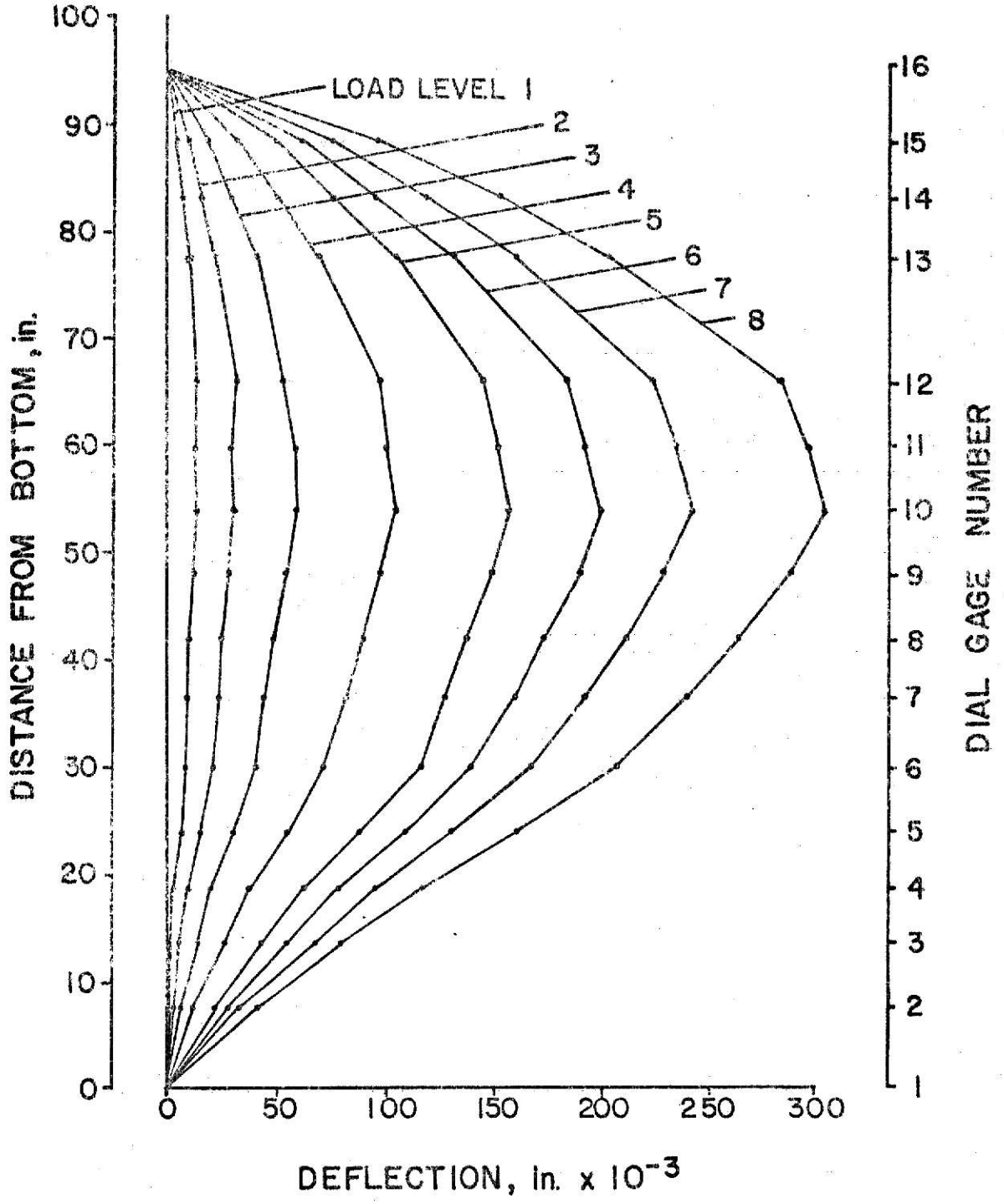

Figure A14 - Deflection Profile Along Vertical Centerline, Plate Number 14 (Adjusted Values)(1 in. = 2.54 cm.)

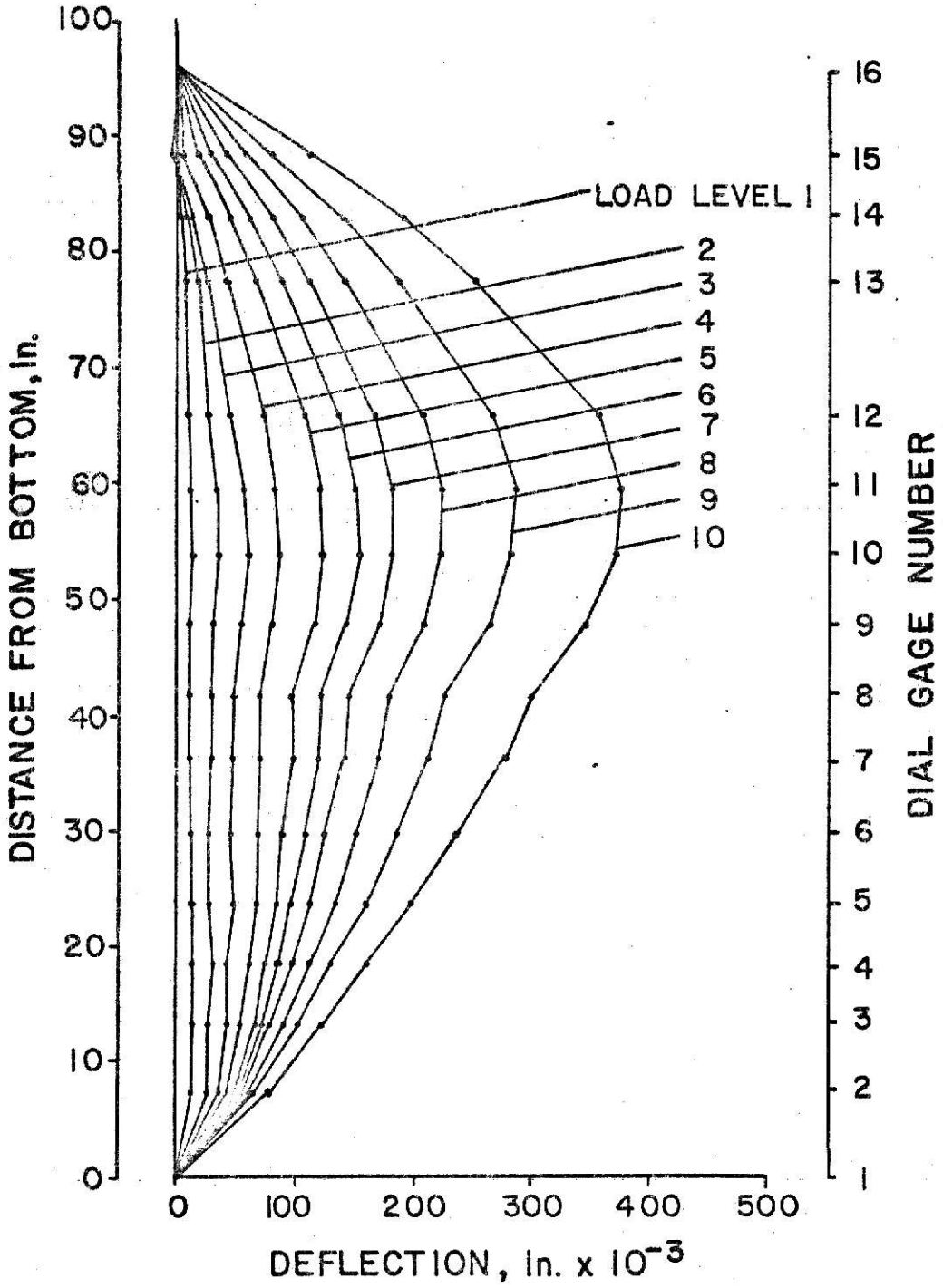

Figure A15 - Deflection Profile Along Vertical Centerline, Plate Number 15 (Adjusted Values)(1 in. = 2.54 cm.)

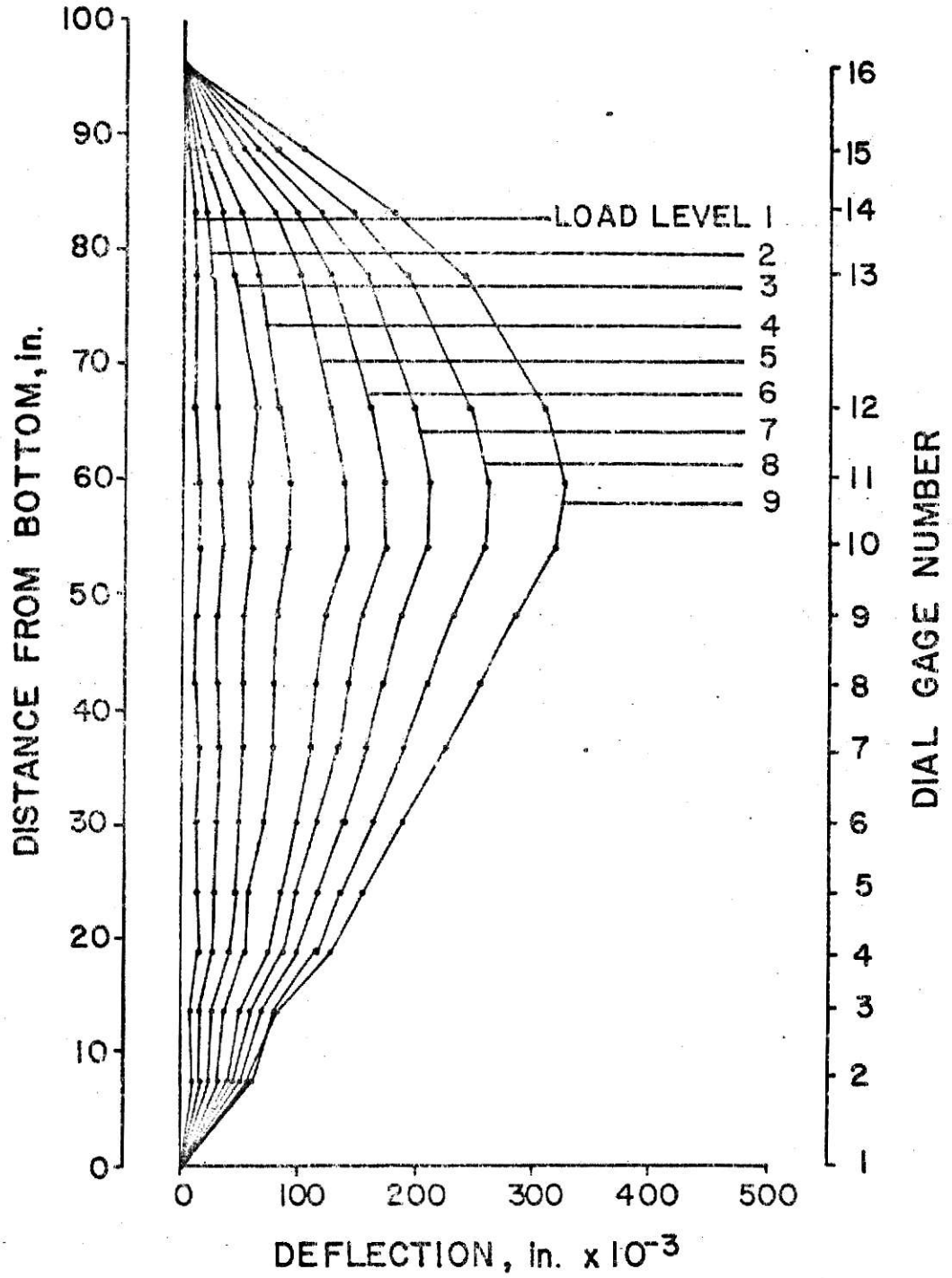

Figure A16 - Deflection Profile Along Vertical Centerline, Plate Number 16 (Adjusted Values) (1 in. = 2.54 cm.)

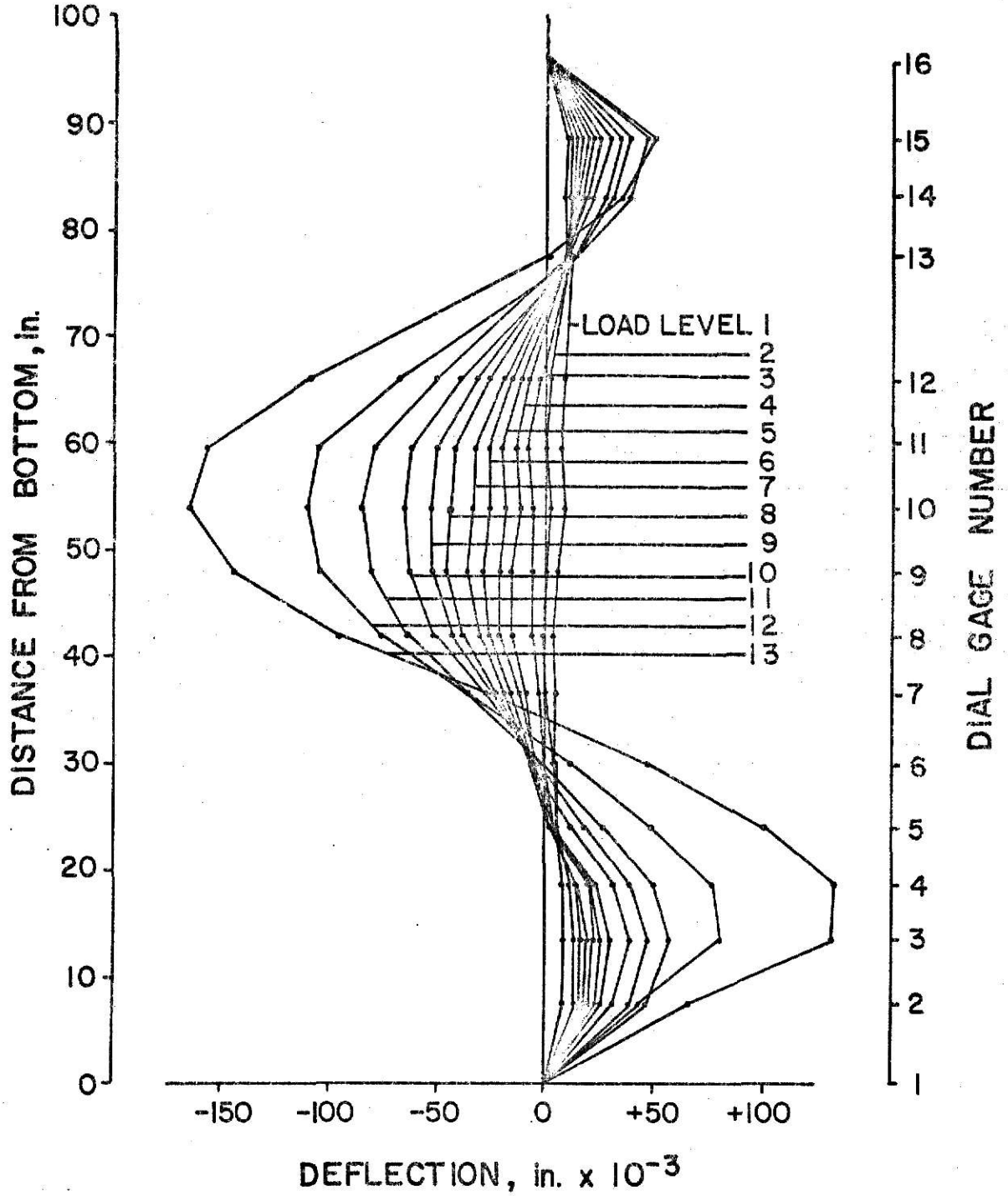

Figure A17 - Deflection Profile Along Vertical Centerline, Plate Number 17 (Adjusted Values)(1 in. = 2.54 cm.)

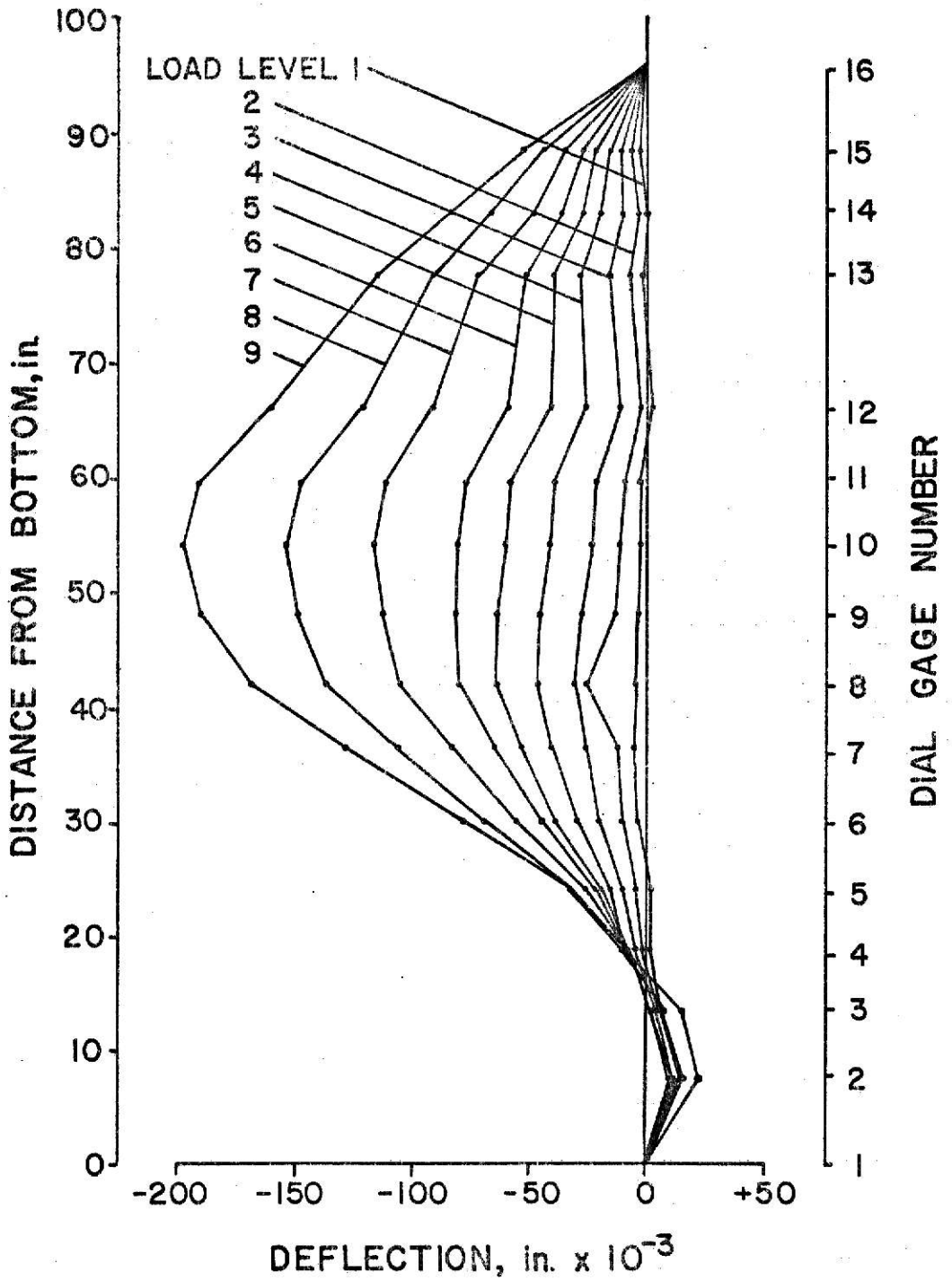

Figure A18 - Deflection Profile Along Vertical Centerline, Plate Number 18 (Adjusted Values)(1 in. = 2.54 cm.)

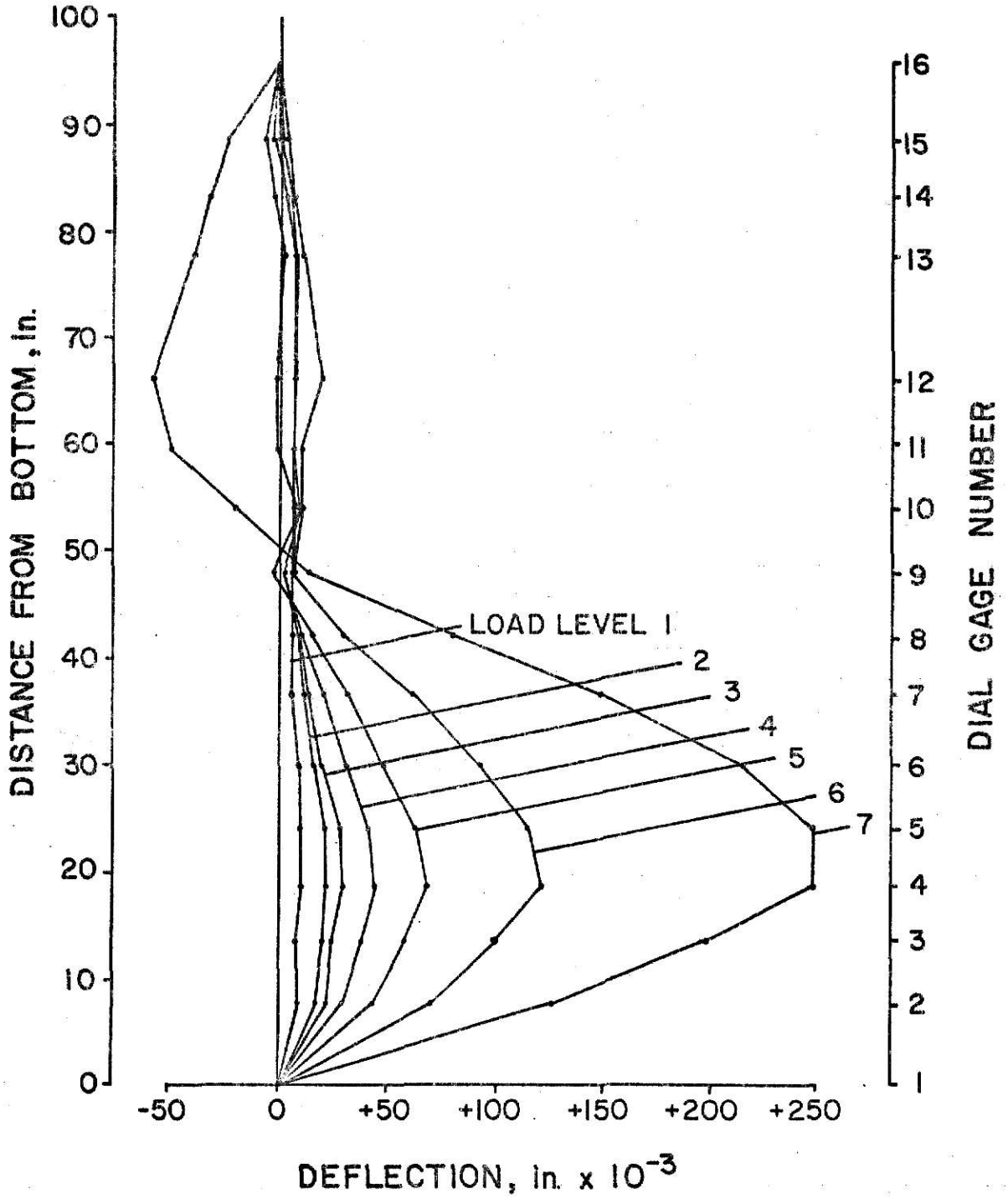

Figure A19 - Deflection Profile Along Vertical Centerline, Plate Number 19 (Adjusted Values)(1 in. = 2.54 cm.)

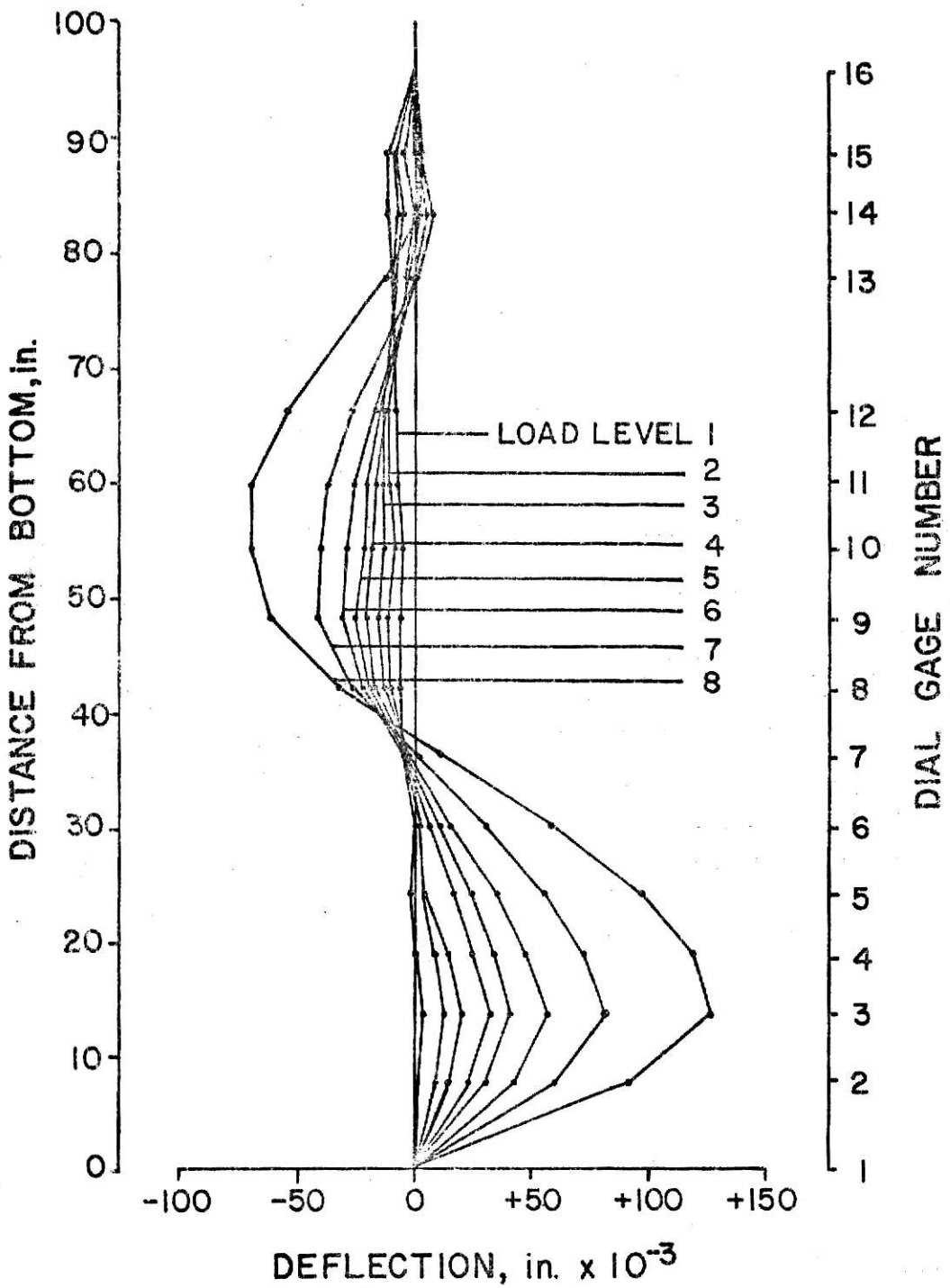

Figure A20- Deflection Profile Along Vertical Centerline, Plate Number 20 (Adjusted Values)(1 in. = 2.54 cm.)

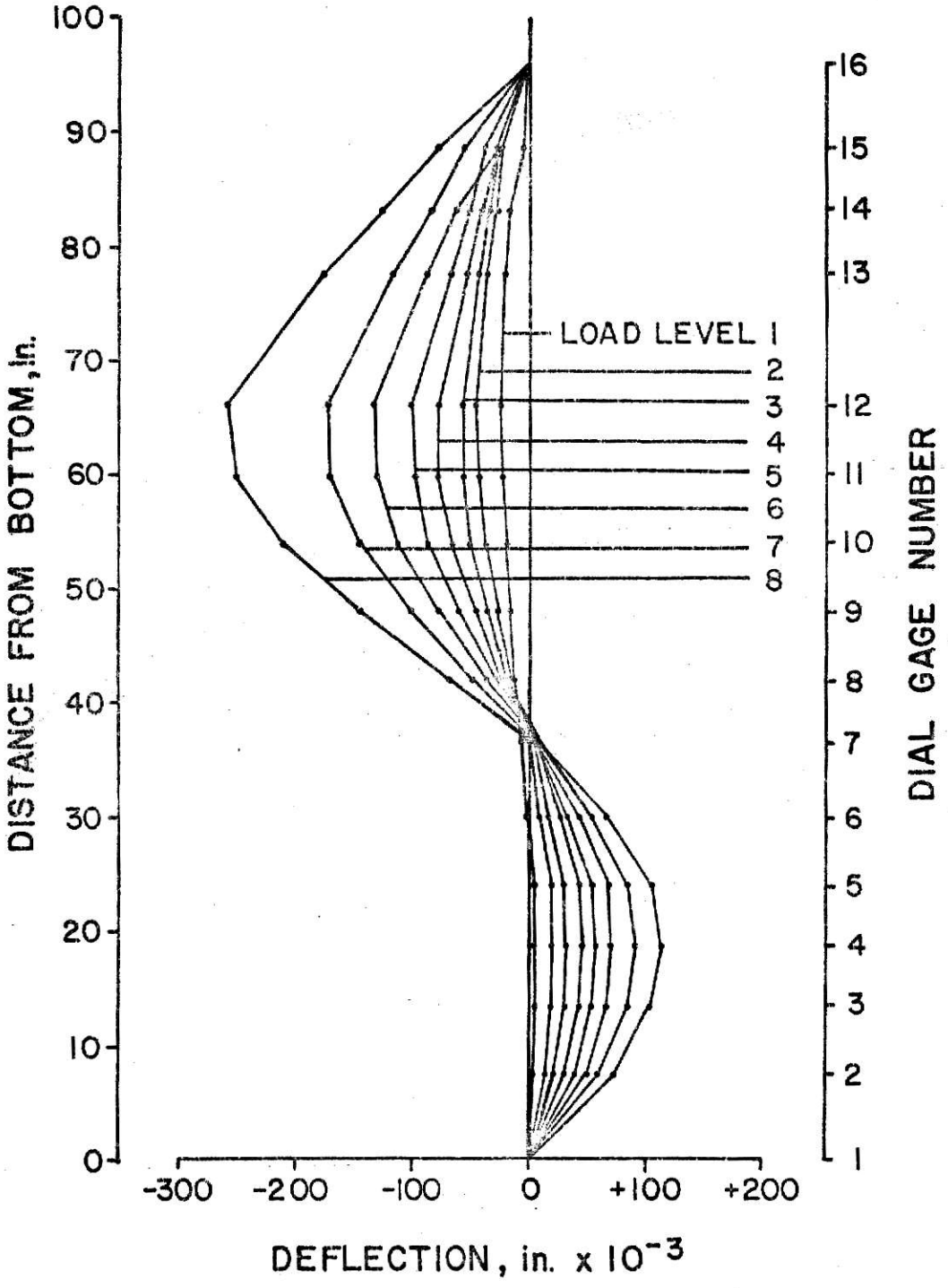

Figure A21 - Deflection Profile Along Vertical Centerline, Plate Number 21 (Adjusted Values)(1 in. = 2.54 cm.)

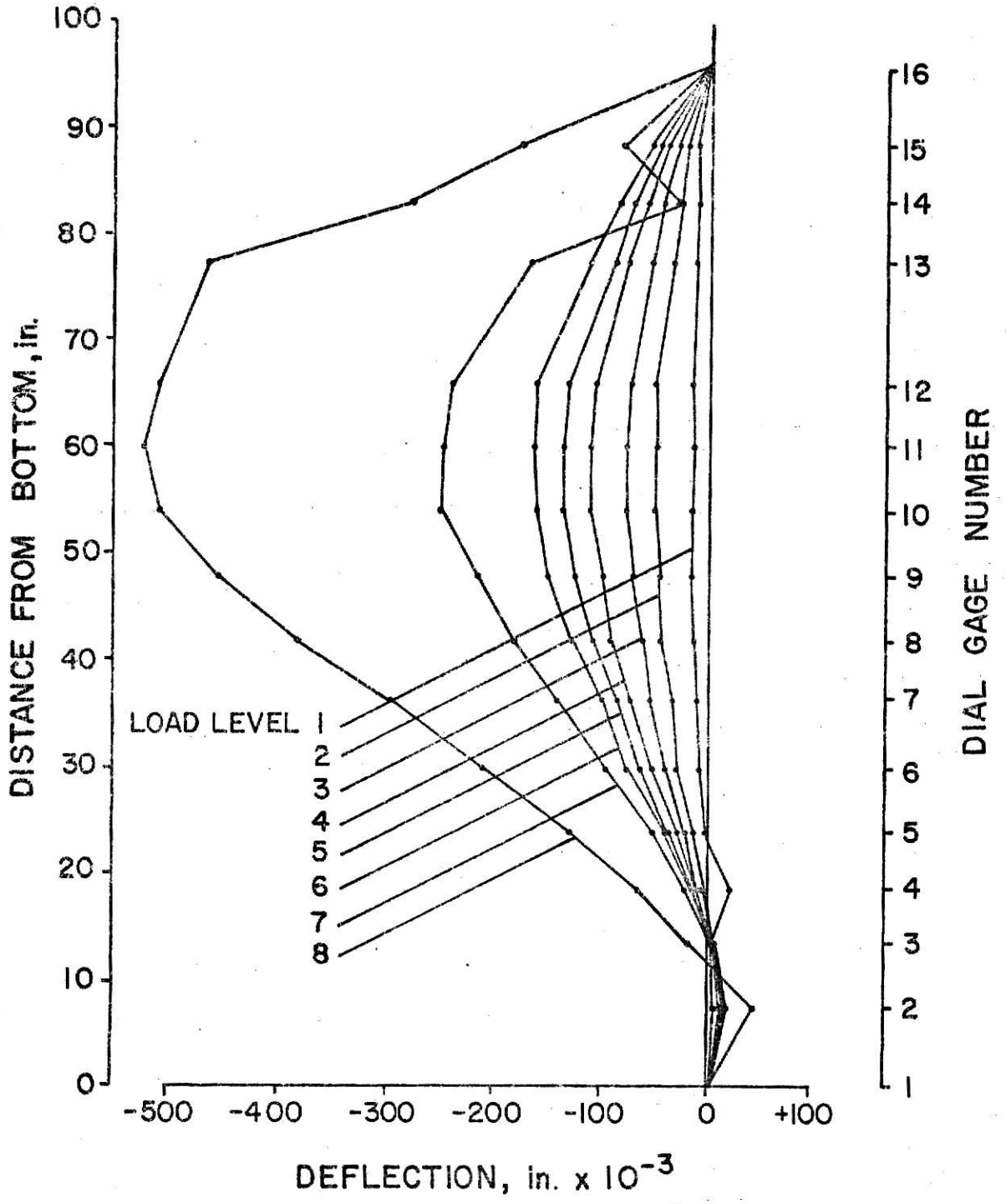

Figure A22 - Deflection Profile Along Vertical Centerline, Plate Number 22 (Adjusted Values)(1 in. = 2.54 cm.)

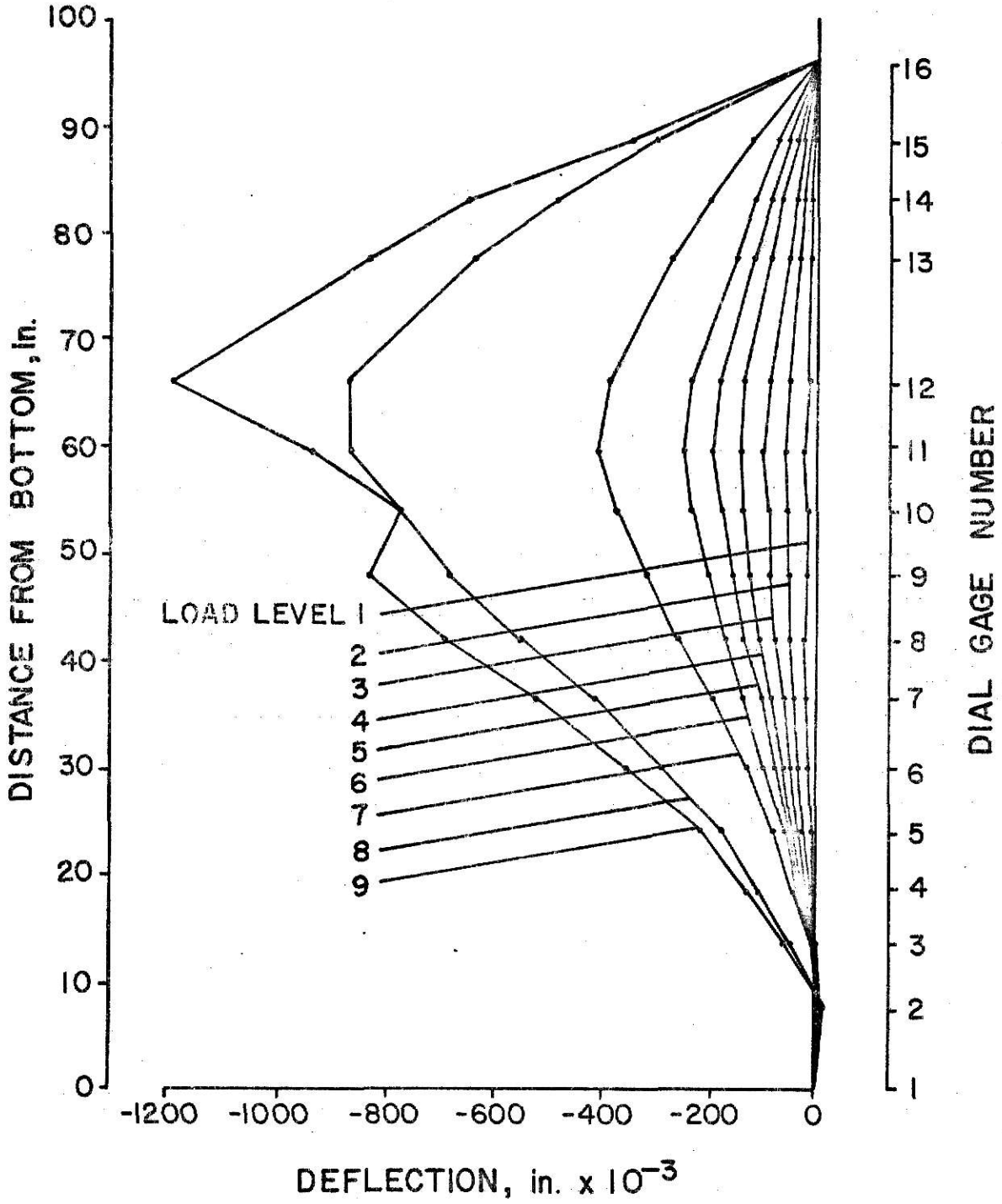

Figure A23 - Deflection Profile Along Vertical Centerline, Plate Number 23 (Adjusted Values)(1 in. = 2.54 cm.)

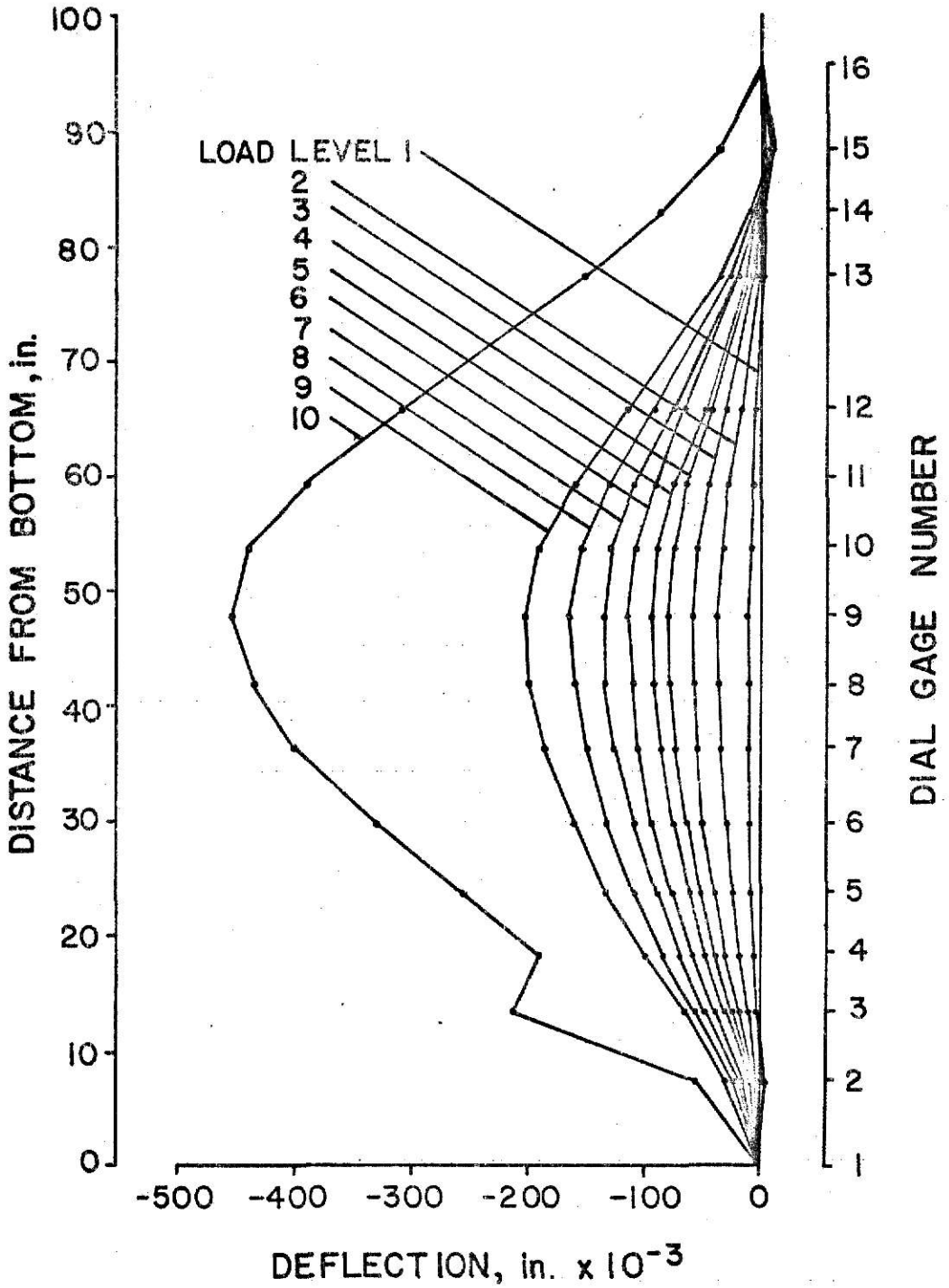

Figure A24 - Deflection Profile Along Vertical Centerline, Plate Number 24 (Adjusted Values)(1 in. = 2.54 cm.)

APPENDIX B

SOUTHWELL PLOTS

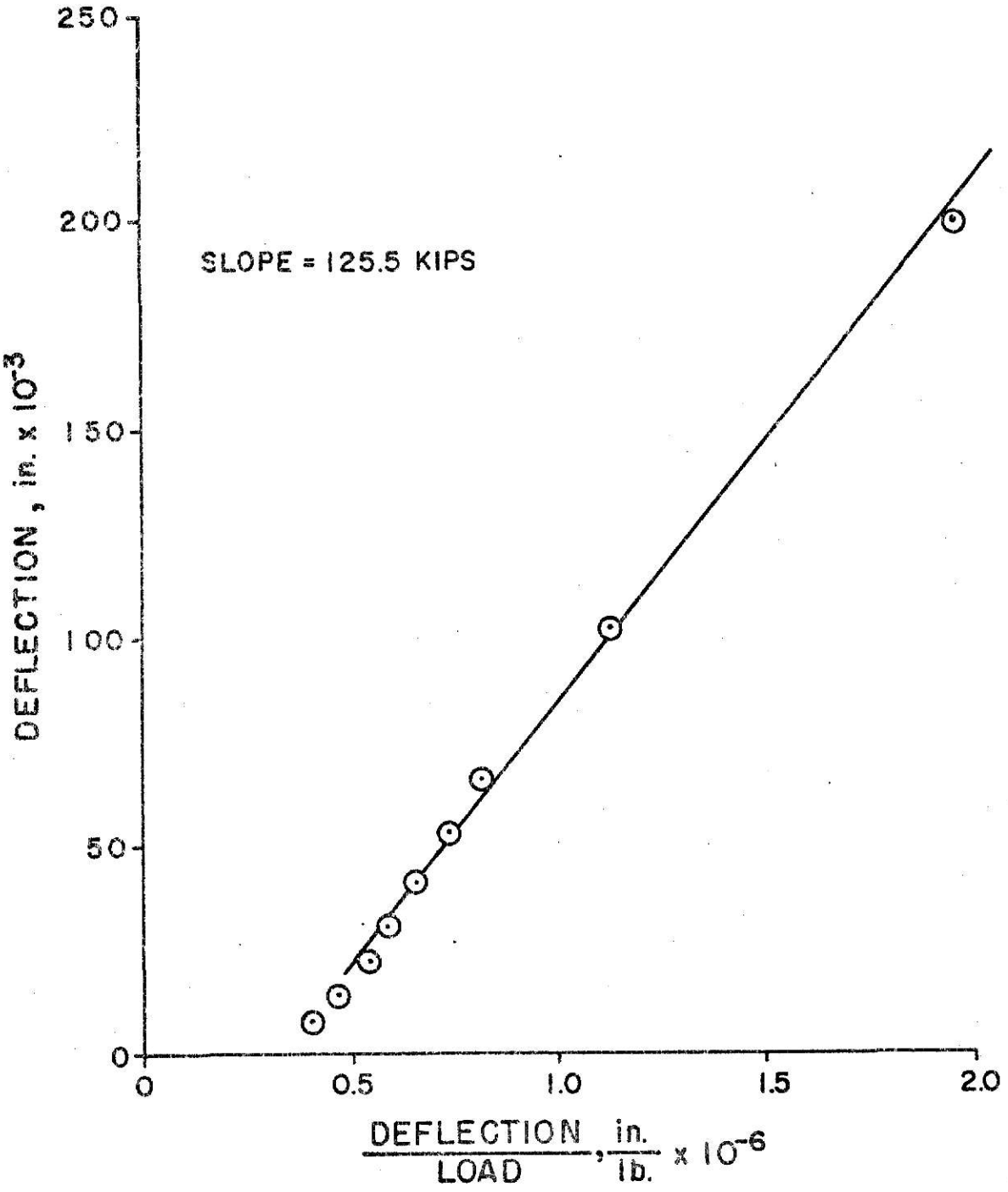

Figure B1 - Southwell Plot, Plate Number 1 (1 in. = 2.54 cm.; 1 in./lb. = 0.57 cm./N; 1 Kip = 4.448 kN)

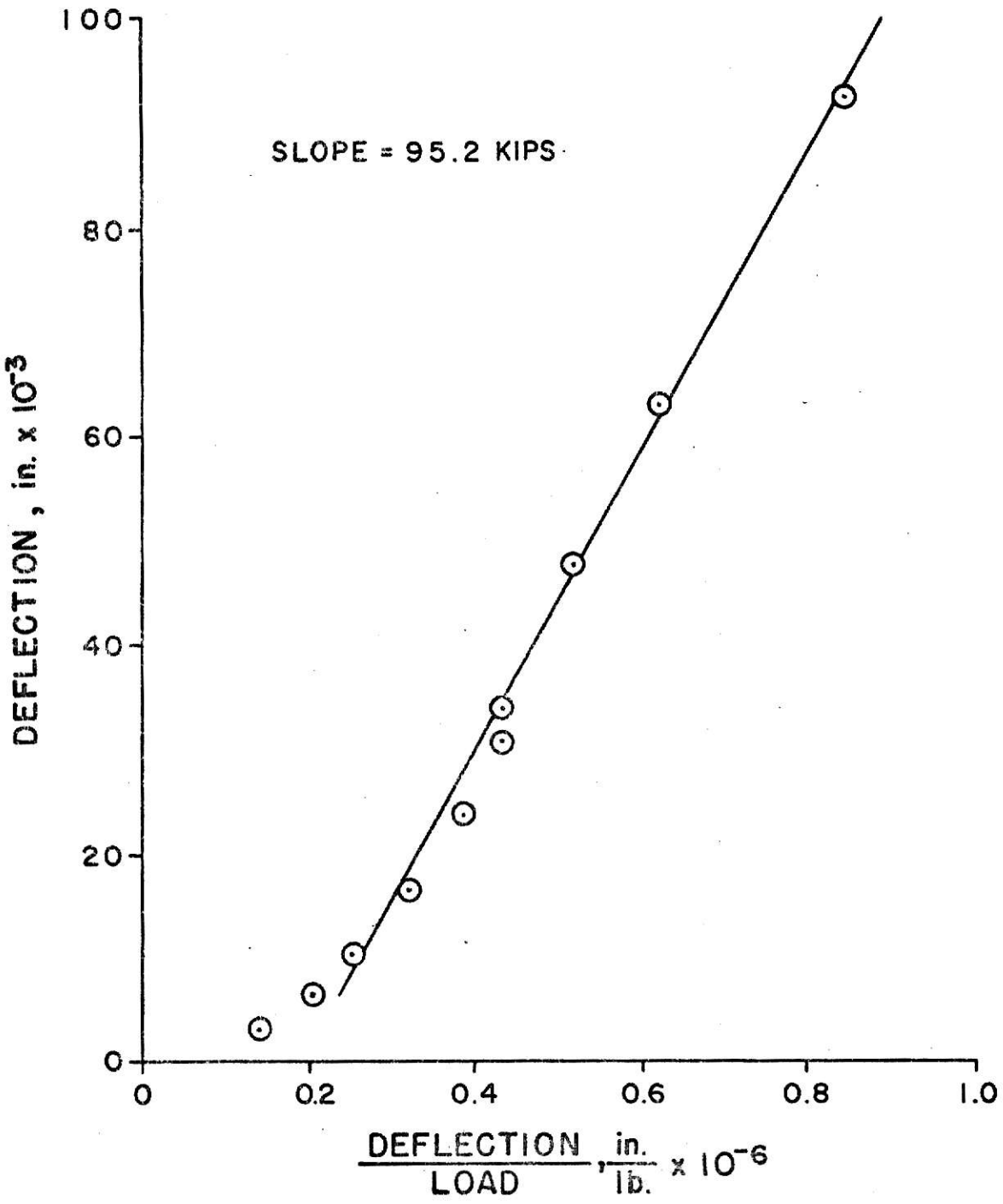

Figure B2 - Southwell Plot, Plate Number 2 (1 in. = 2.54 cm.; 1 in./lb. = 0.57 cm./N; 1 Kip = 4.448 kN)

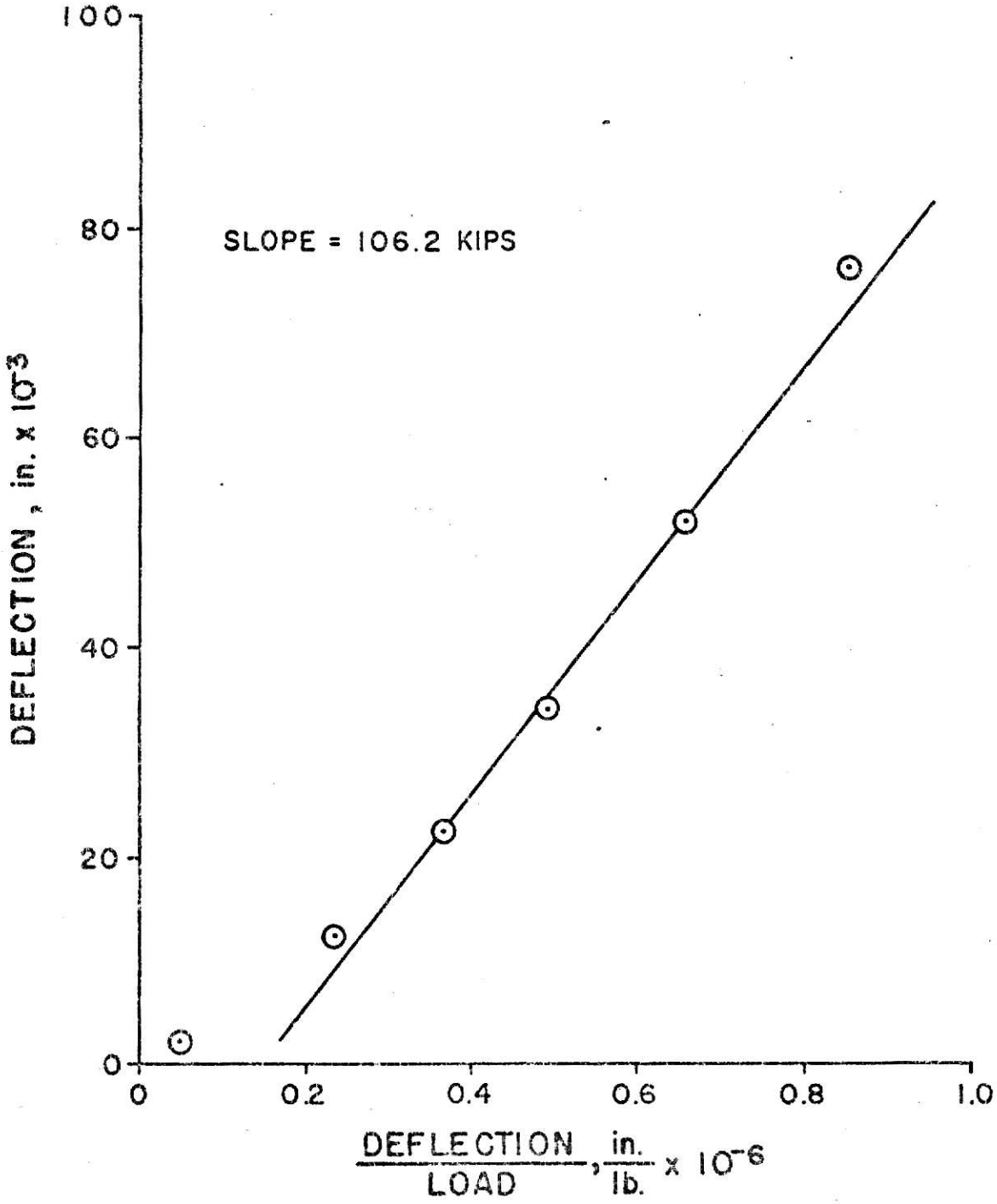

Figure B3 - Southwell Plot, Plate Number 3 (1 in. = 2.54 cm.; 1 in./lb. = 0.57 cm./N; 1 Kip = 4.448 kN)

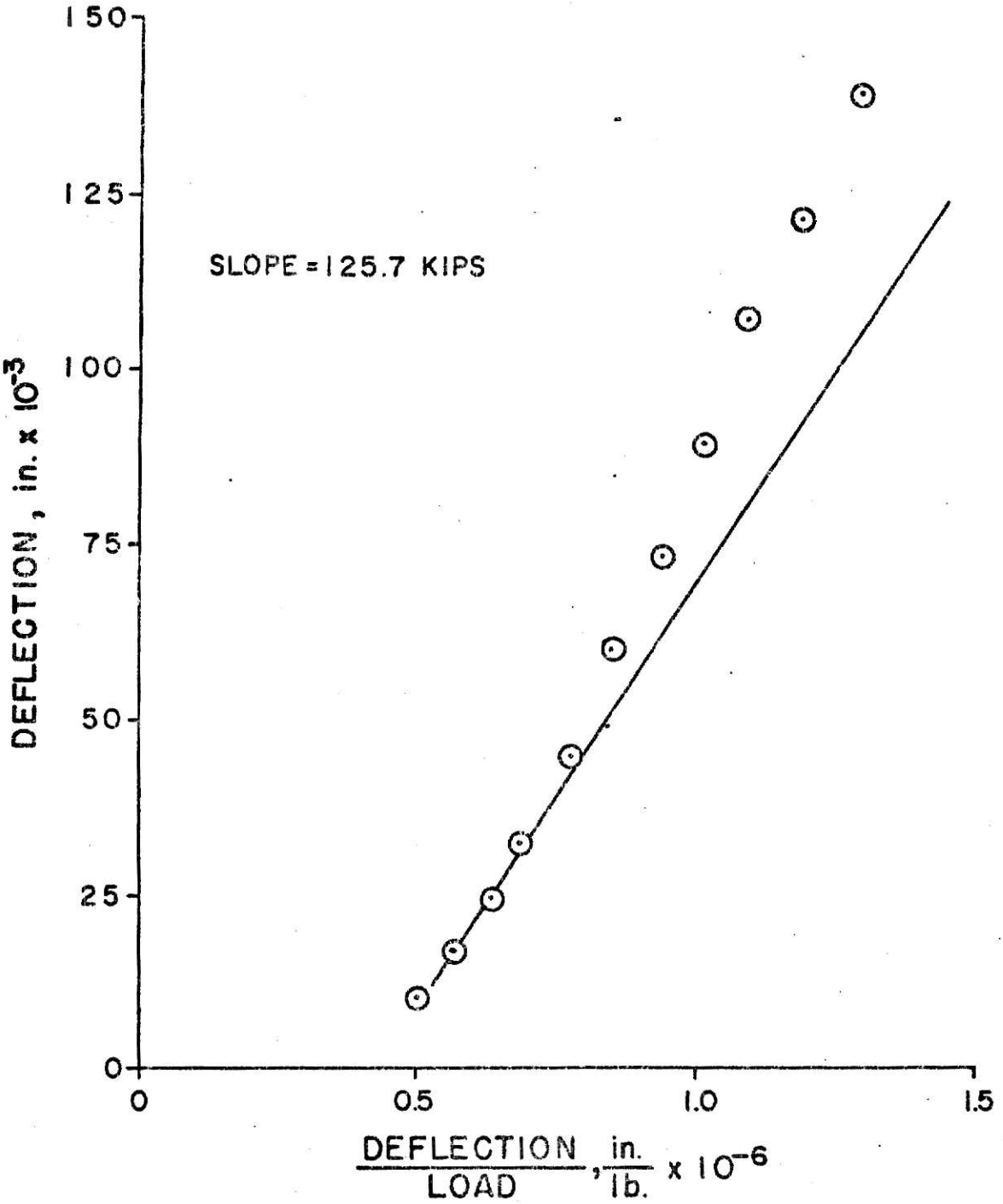

Figure B4 - Southwell Plot, Plate Number 4 (1 in. = 2.54 cm.; 1 in./lb. = 0.57 cm./N; 1 Kip = 4.448 kN)

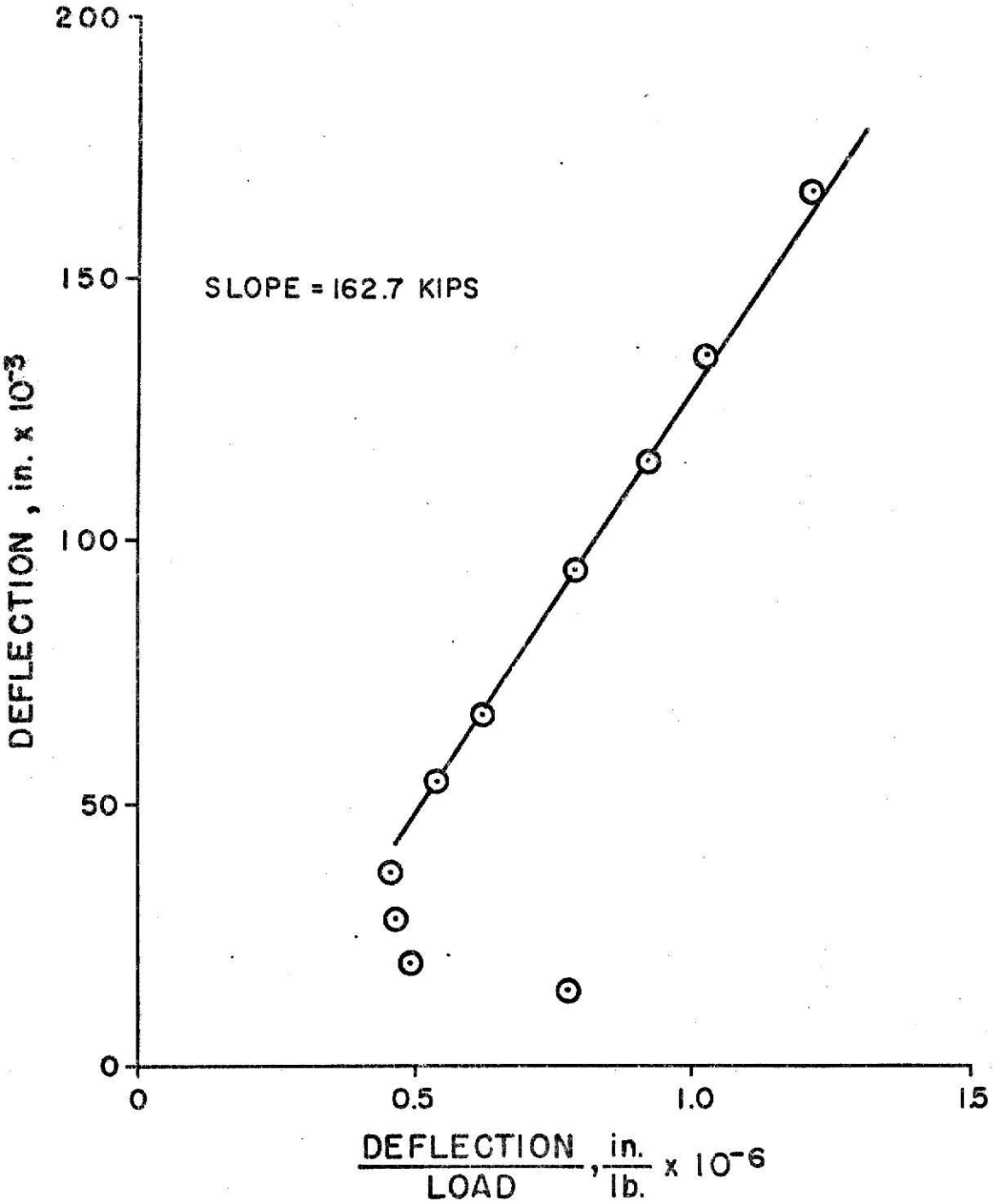

Figure B5 - Southwell Plot, Plate Number 6 (1 in. = 2.54 cm.; 1 in./lb. = 0.57 cm./N; 1 Kip = 4.448 kN)

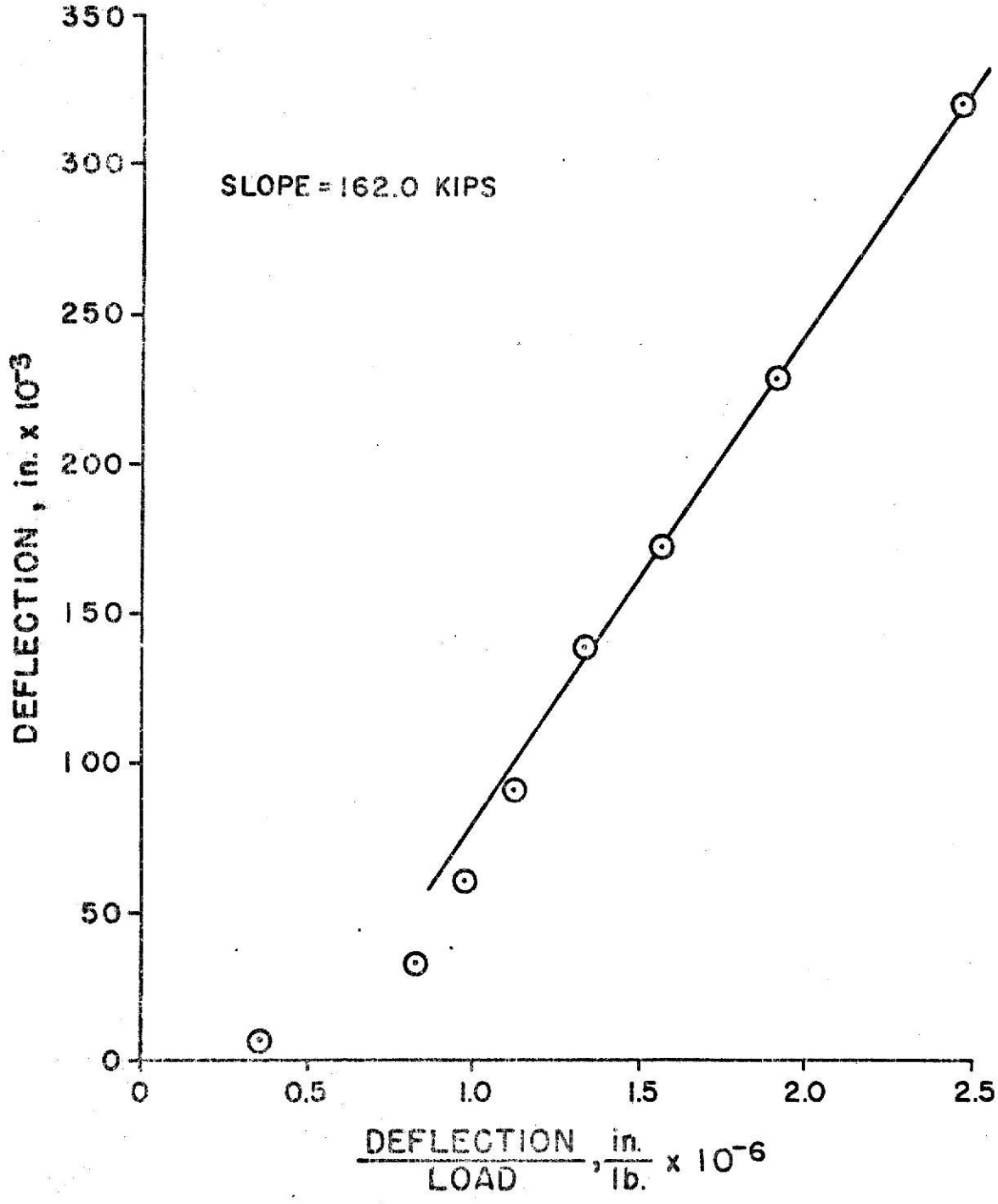

Figure B6 - Southwell Plot, Plate Number 7 (1 in. = 2.54 cm.; 1 in./lb. = 0.57 cm./N; 1 Kip = 4.448 kN)

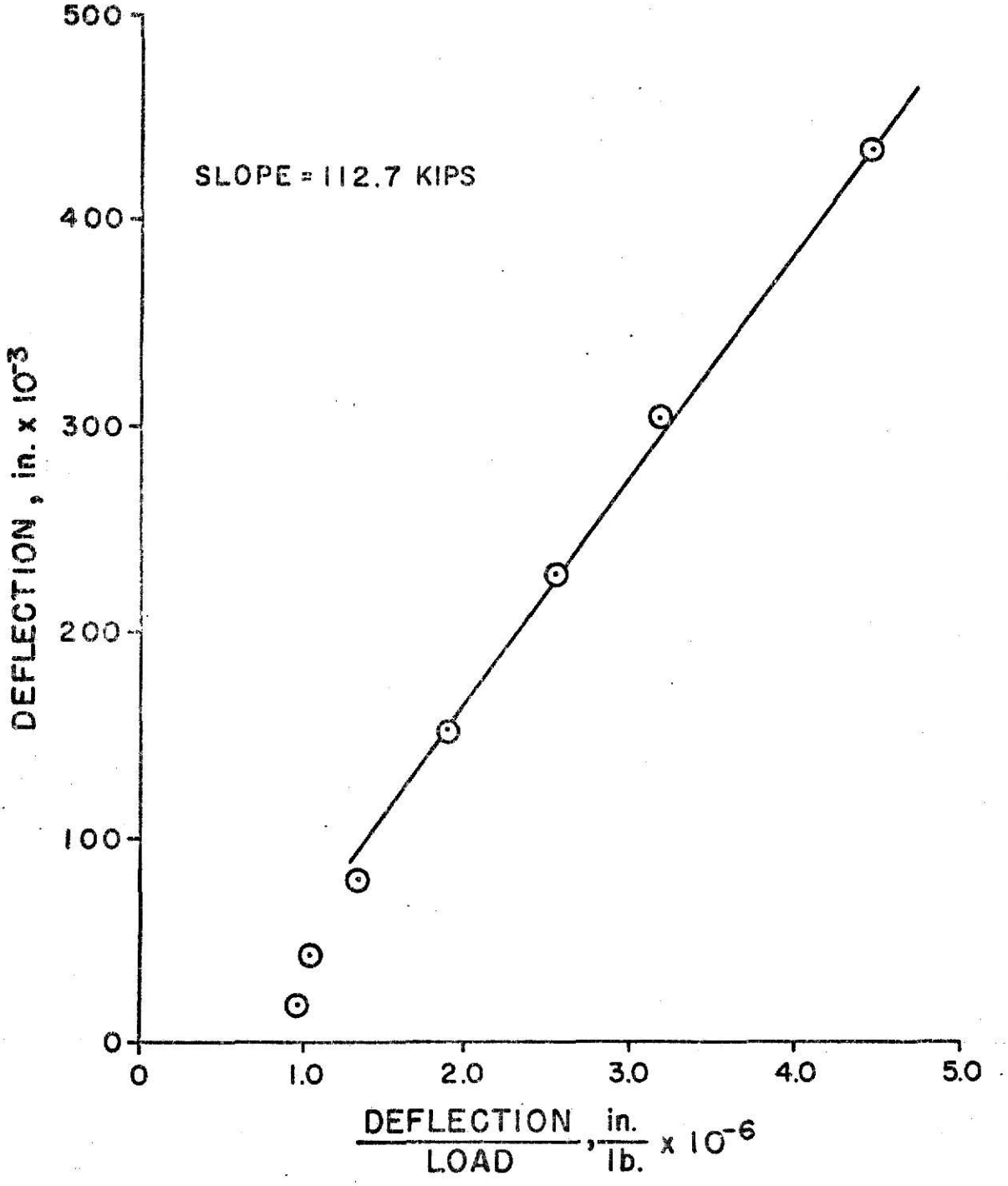

Figure B7 - Southwell Plot, Plate Number 8 (1 in. = 2.54 cm.; 1 in./lb. = 0.57 cm./N; 1 Kip = 4.448 kN)

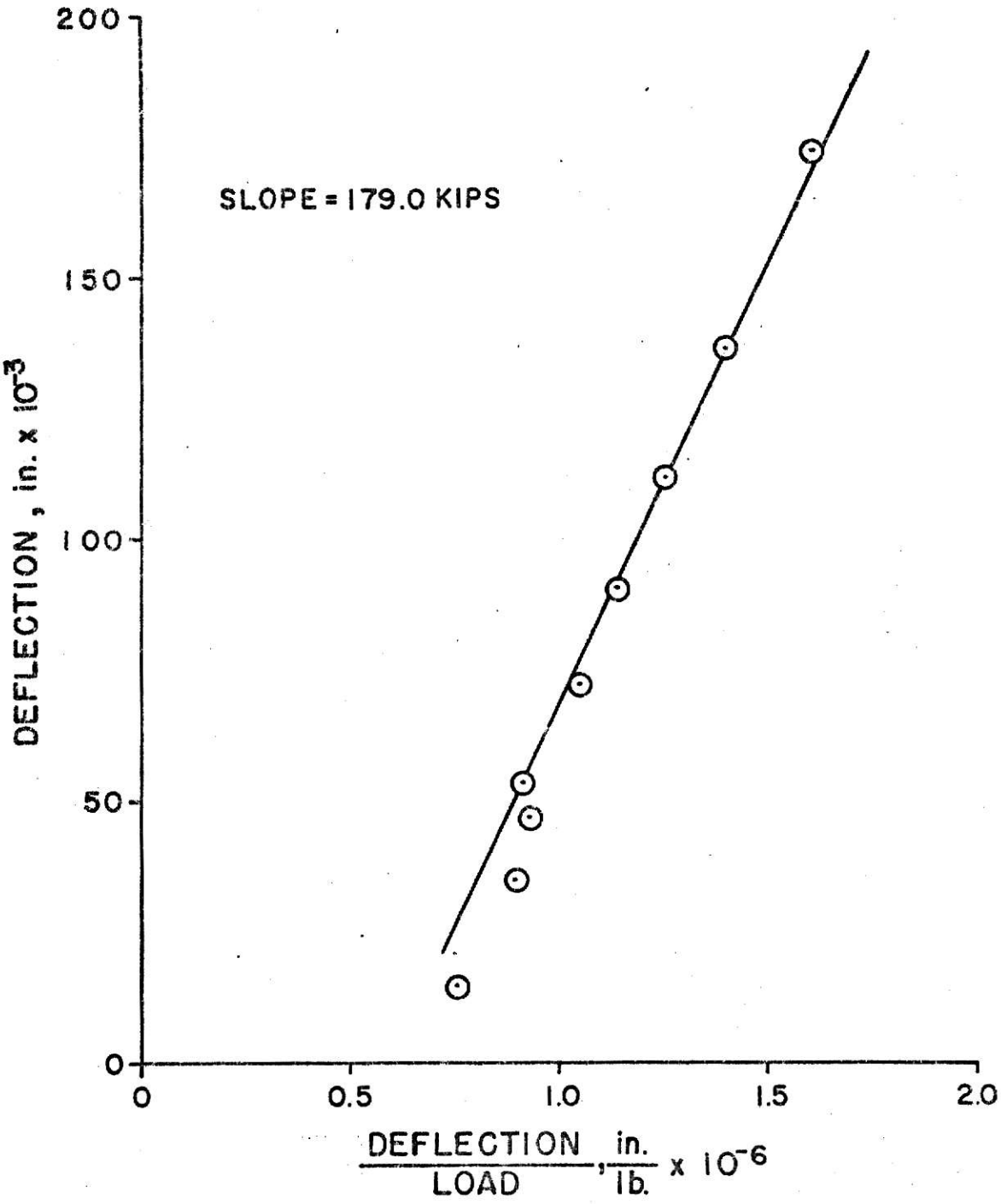

Figure B8 - Southwell Plot, Plate Number 9 (1 in. = 2.54 cm.; 1 in./lb. = 0.57 cm./N; 1 Kip = 4.448 kN)

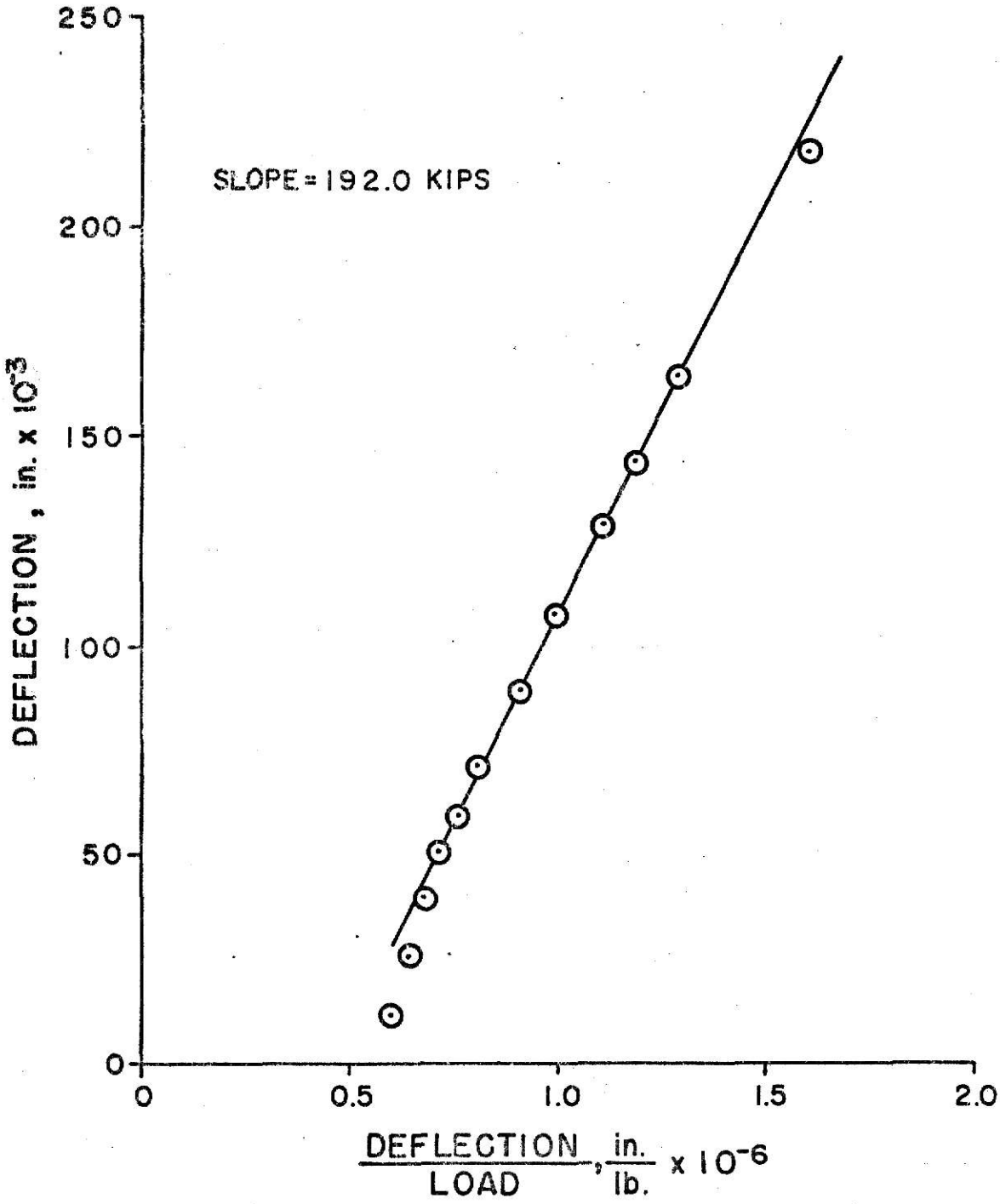

Figure B9 - Southwell Plot, Plate Number 10 (1 in. = 2.54 cm.; 1 in./lb. = 0.57 cm./N; 1 Kip = 4.448 kN)

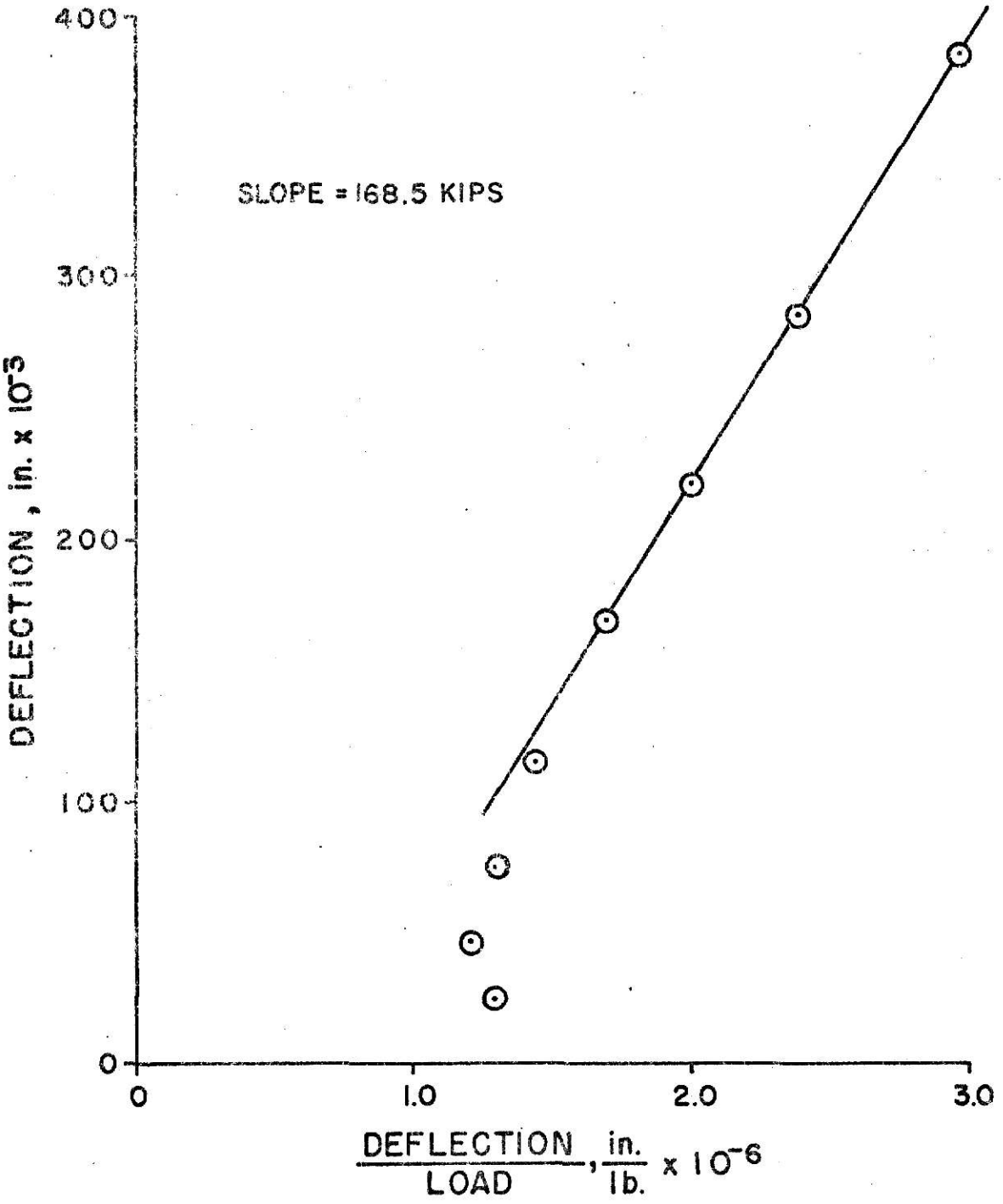

Figure B10 - Southwell Plot, Plate Number 11 (1 in. = 2.54 cm.; 1 in./lb. = 0.57 cm./N; 1 Kip = 4.448 kN)

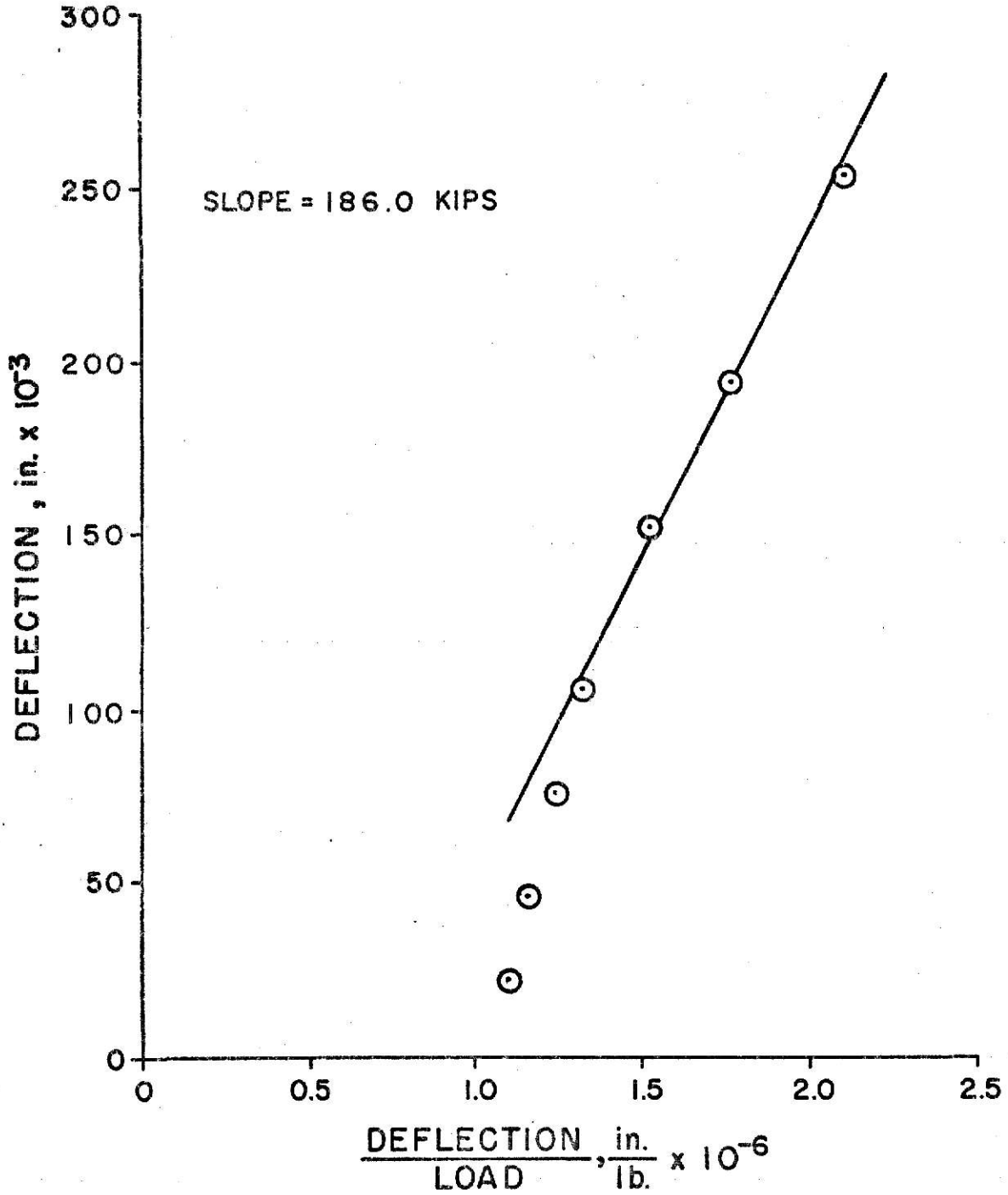

Figure B11 - Southwell Plot, Plate Number 12 (1 in. = 2.54 cm.; 1 in./lb. = 0.57 cm./N; 1 Kip = 4.448 kN)

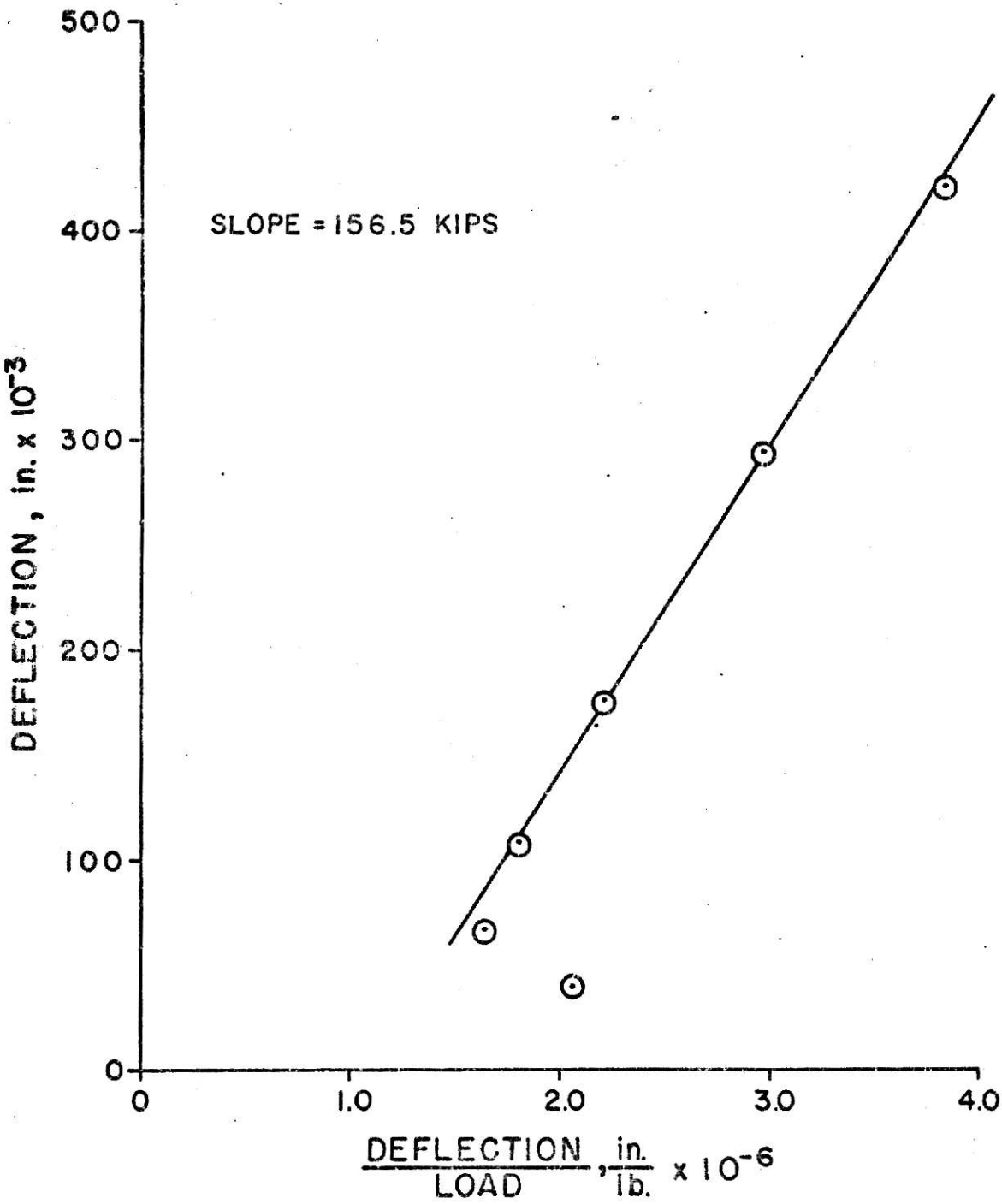

Figure B12 - Southwell Plot, Plate Number 13 (1 in. = 2.54 cm.; 1 in./lb. = 0.57 cm./N; 1 Kip = 4.448 kN)

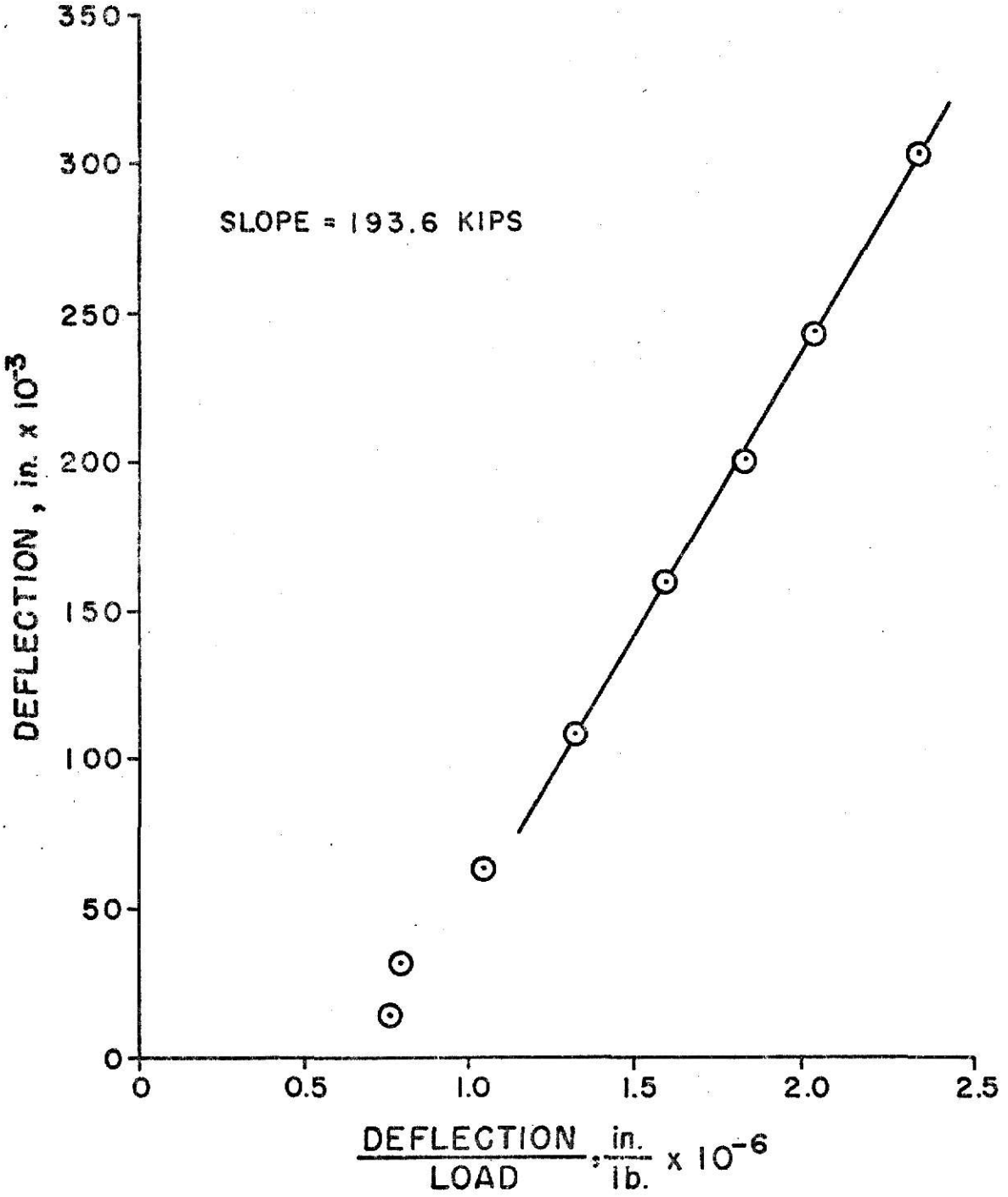

Figure B13 - Southwell Plot, Plate Number 14 (1 in. = 2.54 cm.; 1 in./lb. = 0.57 cm./N; 1 Kip = 4.448 kN)

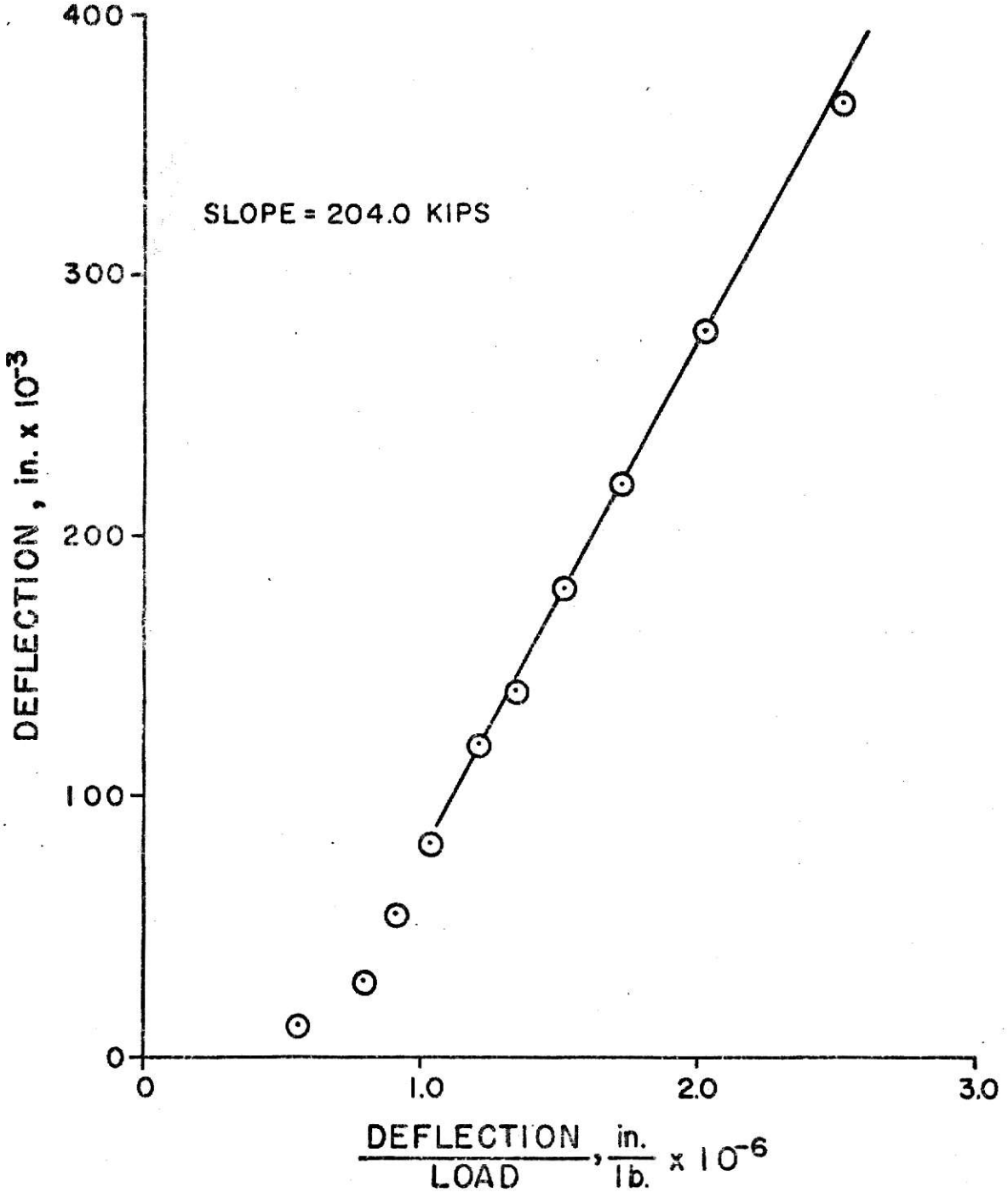

Figure B14 - Southwell Plot, Plate Number 15 (1 in. = 2.54 cm.; 1 in./lb. = 0.57 cm./N; 1 Kip = 4.448 kN)

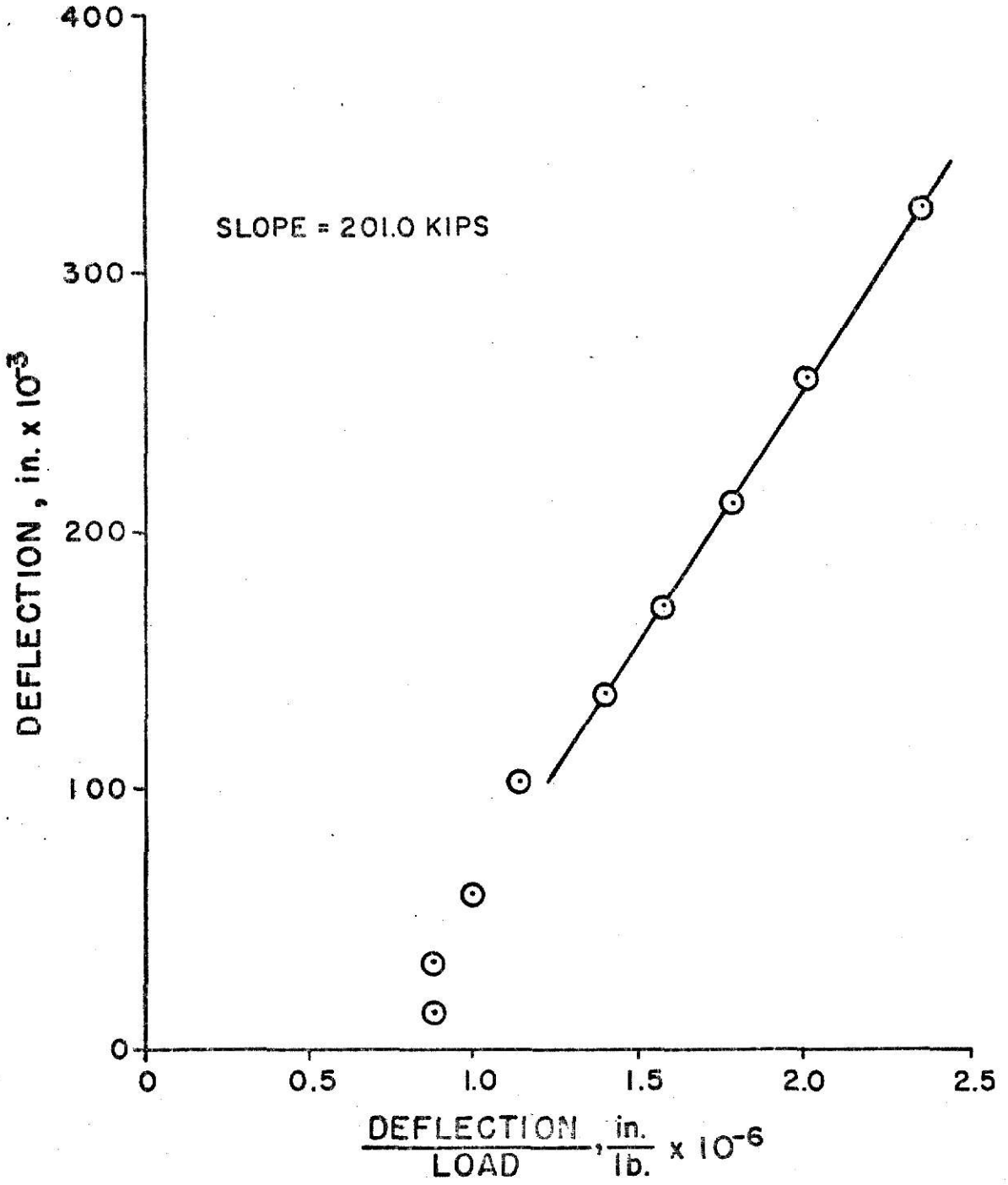

Figure B15 - Southwell Plot, Plate Number 16 (1 in. = 2.54 cm.; 1 in./lb. = 0.57 cm./N; 1 Kip = 4.448 kN)

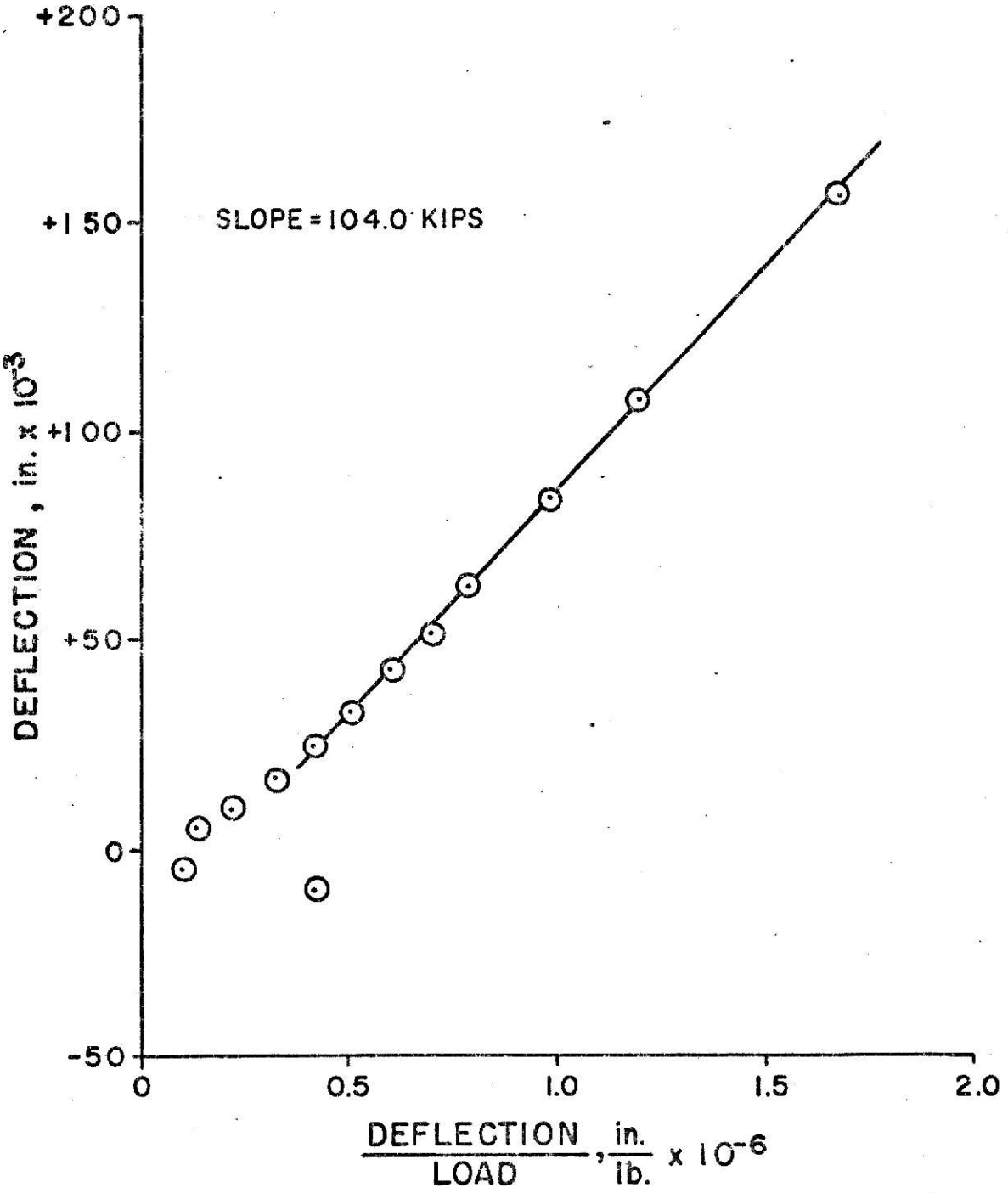

Figure B16 - Southwell Plot, Plate Number 17 (1 in. = 2.54 cm.; 1 in./lb. = 0.57 cm./N; 1 Kip = 4.448 kN)

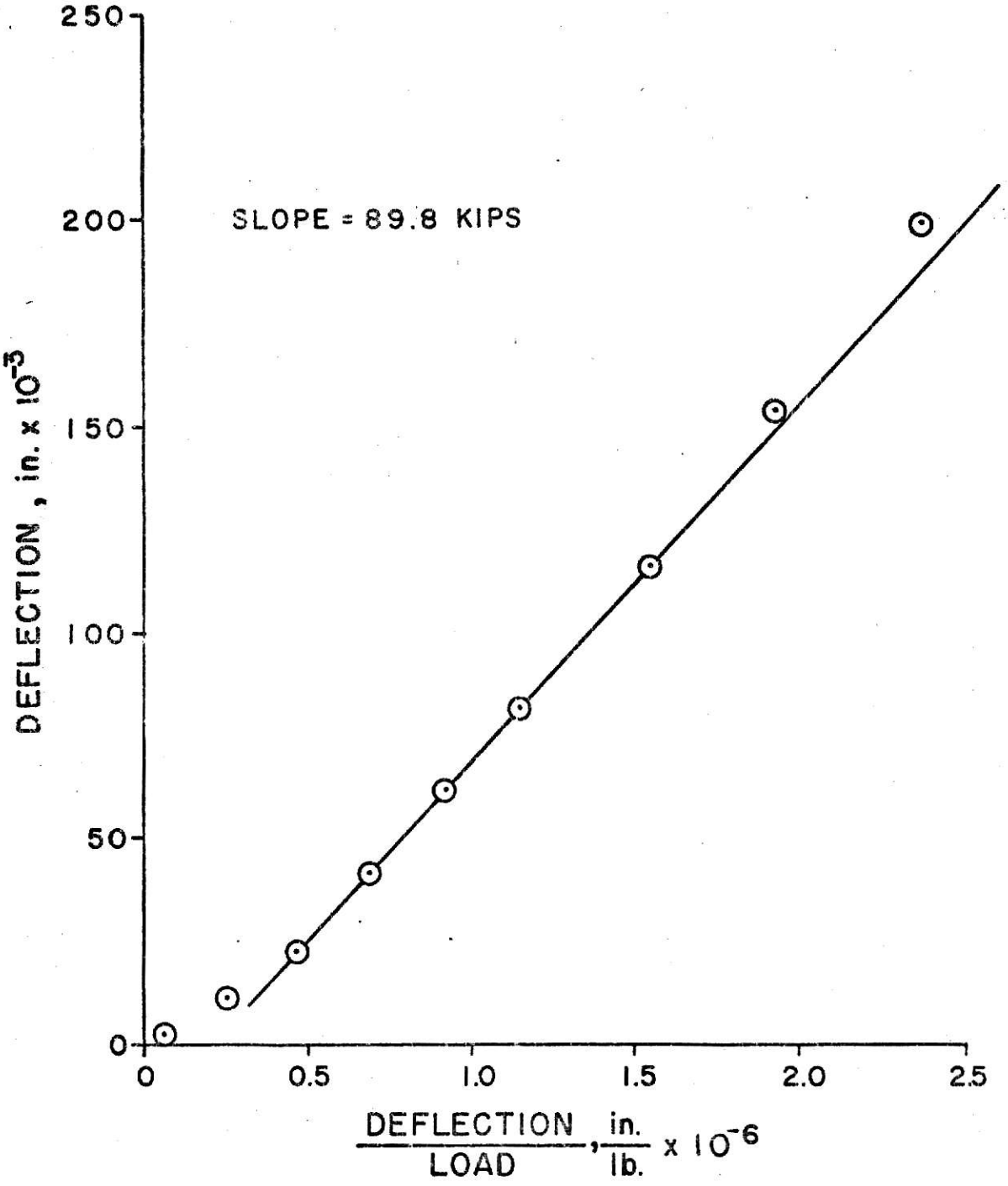

Figure B17 - Southwell Plot, Plate Number 18 (1 in. = 2.54 cm.; 1 in./lb. = 0.57 cm./N; 1 Kip = 4.448 kN)

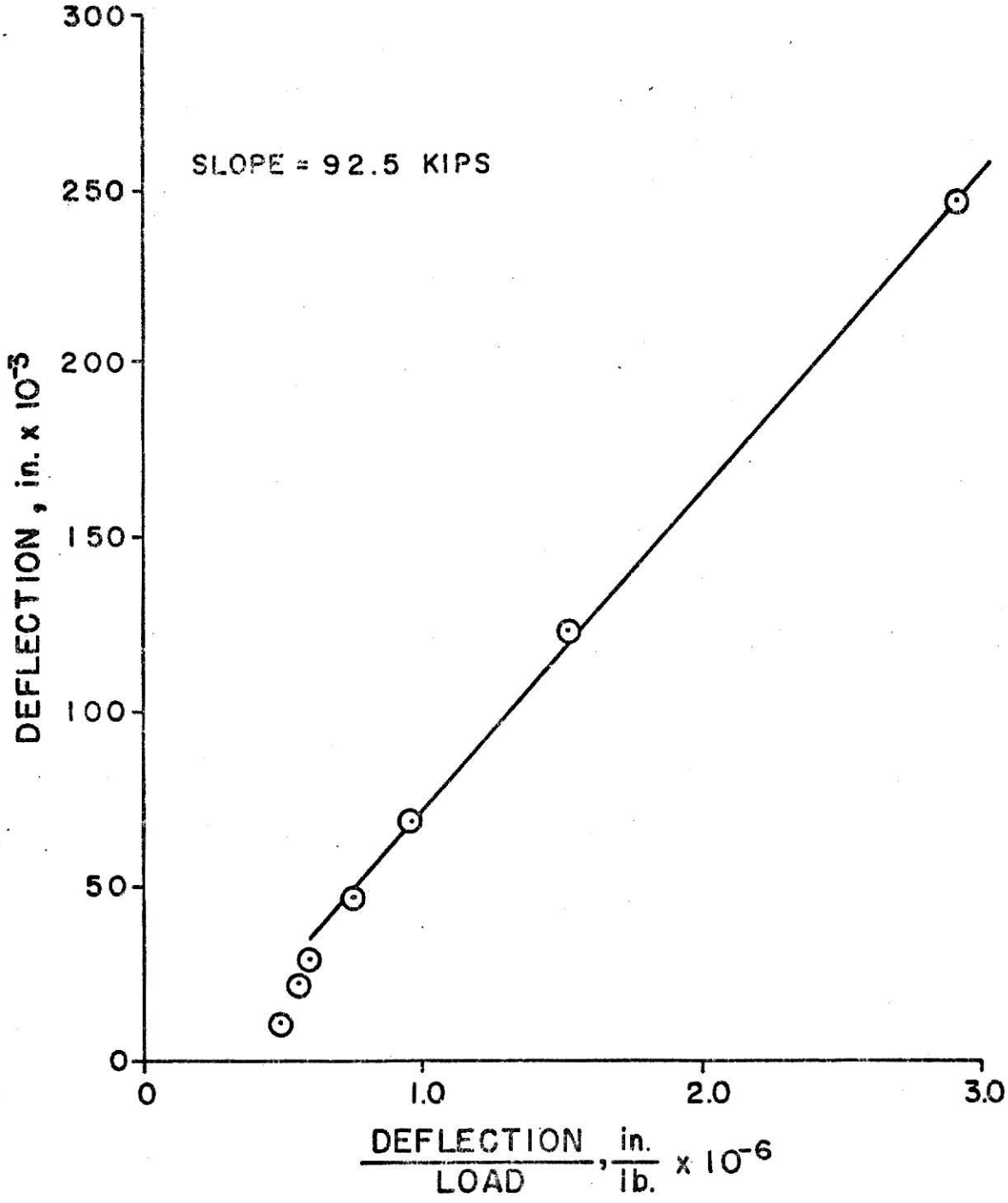

Figure B18 - Southwell Plot, Plate Number 19 (1 in. = 2.54 cm.; 1 in./lb. = 0.57 cm./N; 1 Kip = 4.448 kN)

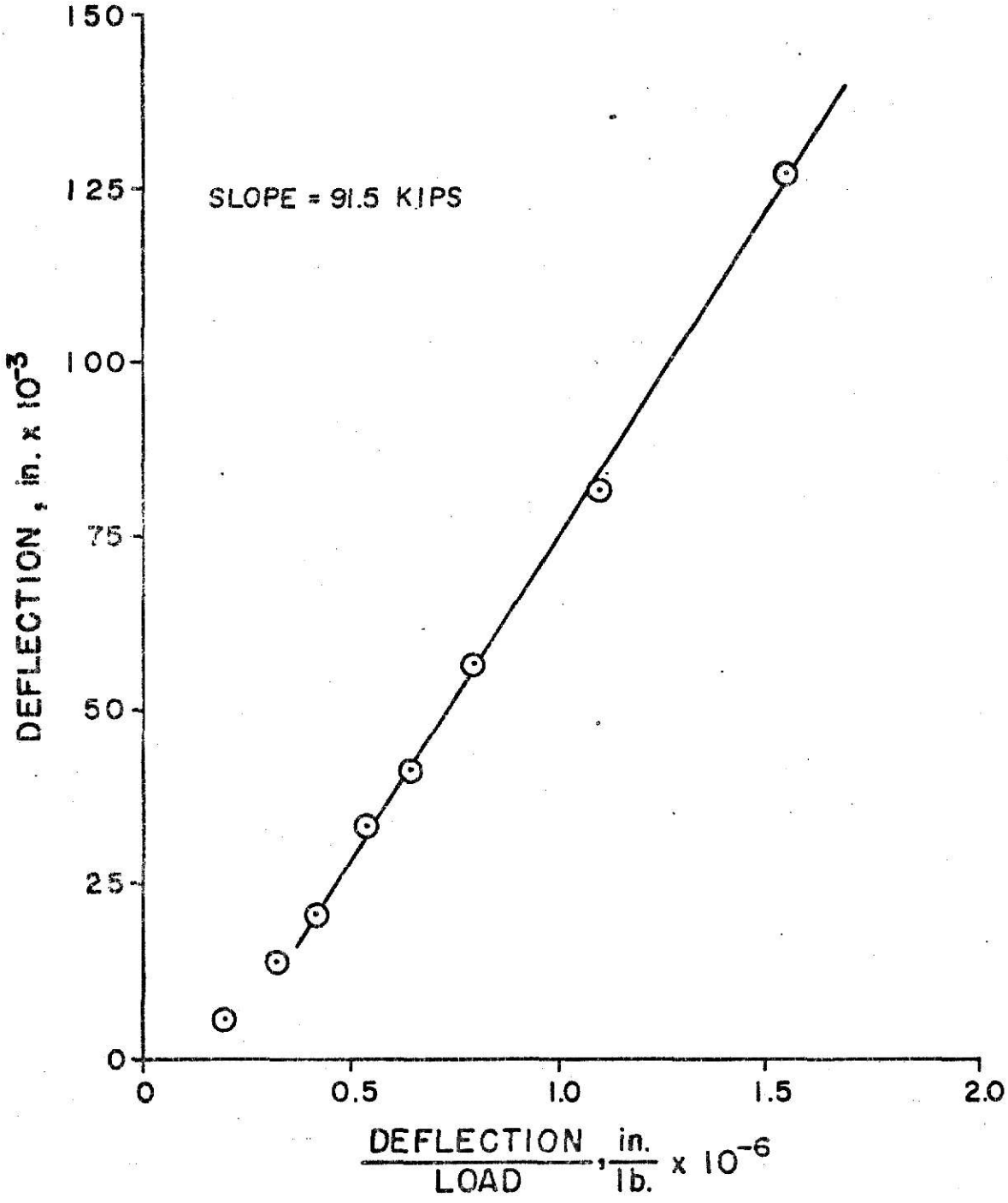

Figure B19 - Southwell Plot, Plate Number 20 (1 in. = 2.54 cm.; 1 in./lb. = 0.57 cm./N; 1 Kip = 4.448 kN)

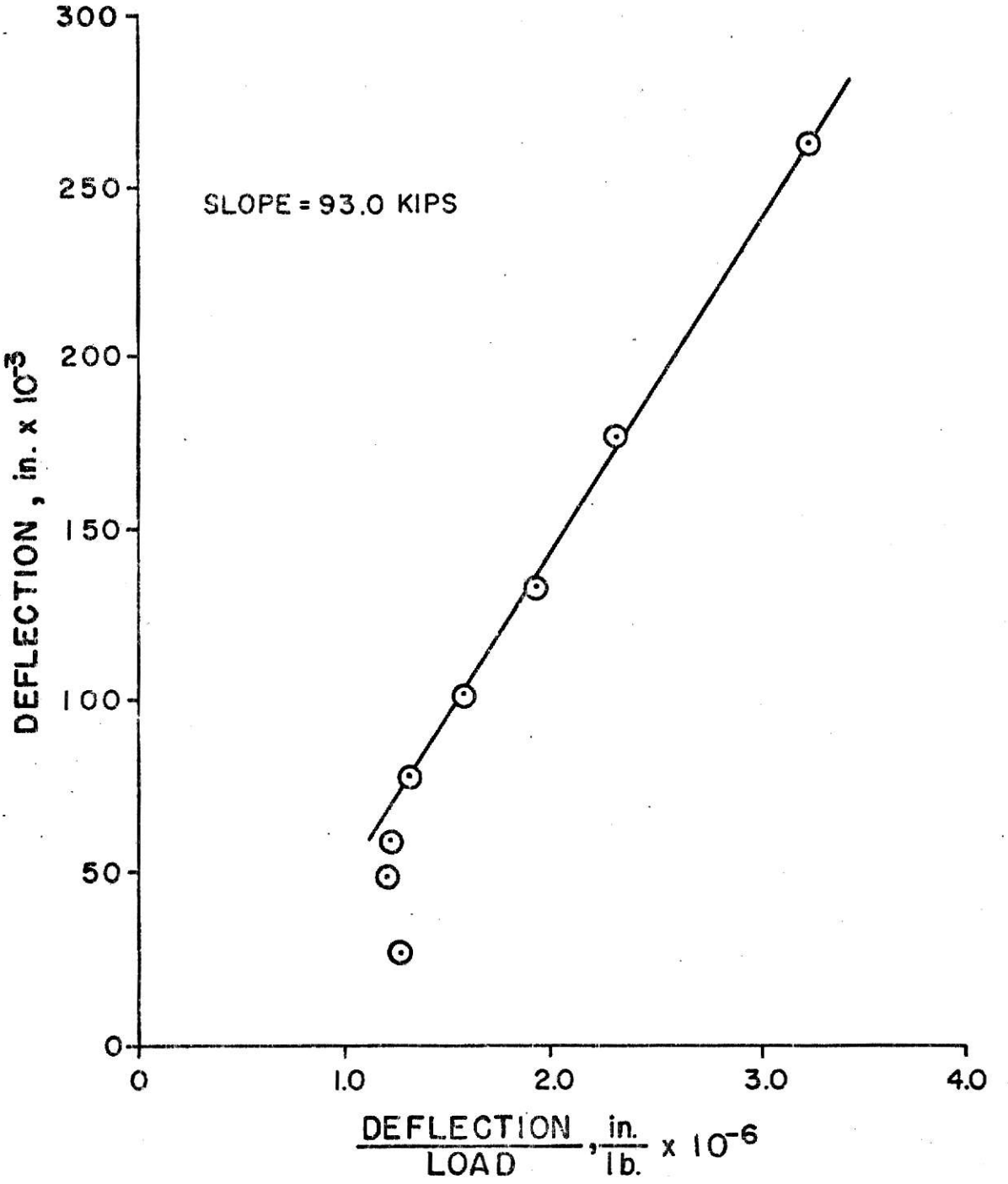

Figure B20 - Southwell Plot, Plate Number 21 (1 in. = 2.54 cm.; 1 in./lb. = 0.57 cm./N; 1 Kip = 4.448 kN)

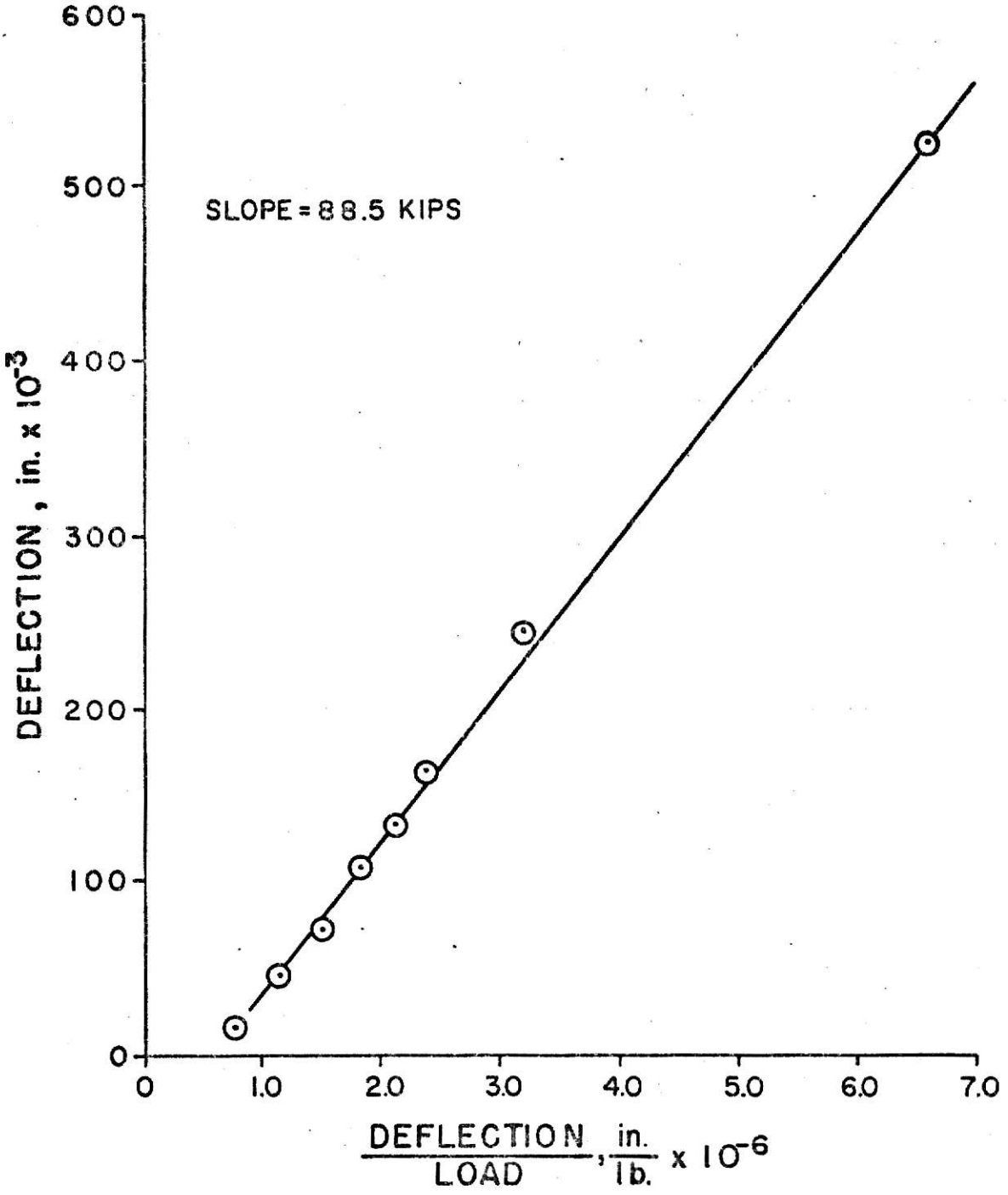

Figure B21 - Southwell Plot, Plate Number 22 (1 in. = 2.54 cm.; 1 in./lb. = 0.57 cm./N; 1 Kip = 4.448 kN)

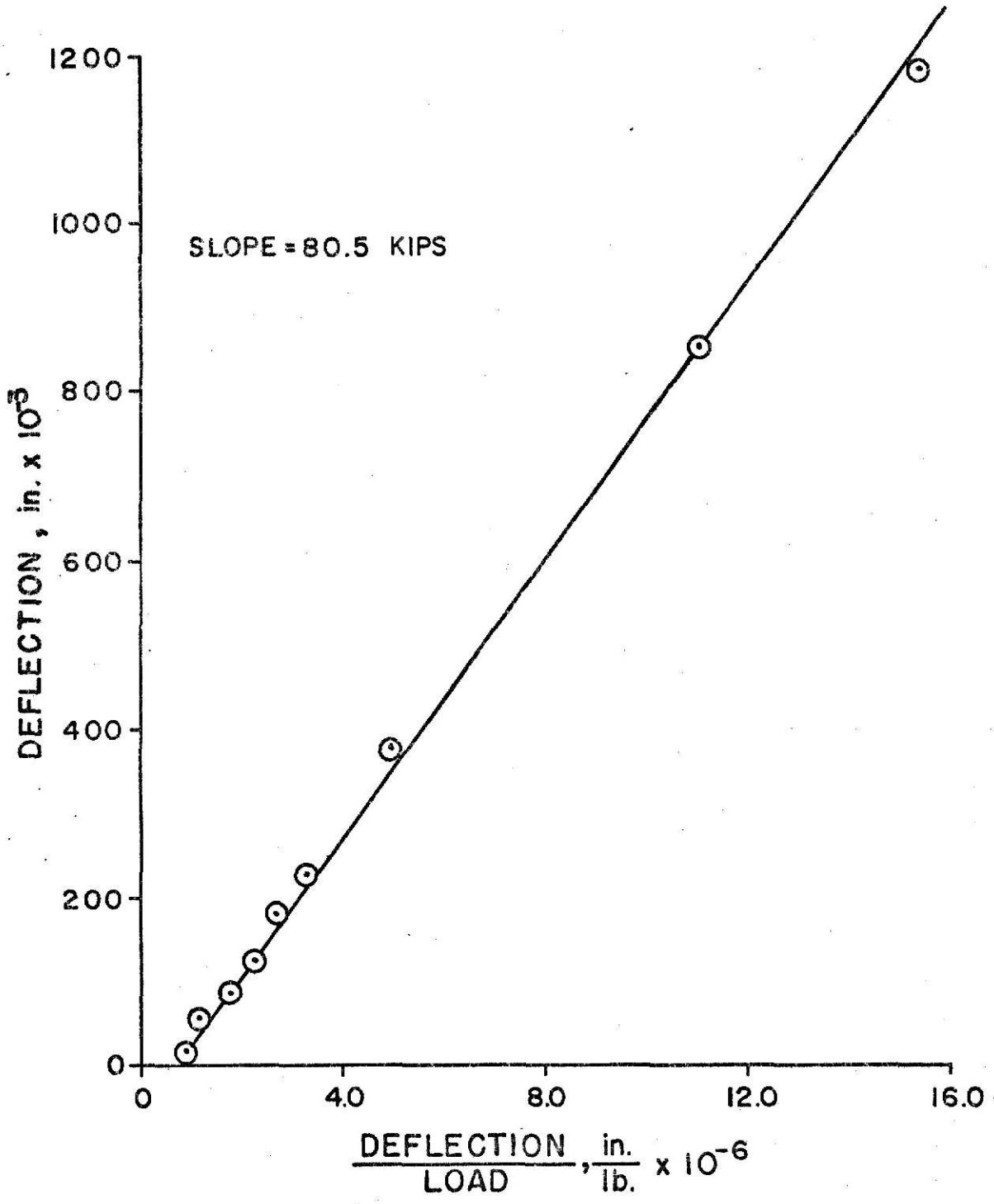

Figure B22 - Southwell Plot, Plate Number 23 (1 in. = 2.54 cm.; 1 in./lb. = 0.57 cm./N; 1 Kip = 4.448 kN)

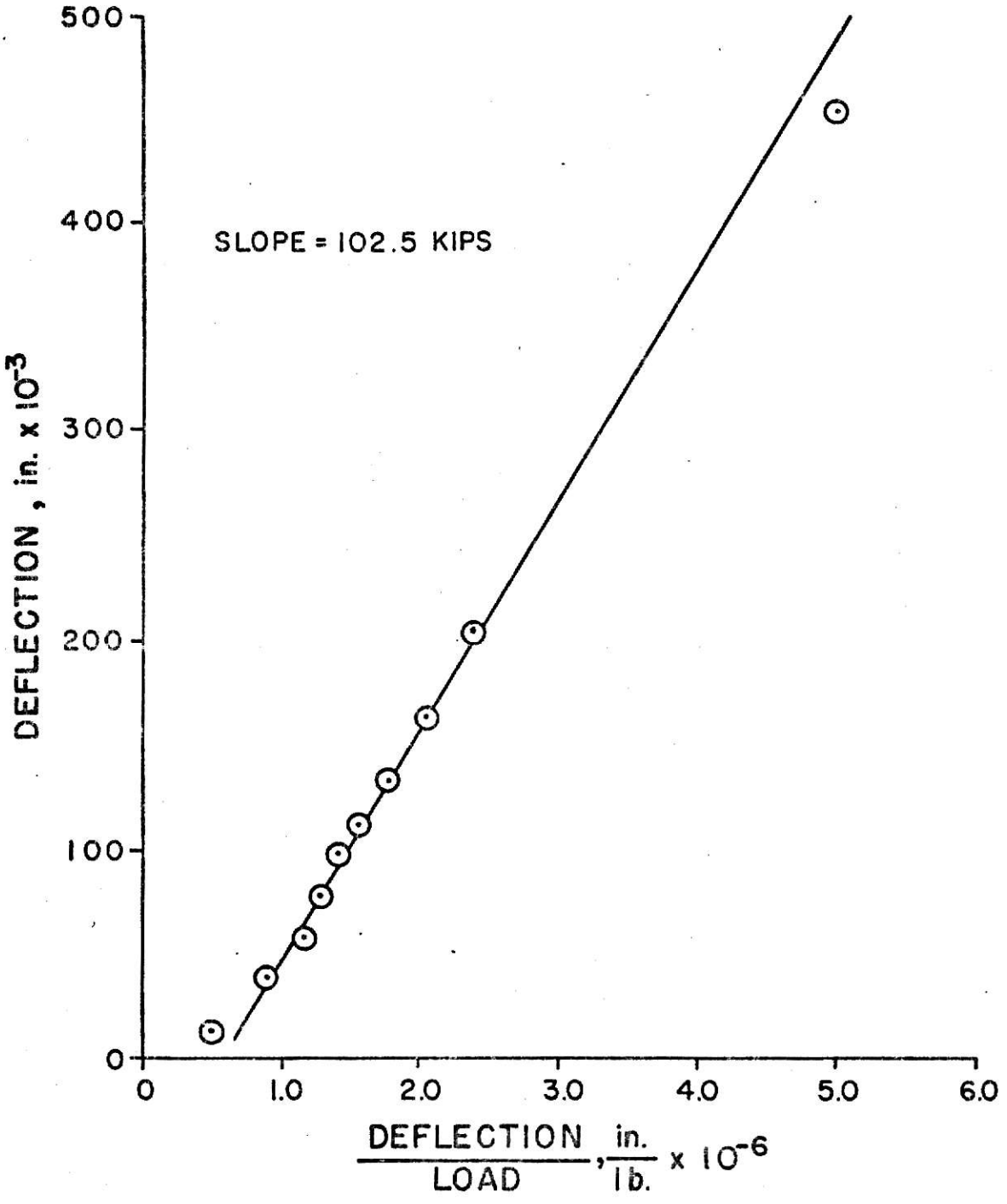

Figure B23 - Southwell Plot, Plate Number 24 (1 in. = 2.54 cm.; 1 in./lb. = 0.57 cm./N; 1 Kip = 4.448 kN)

APPENDIX C

STRAIN VERSUS LOAD PLOTS AT POINT OF BUCKLE

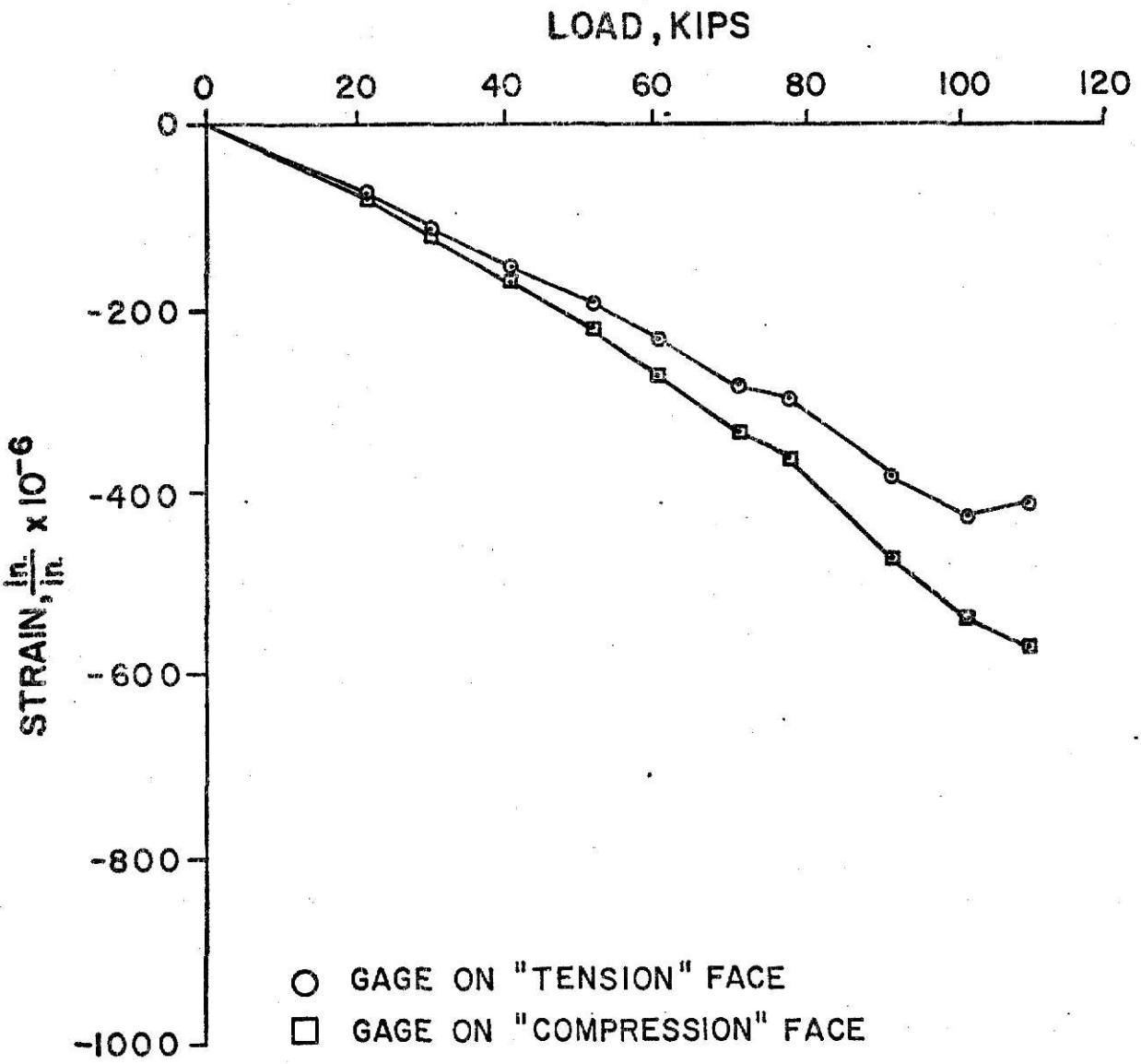

Figure C1 - Strain Versus Load, Midpoint of Plate on Centerline, Plate Number 2 (1 Kip = 4.448 kN)

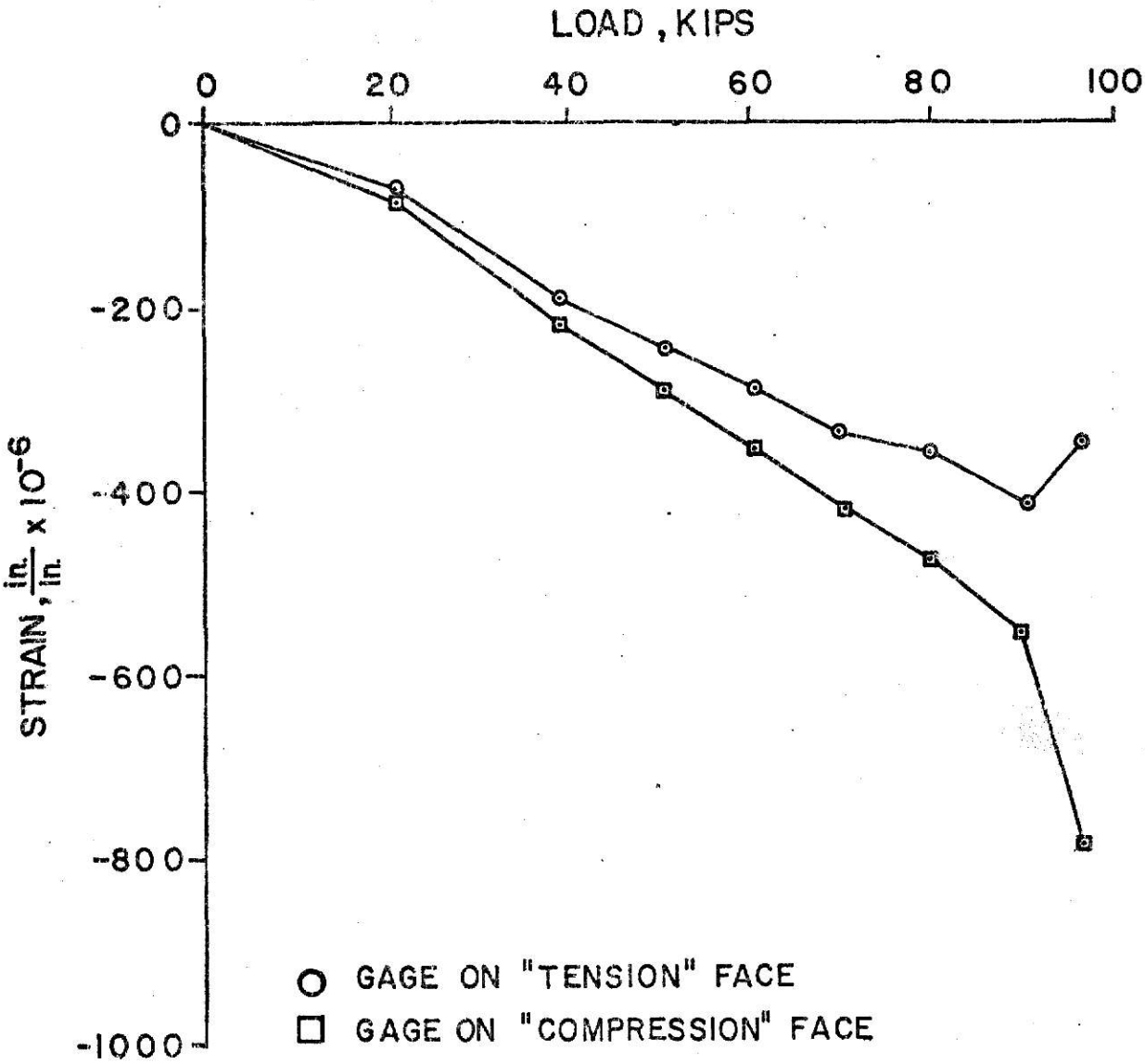

Figure C2 - Strain Versus Load, Midpoint of Plate on Centerline, Plate Number 3 (1 Kip = 4.448 kN)

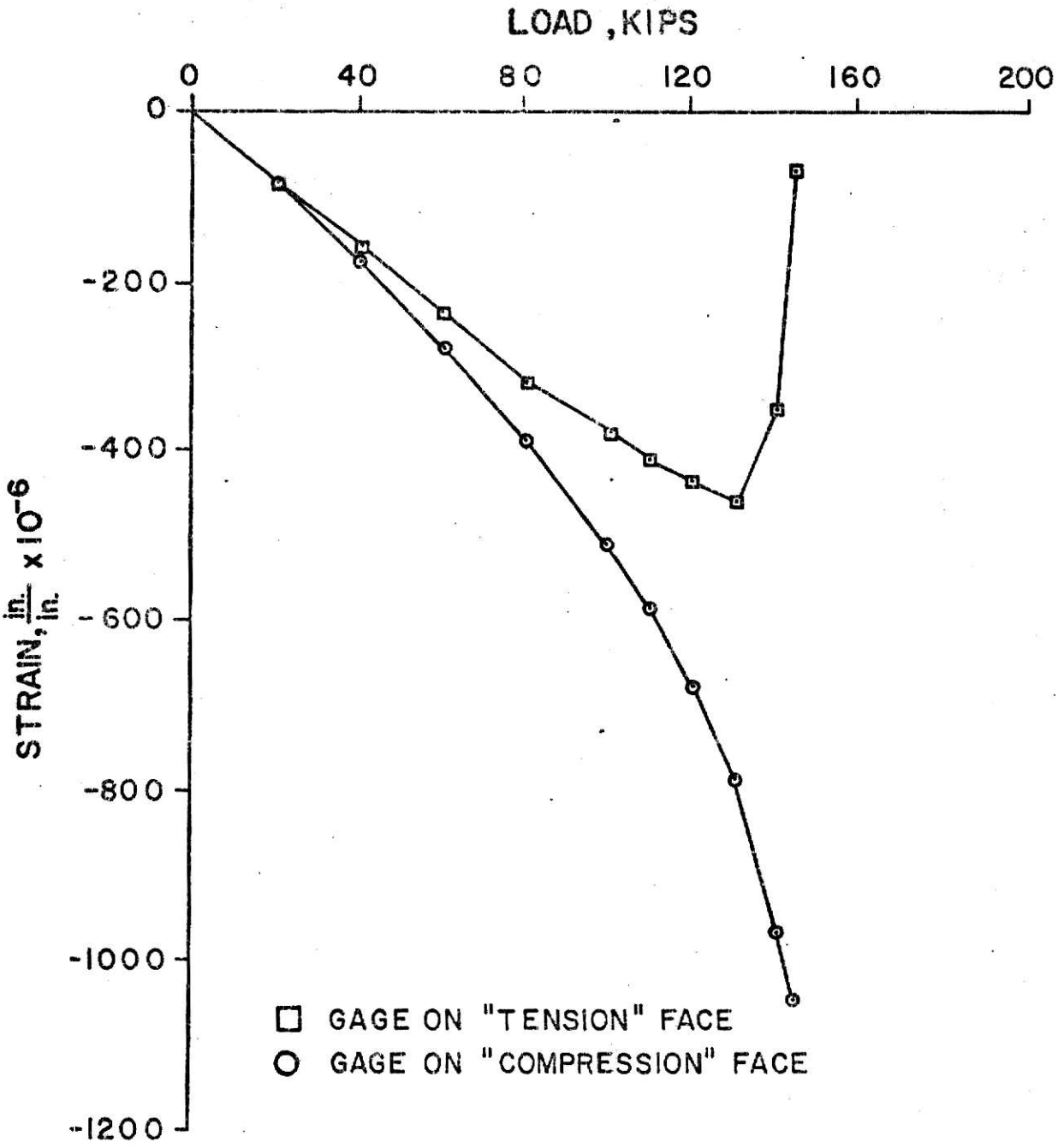

Figure C3 - Strain Versus Load, Midpoint of Plate on Centerline, Plate Number 7 (1 Kip = 4.448 kN)

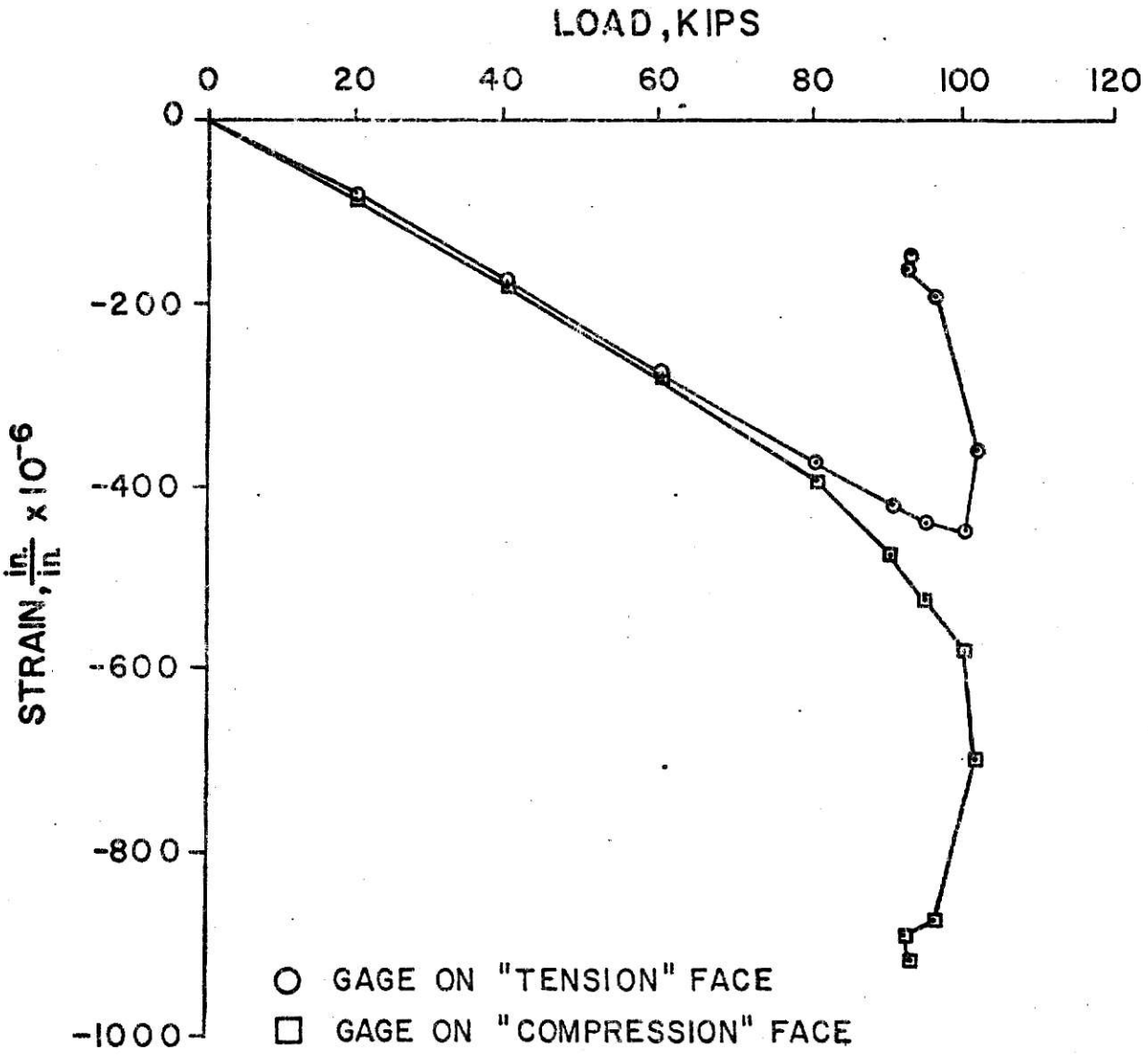

Figure C4 - Strain Versus Load, Top Quarter of Plate on Centerline, Plate Number 8 (1 Kip = 4.448 kN)

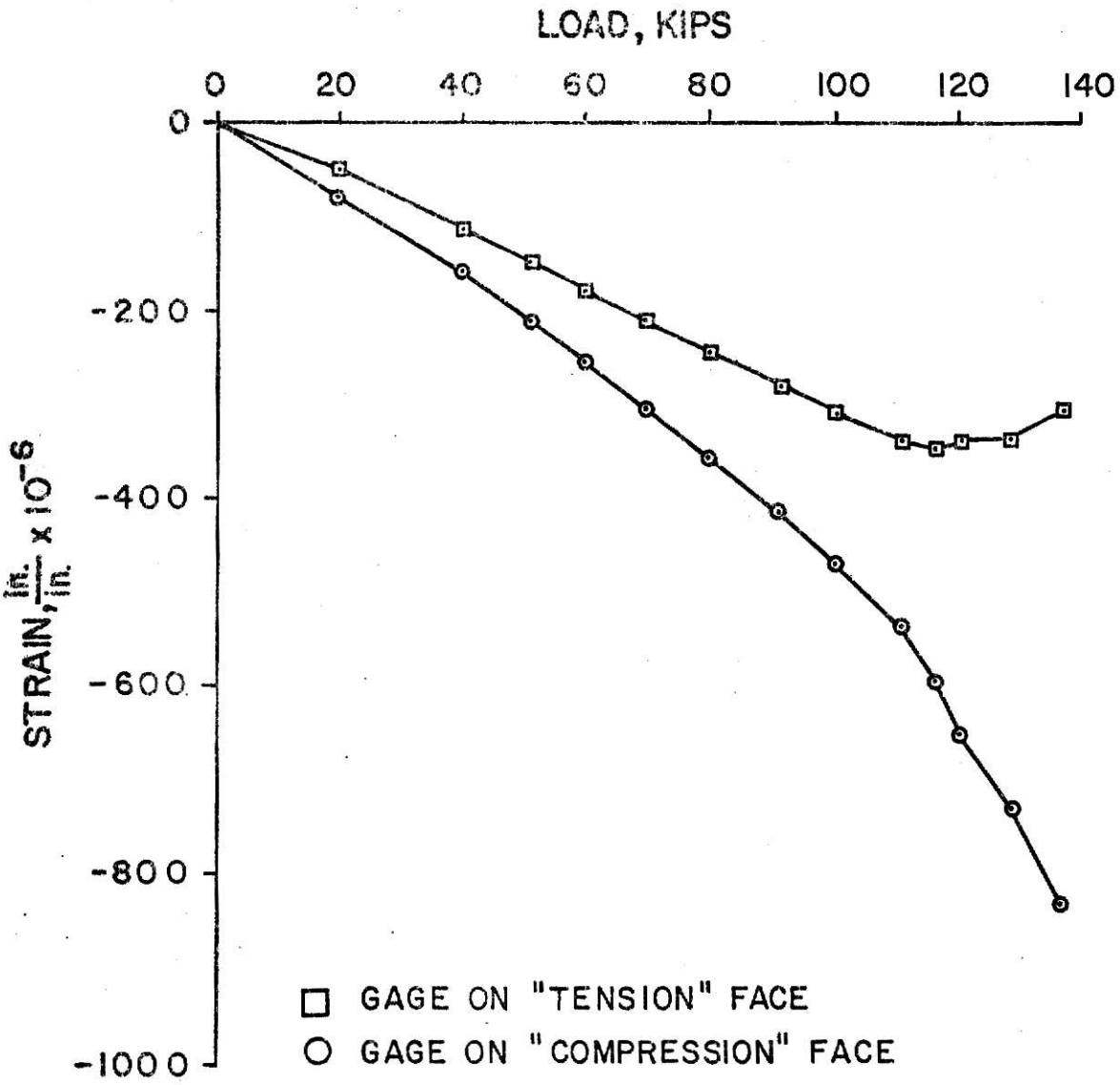

Figure C5 - Strain Versus Load, Midpoint of Plate on Centerline, Plate Number 9 (1 Kip = 4.448 kN)

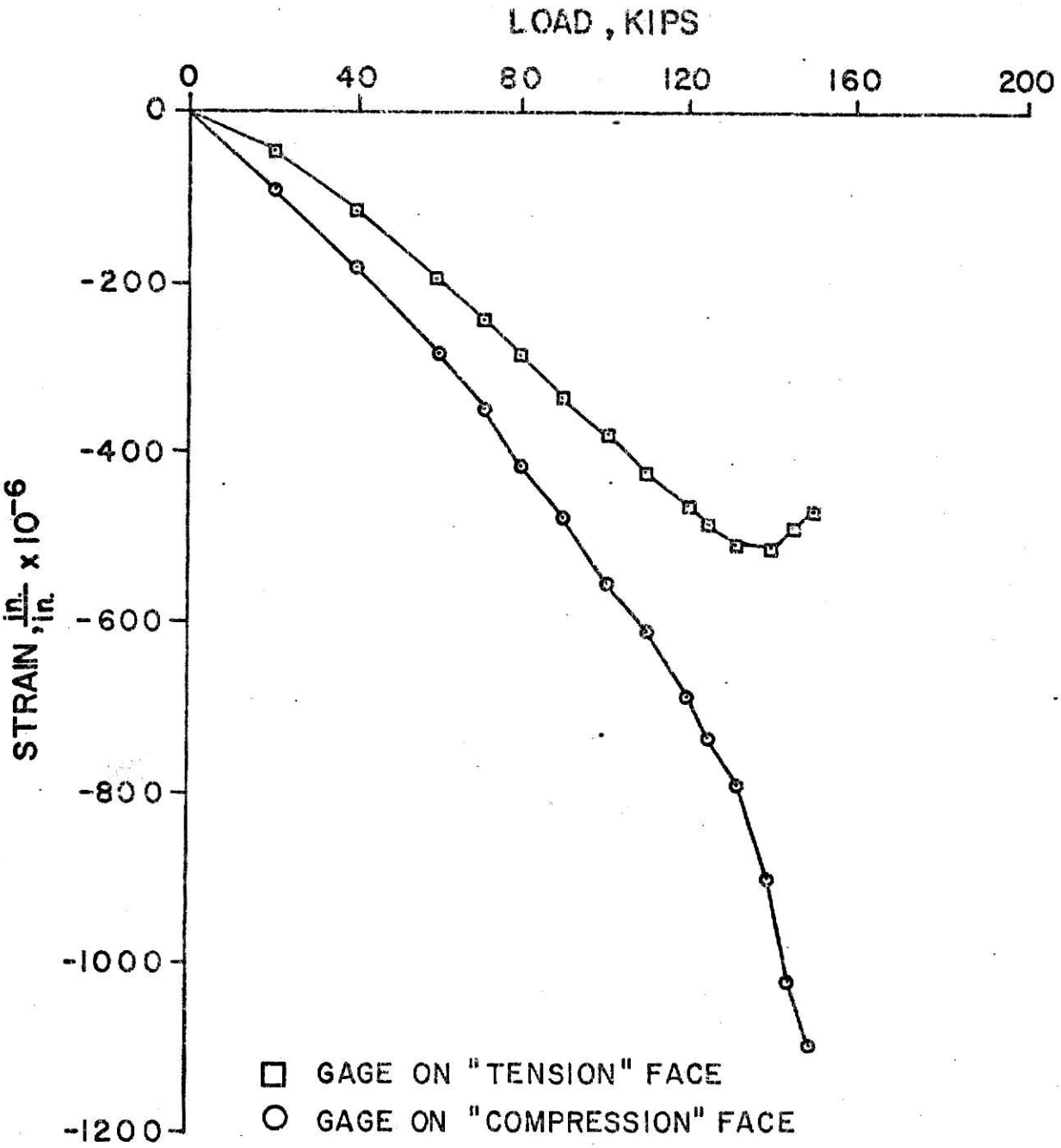

Figure C6 - Strain Versus Load, Midpoint of Plate on Centerline, Plate Number 10 (1 Kip = 4.448 kN)

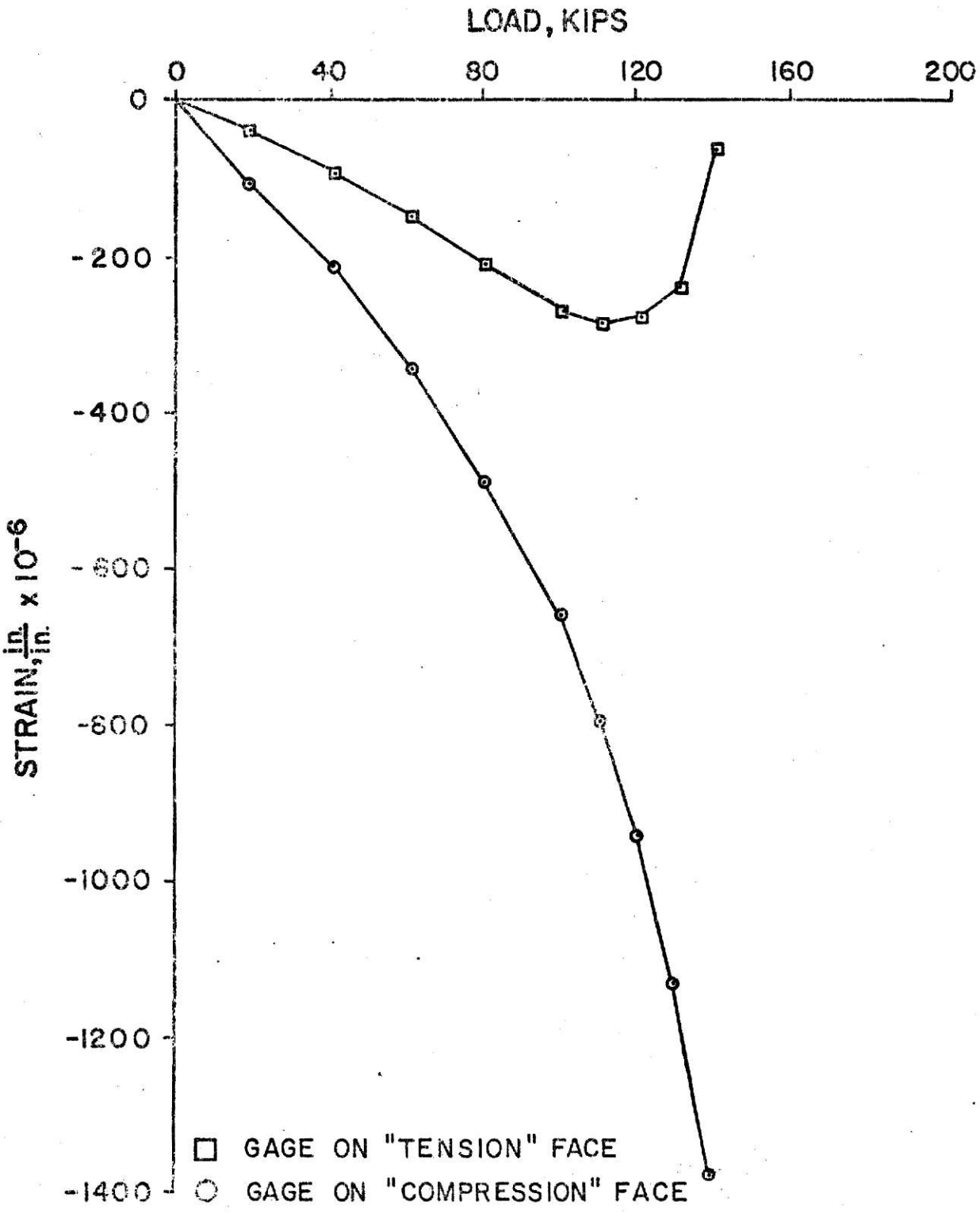

Figure C7 - Strain Versus Load, Midpoint of Plate on Centerline, Plate Number 11 (1 Kip = 4.448 kN)

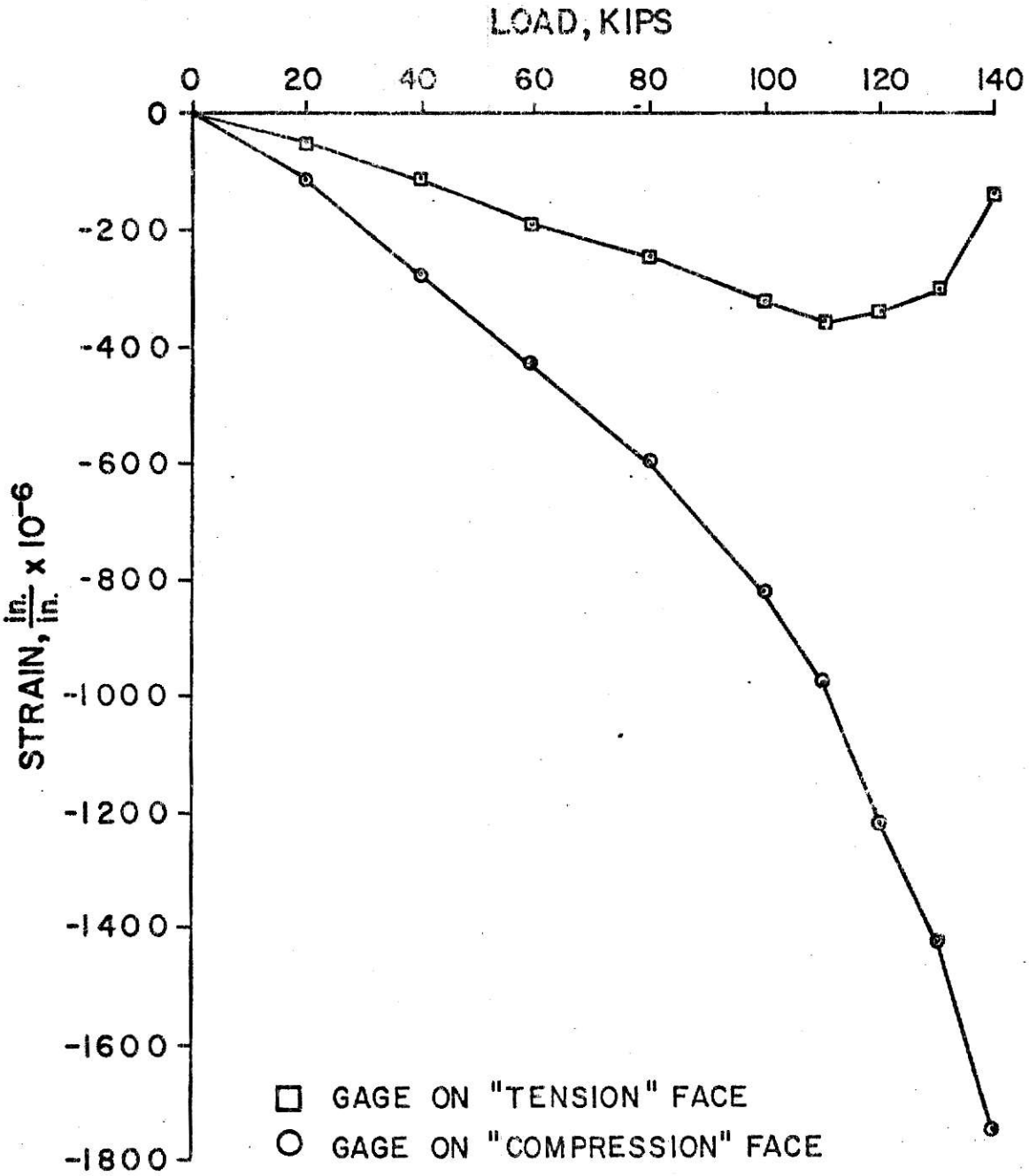

Figure C8 - Strain Versus Load, Midpoint of Plate on Centerline, Plate Number 12 (1 Kip = 4.448 kN)

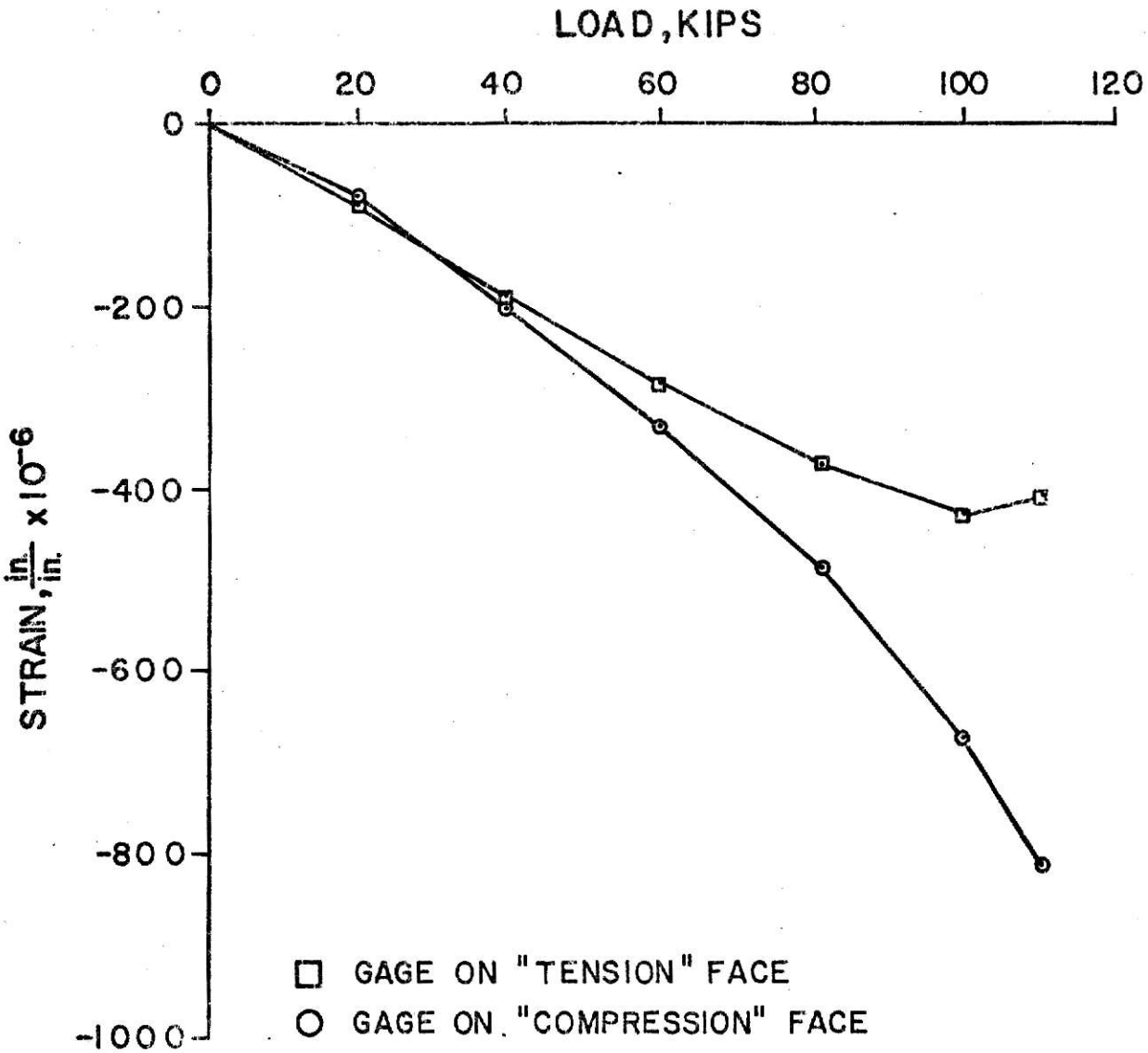

Figure C9 - Strain Versus Load, Midpoint of Plate on Centerline, Plate Number 13 (1 Kip = 4.448 kN)

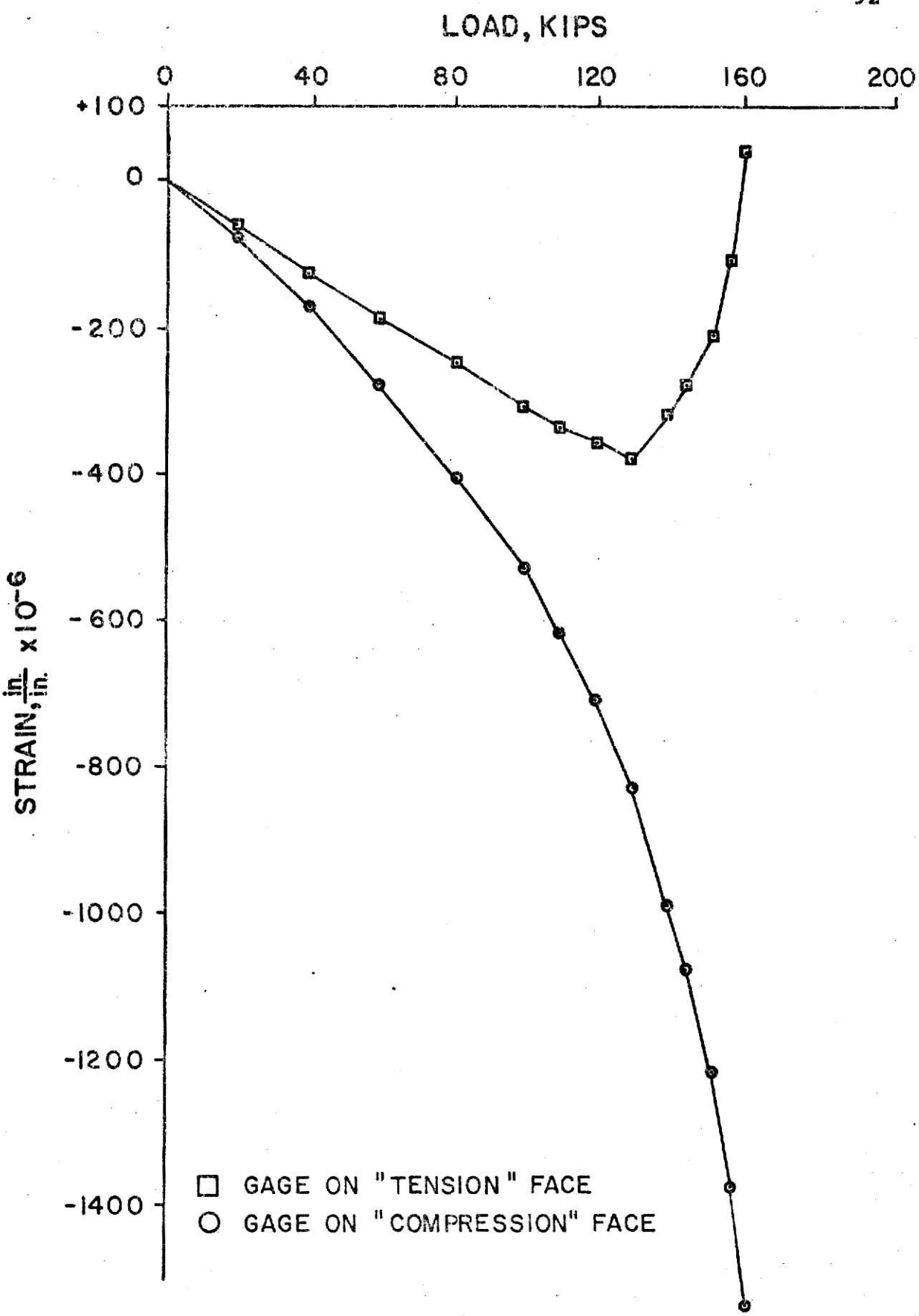

Figure C10 - Strain Versus Load, Midpoint of Plate on Centerline, Plate Number 14 (1 Kip = 4.448 kN)

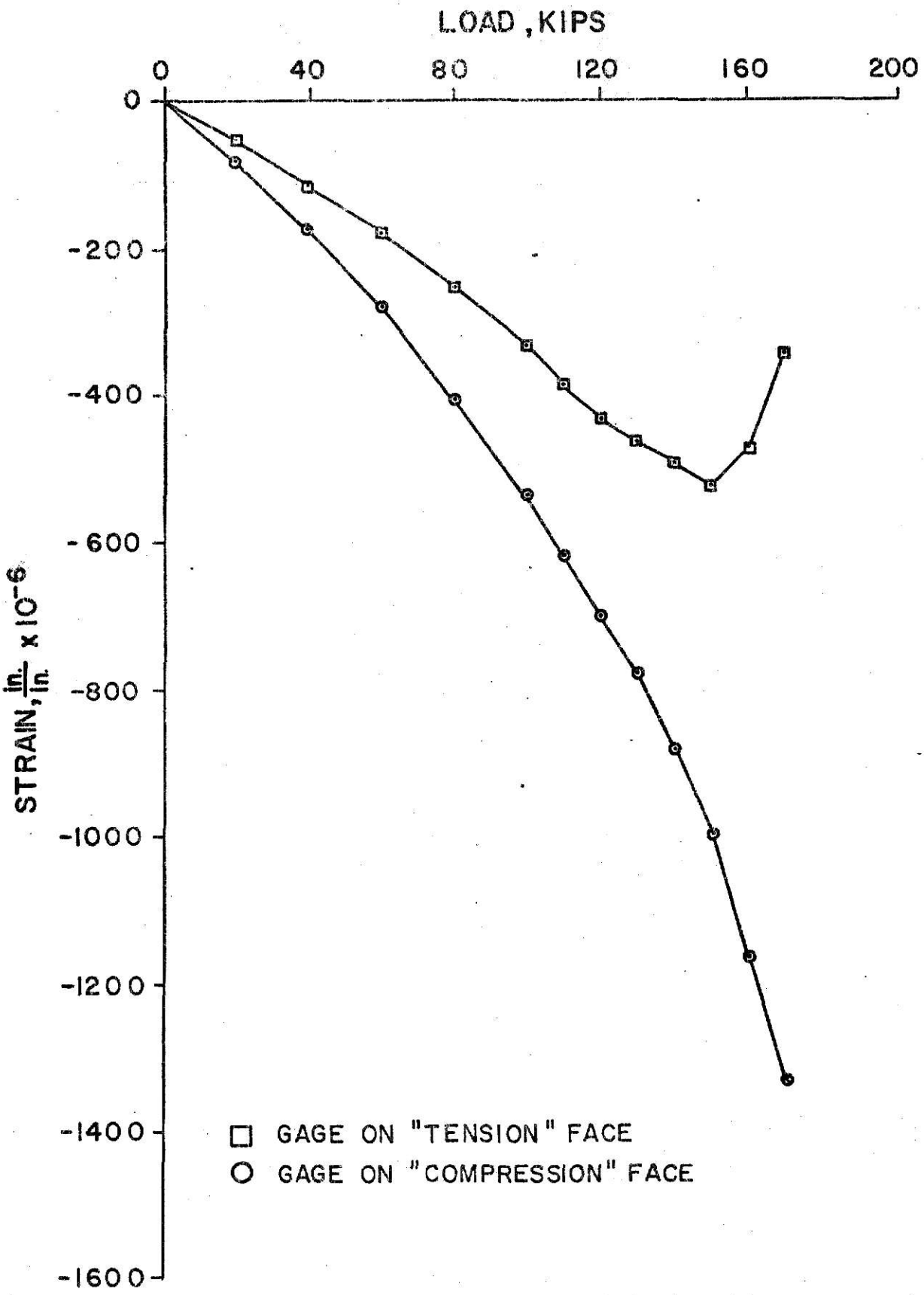

Figure C11 - Strain Versus Load, Midpoint of Plate on Centerline, Plate Number 15 (1 Kip = 4.448 kN)

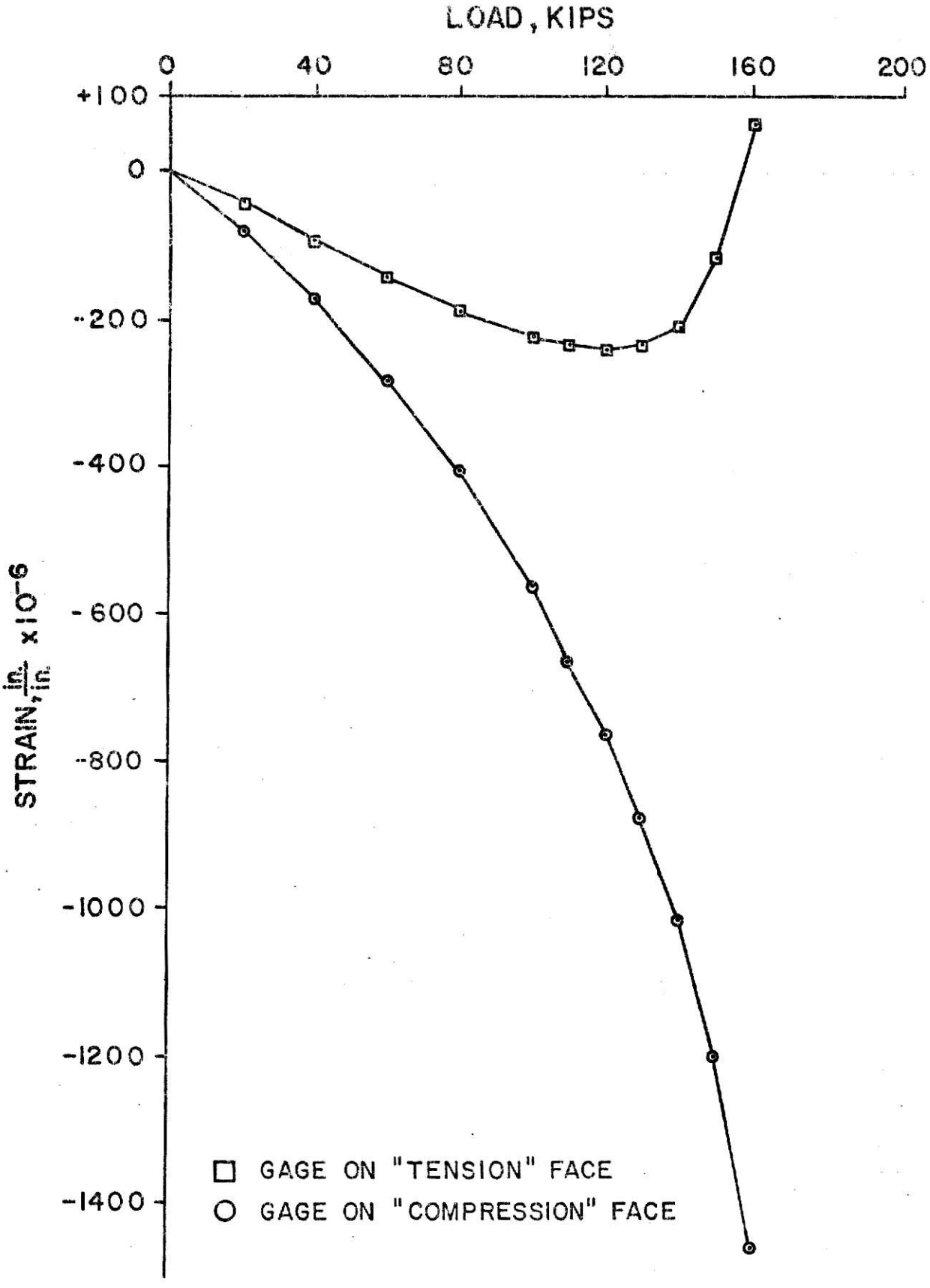

Figure C12 - Strain Versus Load, Midpoint of Plate on Centerline, Plate Number 16 (1 Kip = 4.448 kN)

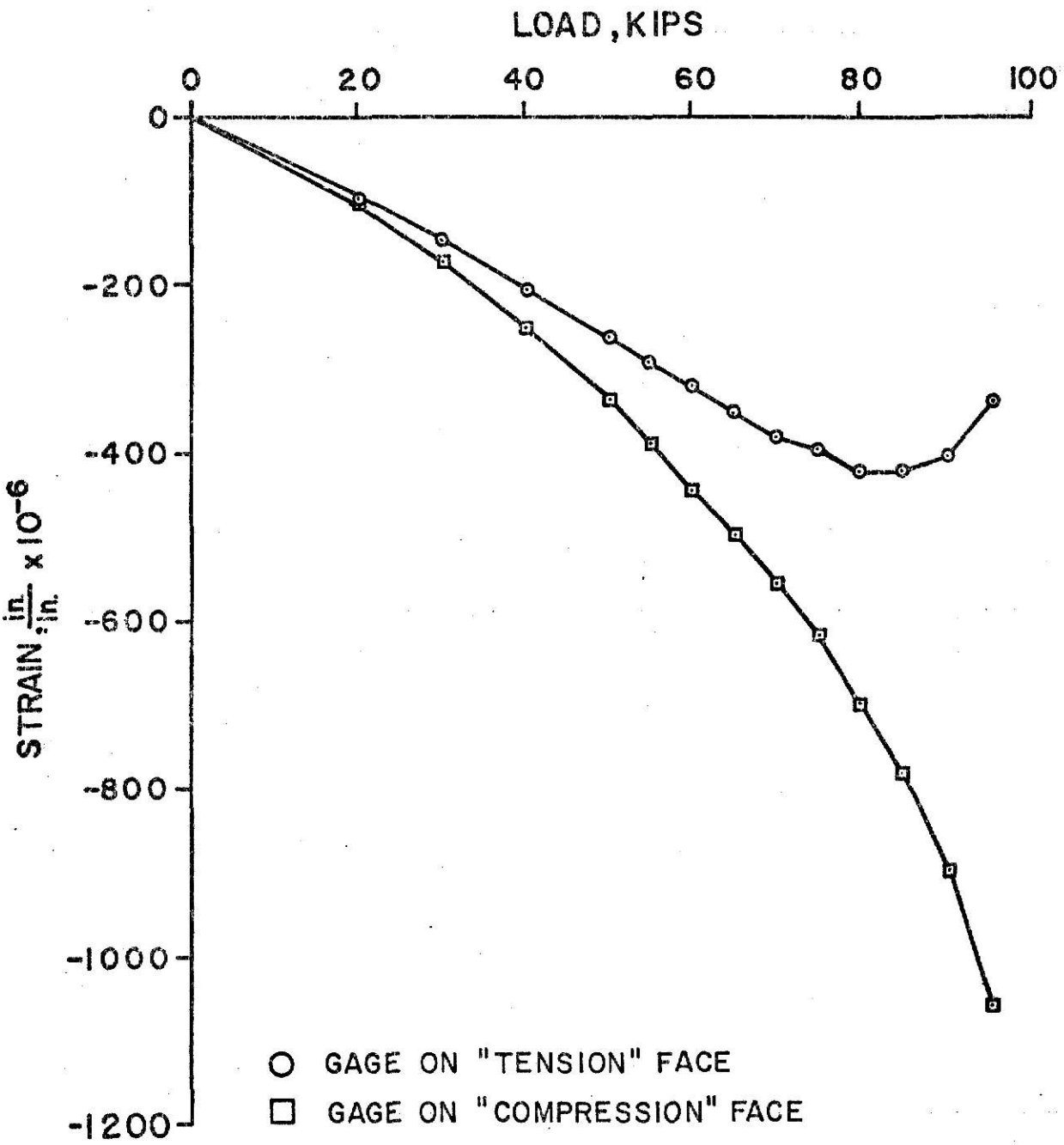

Figure C13 - Strain Versus Load, Midpoint of Plate on Centerline, Plate Number 17 (1 Kip = 4.448 kN)

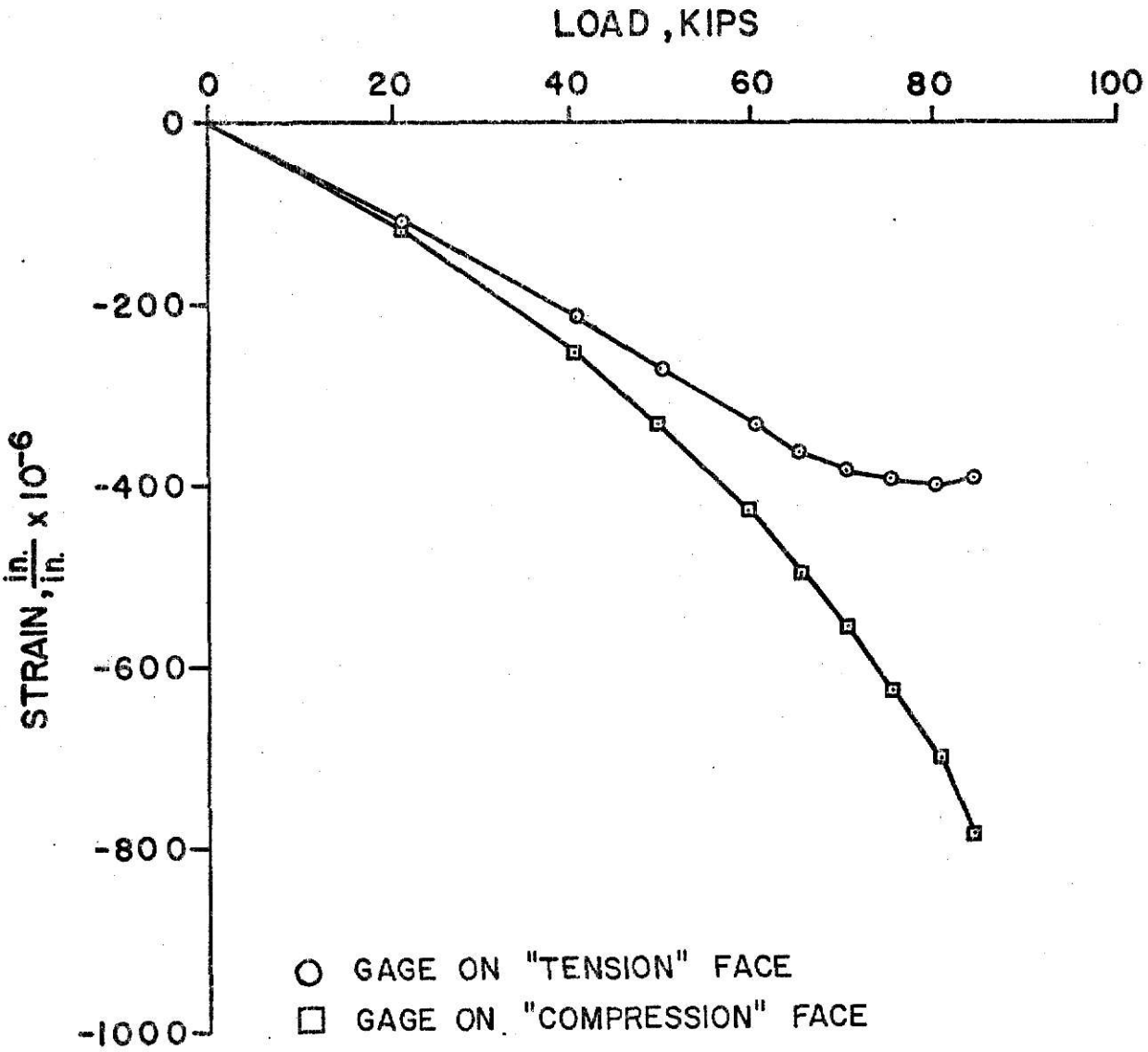

Figure C14 - Strain Versus Load, Midpoint of Plate on Centerline, Plate Number 18 (1 Kip = 4.448 kN)

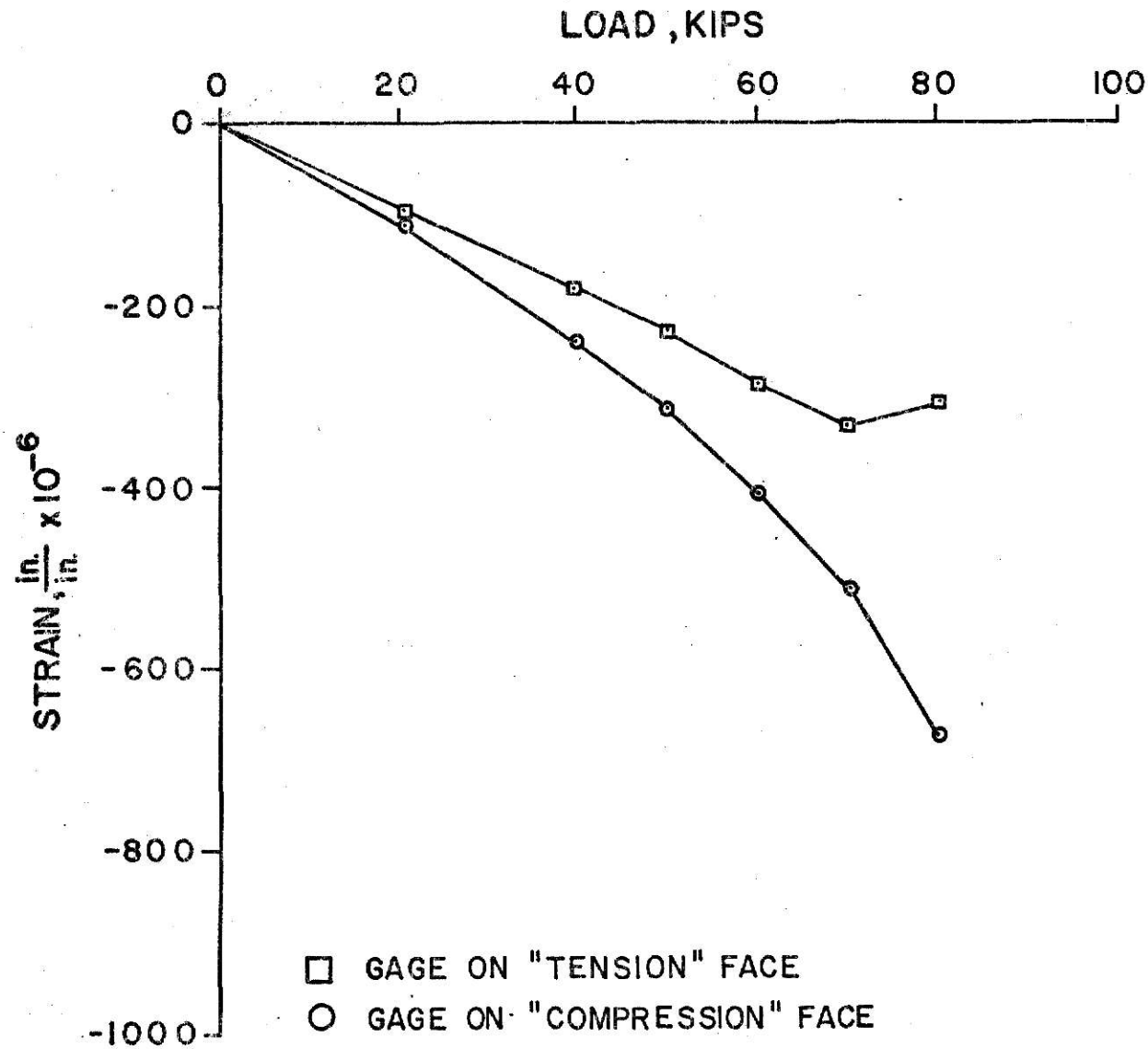

Figure C15 - Strain Versus Load, Bottom Quarter Point of Plate on Centerline, Plate Number 19 (1 Kip = 4.448 kN)

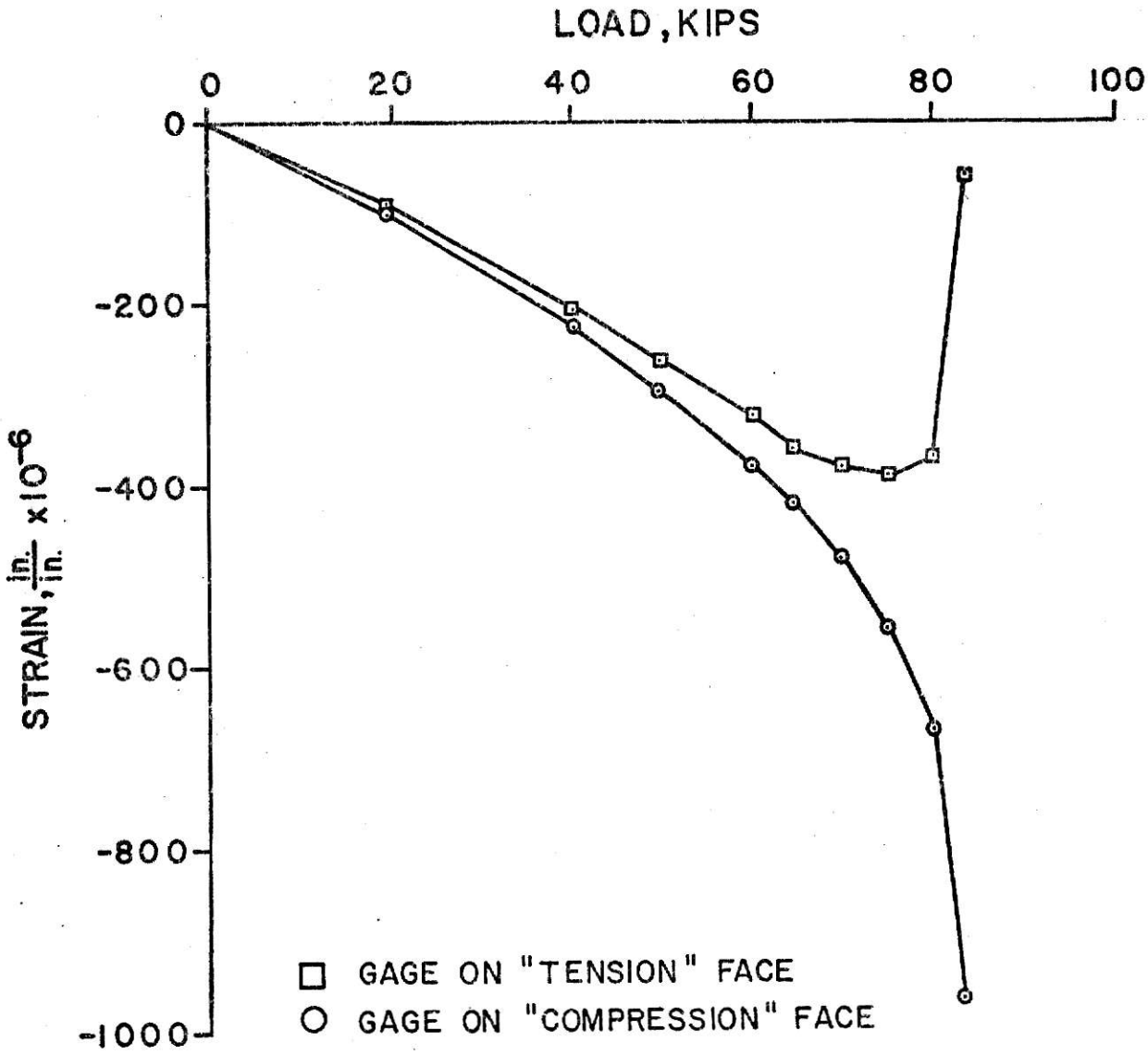

Figure C16 - Strain Versus Load, Bottom Quarter Point of Plate on Centerline, Plate Number 20 (1 Kip = 4.448 kN)

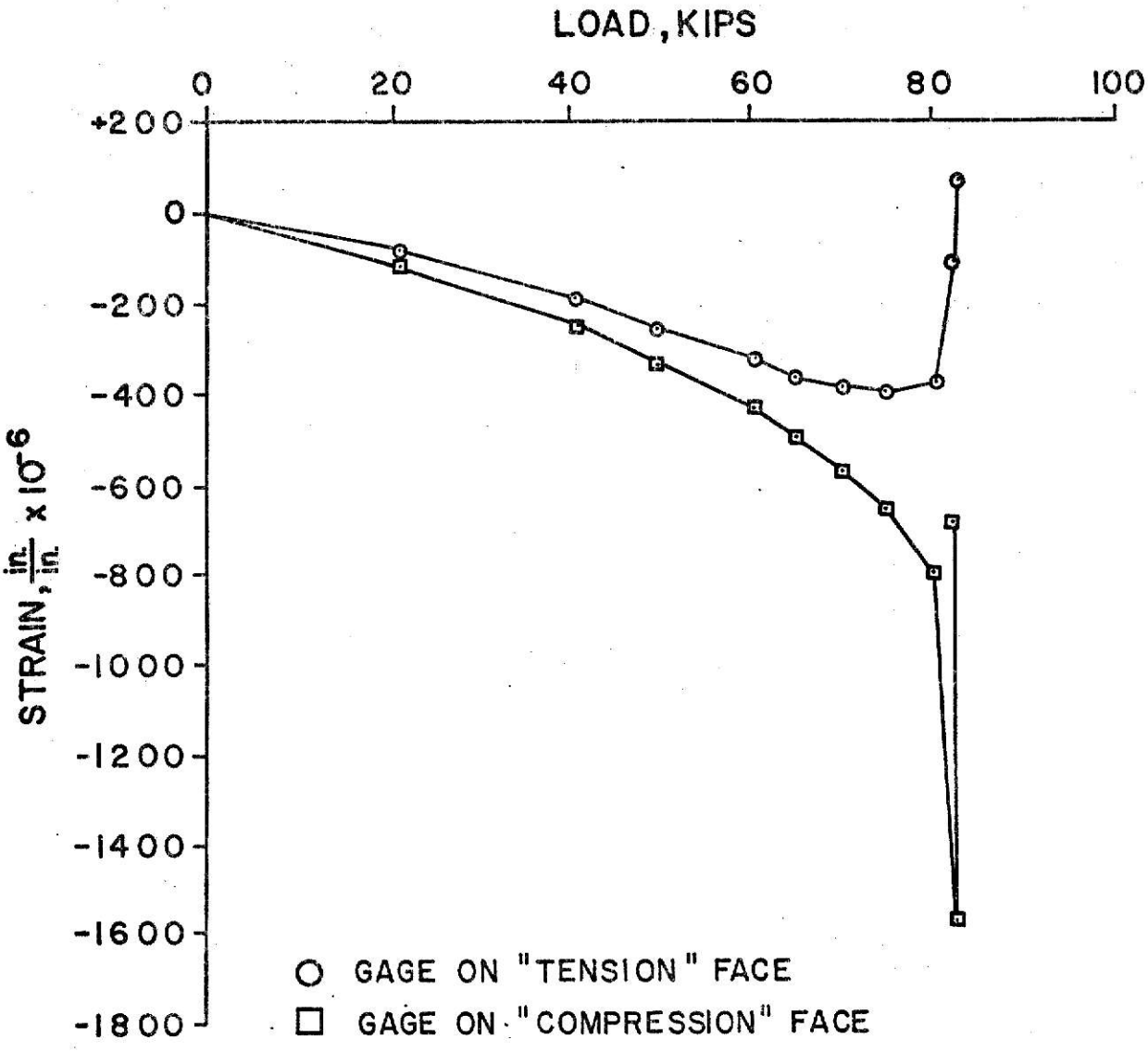

Figure C17 - Strain Versus Load, Top Quarter Point of Plate on Centerline, Plate Number 21 (1 Kip = 4.448 kN)

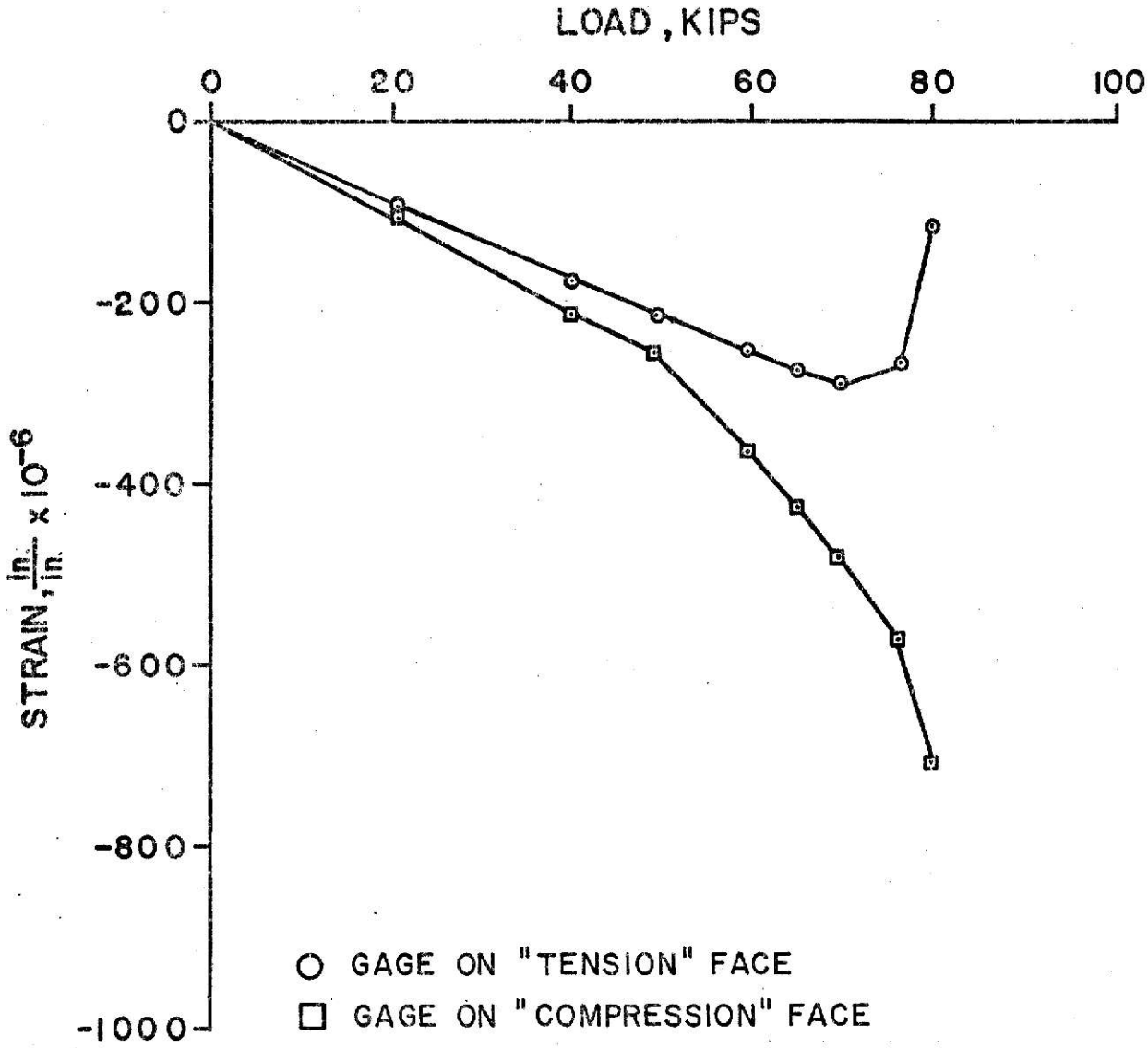

Figure C18 - Strain Versus Load, Midpoint of Plate on Centerline, Plate Number 22 (1 Kip = 4.448 kN)

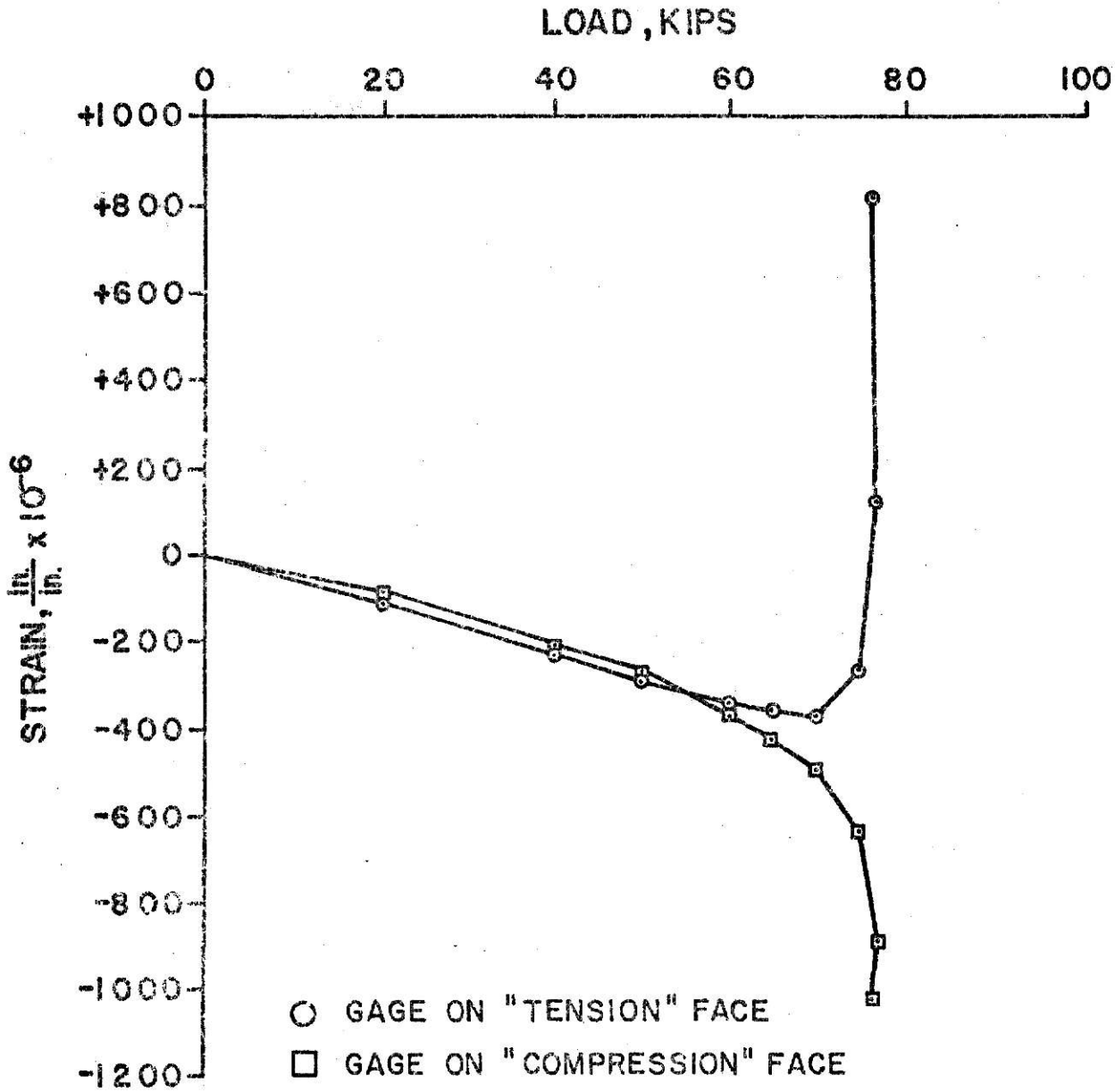

Figure C19 - Strain Versus Load, Top Quarter Point of Plate on Centerline, Plate Number 23 (1 Kip = 4.448 kN)

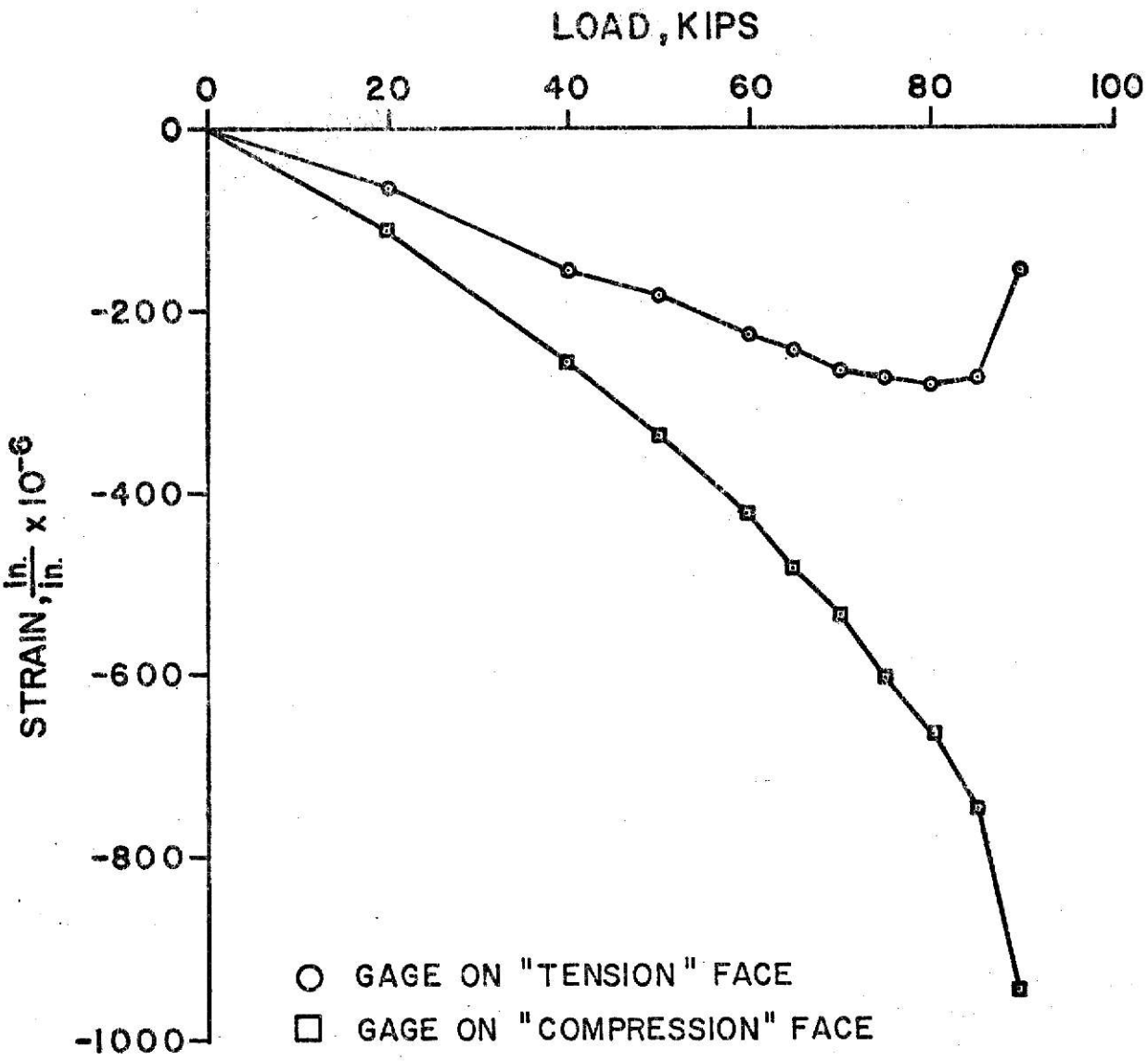

Figure C20 - Strain Versus Load, Midpoint of Plate on Centerline, Plate Number 24 (1 Kip = 4.448 kN)

APPENDIX D

NOTATION

NOTATION

The following symbols are used in this paper:

a = plate length

A_s = total steel area

A_{si} = steel area in i^{th} layer

b = plate width

C = experimental coefficient in "Rankine-Gordon" equation

C = plate stiffness coefficient

C' = plate stiffness coefficient

D = constant in elastic buckling equation

D_s = plate stiffness coefficient

D_{sl} = plate stiffness coefficient

D_{yl} = plate stiffness coefficient

e_{cr} = non-dimensionalized buckling strain

E = Young's Modulus

E_s = steel modulus

f'_c = concrete cylinder strength

f_{cr} = concrete buckling stress

h = plate thickness

l = ratio of plate length to plate width

m = number of half waves of buckled surface in the direction parallel to the applied load

m = buckling node number

p = total steel ratio

p_{cr} = elastic buckling stress

p_i = steel ratio in $i^{\underline{th}}$ layer

P_{cr} = buckling load

P_{cre} = experimental buckling load

P_{crt} = tangent modulus buckling load

P_f = collapse load

$\bar{z}_i$ = distance of $i^{\underline{th}}$ steel layer from middle surface

ε_o = concrete strain at f'_c

ε_{cr} = concrete strain at buckling

ν = Poisson's Ratio

ν_c = Poisson's Ratio for concrete

ACKNOWLEDGMENTS

The principal advisor for this thesis was Dr. Stuart E. Swartz, Associate Professor of Civil Engineering. Dr. Swartz's assistance in all phases of the project and preparation of this paper was invaluable and sincerely appreciated.

Genuine thanks are also extended to Professor Vernon H. Rosebraugh, Associate Professor of Civil Engineering. Professor Rosebraugh's guidance and comments were always of a worthwhile nature.

Appreciation is also put forward to Mr. Wallace M. Johnston of the Applied Mechanics Laboratory for his help during the experimental phase of the project.

REFERENCES

1. Bleich, F., Buckling Strength of Metal Structures, McGraw-Hill Book Co., New York, 1952.

2. Ernst, G. C., "Stability of Thin-Shelled Structures," Journal of the American Concrete Institute, Vol. 24, No. 4, December, 1952.

3. Ernst, G. C., Hromadik, J. J., and Riveland, A. R., "Inelastic Buckling of Plain and Reinforced Concrete Columns, Plates, and Shells," University of Nebraska Engineering Experiment Station, Bulletin No. 3, August, 1953.

4. Rogacki, S. A., "Design of Casting and Testing Apparatus for Reinforced Concrete Panels," Dissertation presented to the Civil Engineering Department, Kansas State University, in partial fulfillment for the requirements for the degree Master of Science, 1972.

5. Swartz, S. E. and Rosebraugh, V. H., "Buckling of Reinforced Concrete Plates," submitted for publication in the Journal of the Structural Division, ASCE.

6. Swartz, S. E., Rosebraugh, V. H., and Rogacki, S. A., "A Method for Determining the Buckling Strength of Concrete Panels," presented at the Third International Congress on Experimental Mechanics, Los Angeles, California, May, 1973.

7. Timoshenko, S. and Gere, R. D., Theory of Elastic Stability, 2nd Edition, McGraw-Hill Book Co., Inc., New York, 1961.

8. Yokel, F. Y. and Dikkers, R. D., "Strength of Load Bearing Masonry Walls," Journal of the Structural Division, ASCE, Vol. 97, No. ST5, May, 1971.

THE DETERMINATION OF THE BUCKLING STRENGTH OF REINFORCED CONCRETE PLATES

by

MARK YALE BERMAN

B. S. C. E., Kansas State University, 1971

AN ABSTRACT OF A MASTER'S THESIS

submitted in partial fulfillment of the

requirements for the degree

MASTER OF SCIENCE

Department of Civil Engineering

KANSAS STATE UNIVERSITY
Manhattan, Kansas

1973

ABSTRACT

This thesis presents the buckling characteristics of twenty-four reinforced concrete plates that were tested in uniaxial compression, along with correlations with theoretical approaches. Centerline deflection plots, Southwell plots, and strain versus load plots are presented for the points of buckle for each plate. Methods of determining the experimental buckling load are presented, along with a discussion of the available theories for predicting the buckling loads of reinforced concrete plates. The experimental setup is explained, and explanations of the experimentally determined parameters are also given.

It is determined that the strain versus load method of designating the buckling load was the most accurate one, and reasons for the inadequacy of the other methods are presented. The isotropic-tangent modulus theory is found to be the most accurate approach in theoretically predicting the buckling characteristics of the plates, and correlations are made with the experimental buckling load, the experimental collapse load, and the total steel ratio. The common parameter used in the correlations was a non-dimensionalized form of concrete buckling stress. The "Rankine-Gordon" formula is found to be unacceptable in predicting buckling stresses, and the total steel ratio is determined not to be a major factor. Further suggestions as to future research are also given.